AD NUMBER

AD858662

NEW LIMITATION CHANGE

TO

Approved for public release, distribution unlimited

FROM

Distribution authorized to U.S. Gov't. agencies and their contractors; Administrative/Operational Use; 30 Apr 1968. Other requests shall be referred to Air Force Materials Laboratory, Research and Technology Division, Wright-Patterson AFB, OH 45433.

AUTHORITY

AFSC ltr, 26 May 1972

CONTRACT AF 61 (052) - 916

FINAL SCIENTIFIC REPORT

CHATTER BEHAVIOR OF HEAVY MACHINE TOOLS

1 January 1966 - 31 March 1968

Professor Dr.-Ing. Dr. h. c. H. Opitz

Direktor des
Laboratoriums für Werkzeugmaschinen und
Betriebslehre der Technischen Hochschule
Aachen

The research reported in this document has been sponsored by the AIR FORCE MATERIALS LABORATORY Research and Technology Division, AFSC through the European Office of Aerospace Research (OAR), United States Air Force under Contract AF 61 (052)-916.

CONTRACT AF 61 (052) - 916

FINAL SCIENTIFIC REPORT

CHATTER BEHAVIOR OF HEAVY MACHINE TOOLS

1 January 1966 - 31 March 1968

Professor Dr.-Ing. Dr. h. c. H. Opitz

Direktor des
Laboratoriums für Werkzeugmaschinen und
Betriebslehre der Technischen Hochschule
Aachen

The research reported in this document has been sponsored by the AIR FORCE MATERIALS LABORATORY (Research and Technology Division, AFSC) through the European Office of Aerospace Research (OAR), United States Air Force under Contract AF 61 (052)-916.

Foreword

This Final Scientific Report covers the work performed under Contract AF 61(052)-916 during the period from 1 January 1966 to 31 March 1968 which terminates this program. It is published for information only and does not necessarily represent the recommendations, conclusions or approval of the Air Force.

This contract with the "Laboratorium für Werkzeugmaschinen und Betriebslehre der Technischen Hochschule Aachen" was initiated under Manufacturing Methods Project "Chatter Behavior of Heavy Machine Tools". It has been accomplished under the technical direction of Mr. Floyd L. Whitney of the Advanced Fabrication Techniques Branch, MATF, Manufacturing Technology Division, Air Force Materials Laboratory, Wright-Patterson Air Force Base OHIO.

Closely related efforts in the field of vibration analysis are covered under Contracts AF 33 (615)-2661 at the Cincinnati Milling and Grinding Machines, Inc., Cincinnati, Ohio; AF 33 (615)-2664 at the Department of Mechanical Engineering University of Cincinnati; AF 61 (052)-961 at the "Institut für Werkzeugmaschinen und Betriebswissenschaften der Technischen Hochschule München" and AF 61 (052)-966 at the "Laboratorium für Werkzeugmaschinen und Betriebslehre der Technischen Hochschule Aachen".

The principal investigator of this project is Professor Dr.-Ing. Dr. h.c. D. Sc. H. Opitz. Chief engineer is Dr.-Ing. A. Mussenbrock. The work on the project was performed by the following research group:

Research engineers on chatter analysis and investigations of the cutting process are Dipl.-Ing. H. Kubeth, Dipl.-Ing. F. Bernardi and Dipl.-Ing. K. Beckenbauer.

Research engineers on structure analysis are Dr.-Ing. W. Döpper and Dipl.-Wirtsch.-Ing. H. Groth.

Abstract

This project has been engaged in a program of research which was directed at the problem of determining and improving the dynamic stability of machine tool-metal cutting systems. Such a study will provide machine tool manufacturers with the necessary analytical methods, tests and specification techniques to assure a chatter free cutting process for large machine tools.

Based upon the theory of regenerative chatter the system machine-tool - cutting process is reduced to a nonintermeshed closed control loop, of which the stability behavior is representative for the chatterfree cutting performance. For economically carrying out the stability analysis digital computer programs have been developed. Results of practical chatter investigations are finally detailed.

The discussion of different possibilities to provide data for chatter specifications showed, that further practical investigations must be carried out, before one of the discussed procedures can be finally stated to be fully suitable and before machine tool chatter specifications can be published respectively.

Methods and digital computer programs have been developed and tested for the precalculation of the static and dynamic properties of machine tool systems already in the status of design. A short general view over this research work is presented.

For calculating the deformation of columns with square and rectangular cross-section equations have been derived. They include the influence of shear force and a cross-sectional distortion under torsional loads can be considered as well. In model tests these equations have been proved. Furthermore the influence of different types of ribbing on the static and dynamic behavior of columns has been determined.

Table of Contents

List of Figures

List of Figures (Continued) Page

List of Figures (Continued) Page

List of Figure (Continued) Page

List of Figures (Continued) Page

Nomenclature

$A\ (i\omega)$	resultant directed response locus	
A	area	(mm^2)
B	milling breadth	(mm)
C	connection matrix	
c	damping coefficient	(kps/cm)
D	damping factor	
D	diameter of cutter	(mm)
d	vector of deformation	
d	vector of rigid body deformation	
E	modulus of elasticity	(kp/mm^2)
e	vector of member deformation	
F	flexibility matrix	
F	force per unit length	(kp/mm)
F	force, cutting force variation	(kp)
F_o	static cutting force	(kp)
$F_o\ (i\omega)$	response locus of the open control loop	
F_A	thrust force	(kp)
F_H	main cutting force	(kp)
f	frequency	(cps)
f_R	chatter frequency	(cps)
f_z	tooth mesh frequency	(cps)
G	modulus of elasticity	(kp/mm^2)
$G\ (i\omega)$	machine response locus	
H	equilibrium matrix	
h	height of cross section	(mm)
I	moment of inertia	(mm^4)
IF	influence matrix	
Im	imaginary part	($\mu m/kp$)
K	operand	
K	stiffness matrix	
K	stiffness	(kp/cm)

k_c	chip thickness coefficient	(kp/cm)
k_{cw}	chip thickness coefficient related to the deapth of cut	(kp/cm^2)
$k_{st,s}$	specific cutting force	(kp/mm^2)
L	length	(mm)
M	moment	(mkp)
Md	torsional moment	(mkp)
m	positive integer number	
m	mass	(kps^2/cm)
N_e	installed power	(kW)
n	rotational speed	(rev/min)
P	force	(kp)
P	vector of loading	
Q	shear force	(kp)
R, R_A, R_H	angular functions	
Re	real part	(μm/kp)
R_m	time-averaged direction coefficient	
R (t)	time-variant direction coefficient	
s	feed rate	(mm/min)
s_z	feed rate per tooth	(mm/tooth)
T	revolution time	(s)
t	time	(s)
U	circumference	(mm)
u	chip thickness variation	(cm)
v	cutting speed	(cm/s)
w	deapth of cut (milling)	
	width of cut (turning)	(mm)
x,y,z	co-ordinate axes, displacements	(μm)
z	number of tooth on cutter	
z_c	number of tooth in contact	
z_a	output	
z_e	input	
α_H	clearance angle	(^{o})
β	cutting force angle	(^{o})
γ_H	rake angle	(^{o})

η	efficiency	(%)
η	frequency ratio	
κ_r	side cutting edge angle	(^{o})
κ	shear force deformation coefficient	
λ	inclination angle	(^{o})
ρ	phase shift between force and displacement	(^{o})
φ	torsional angle	(^{o})
φ	angular position of tooth	(^{o})
φ_A	exit angle	(^{o})
φ_E	entrance angle	(^{o})
ω	frequency	(sec^{-1})
ψ	phase shift between cutting force-and chip thickness variation	(^{o})
τ	shear stress	(kp/mm^2)
τ	delay time between two cuts	(s)

Introduction

In machining processes on cutting machine tools often intense vibrations occur, which can shorten the tool life, increase the wear of the machine and cause insufficient accuracy and surface quality of the workpieces. Because of these vibrations - in general called chatter vibrations - in many cases the performance of the machining operation can even be impossible without changing the given cutting conditions. In the plant a change of the cutting conditions is not necessarily but actually in most of the practical cases connected with a decrease of cutting performance, which means a forfeiture of profit for the machine tool user. This aspect becomes specially important for machines which require high amounts of investment, as for instance large and heavy machine tools and NC machines.

The above listed reasons caused the United States Air Force Materials Laboratory, Research and Technology Division, to sponsor a research program for the investigation of the dynamic and chatter behavior of machine tools in general.

This Final Scientific Report covers the work performed under Contract AF 61 (052)-916 at the Laboratorium für Werkzeugmaschinen und Betriebslehre der Technischen Hochschule Aachen. The research work was initiated on 1 January 1966 and terminated on 31 March 1968. This contract is the continuation of the research work conducted at the same institute under Contract AF 61(052)-713 during the period from 1 June 1963 to 30 November 1964.

Under the preceding contract, which for the first time dealt with systematical investigations into the static and dynamic properties and the chatter behavior of heavy machine tools, fundamental research work on the field of the development of measuring equipment and test procedures as well as initial theoretical investigations concerning the chatter behavior in face milling operations have been carried out. Additionally

initial steps have been done to calculate the static and dynamic properties of machine tool elements by means of electronical computers.

The aim of this new contract, in which the important results of the preceding contract have been used, was to improve the dynamic and chatter behavior of cutting machine tools in general and therewith to get higher profit from the machine tool capacity. The total research work is directed at improving the behavior of actual machines in the shop and of machine tools being in the status of design.

The object of the first section "Chatter Analysis" was to investigate the theoretical relationships in machine tool chatter and to get knowledge about the effect of the machining parameters and structural characteristics upon the chatter behavior. Extensive theoretical and experimental investigations have been discussed in the Quarterly Technical Reports (see Ref. 11-18). The most important results and especially the practical application of the developed procedures are detailed in the first part of this report. In this part a mathematical model being generally valid, is established, by means of which the stability of milling and turning operations can be analyzed. In this model certain simplifications of the exact mathematical relations are included, which however have negligible influence upon the accuracy of the results for the practically interesting conditions. These simplifications have only been introduced in order to make the chatter investigation to be carried out easily and economically.

One essential purpose of the theoretical chatter analysis is to provide the necessary data for chosing the machining conditions in such a manner, that a high chatter free cutting performance can be reached. In order to take into account and to vary the practically interesting parameters easily in the theoretical calculation different digital computer pro-

grams have been developed, by means of which the stability analysis can be carried out. In many application cases a very good correlation between theoretical and experimental borderlines of stability has been obtained.

An additional purpose of the research work in the section Chatter Analysis was to study the basis for establishing dynamic specifications for machine tools. Dynamic (chatter) specifications, which are demanded for since about 10 years chiefly by the machine tool users, shall complete the geometrical specifications after Schlesinger. Dynamic specifications shall enable machine tool users to judge and to compare the machines reliably with regard to their chatterfree cutting performance.

Investigations on milling machines and lathes of various types and manufacturers gave the possibility to study the conditions for the establishment of general dynamic specifications. From these extensive investigations on principle different possibilities can be derived for testing and specifying machine tool chatter behavior. These procedures will be discussed in the second section "Chatter Specifications". However, considering the numerous aspects concerning chatter specifications, which were unknown until now and therefore were not taken into account when initiating this program, it can be stated here beforehand, that it seems very premature to establish and to publish chatter specifications at this time.

Another part of this contract dealt with structur-analysis. From the above mentioned point of view and in a lot of other cases it would be very helpful for surely being able to precalculate the static and dynamic behavior of machine tool parts and systems of these elements which consequently give a machine tool.

Within this part of the contract some methods were developed to calculate the later behavior already in the status of

design (see Ref.[2 + 18]). Starting from a flux of force analysis over some total machine constructions the steps for developing the methods, programing and testing them was fixed.
During this work problems occured with respect to an economical preparation of input data as for example cross section values. For this purpose additionally a methode was found and will be fully described.
The methods carried out here may be called solving a lot of so far not or unsufficiently solved problems by aid of a computer during the design process. The usefulness and accuracy of the suggested ways are shown within the several Quarterly Technical Reports comparing measured and computed results about representative structures.

However, it has to be pointed out already, in the foreword that still problems occur when applying the methods to arbitrary chosen systems with respect to the boundary conditions in form of so far unknown static and dynamic behavior of the connection points between elements and to the foundation.

Besides the computation of the static and dynamic behavior of machines or structural elements it is still necessary to test actual structures themselves or models. In order to determine the influence of internal ribs and wall ribs on the behavior of column models with different types of ribbing have been tested. These tests point out some interesting aspects for designing columns. In addition to the tests an analysis of the deformation of columns loaded by a single force or a couple of forces is given especially with respect to the deformation due to shear force and cross-sectional distortion caused by torsional loads.

1. Chatter Analysis

Vibrations on machine tools occuring relatively between workpiece and tool can be reduced to different exciting mechanisms which however in a certain case can only be distinguished hardly. According to the fundamental research work into the vibration behavior of machine tools conducted especially by Tobias and Tlusty-Polacek, the observed vibration phenomena can be classified into two main groups:

Forced vibrations
Self excited vibrations.

Forced vibrations are often generated by external forces, which are transferred by the machine foundation. Unbalance, errors and defects in gear drives and bearings have unfavourable effect chiefly in these cases, where their frequency correlates to a natural frequency of the machine. In these cases resonances are excited with often very great vibration amplitudes at the cutting point. In the shop the disturbance sources in general can be localized and removed easyly.

In this connection the periodic forces in interrupted cutting processes and especially in face milling by the tooth mesh impacts as well as by the varying number of teeth being in contact with the workpiece are of high importance. Forced vibrations, as they can be observed in face milling, are characterized by the function of the vibration amplitude at the cutting point versus the deapth of cut, which is given in Figure 1.1 a. It can be seen, that until a certain deapth of cut the relationship between vibration amplitude and deapth of cut is almost linear. As it was stated in practical cutting tests, the vibration amplitudes keep almost constant with increasing deapth of cut above this point. In the plant resonances excited by periodic forces in general can be avoided by suitably choosing the cutting conditions. In many cases of milling a slight change of the rotational speed is already successful.

However, in face milling operations it is sometimes difficult to distinguish forced vibrations from self excited vibrations immediately. For self excited vibrations the function vibration amplitude versus deapth of cut, plotted in Figure 1.1 b is characteristic. It can be seen, that the vibration amplitude increases suddenly, when exceeding a certain deapth of cut, the socalled critical deapth of cut. An important characteristic of self excited vibrations is, that they can arise due to a single disturbance and then continue and increase respectively without any other external force acting. The energy being necessary for the vibration, is here produced by the cutting process itself. In the following the term "Chatter" is exclusively reserved for vibrations, which occur due to self-excitation. Many theories have been developed in the last years in order to explain the observed self-excited vibrations by different physical effects.

However, as it was found out by Fishwick Gurney, Tobias [4,6,21] and Tlusty-Polacek [1] , in turning processes the socalled regenerative effect is mainly the cause for chatter. Research work performed by Péters-Vanherck [20] as well as the investigations performed under Contract AF 61 (052)-713 [10] showed, that the regenerative effect is valid in milling operations too.

In a stationary cutting process a static cutting force is acting, which causes a static deformation of the elements in the flux of force. If this static force is superimposed by a dynamic force - for example an initial disturbance due to material inhomogeneity - an additional relative displacement is excited between workpiece and tool, which produces a chip thickness variation and a wavy workpiece surface. The amount of the displacement and thus the deapth of the waves is dependent on the dynamic compliance of the machine. If the tool cuts this wavy surface again, a dynamic cutting force is generated, which acts upon the machine too. This mechanism can be represented

by the block diagram in Figure 1.2. The stability of this closed control loop and there with the chatter behavior depends on the properties of the machine on one hand and on different parameters given by the cutting process on the other hand.

For the stability analysis the milling process was at first replaced by a model similar to that used already for turning processes by Tobias, Tlusty and Péters. Hereby it is assumed, that the chip thickness variation takes place in the middle of the arc of contact and that the cutting forces acting at the cutter teeth can be taken as one resultant force acting in the middle of the arc of contact too. With this assumptions the machine dynamics can be measured as directed response locus, i. e. excitation in the direction of the resultant force and measurement in the direction of the maximum chip thickness variation. The stability analysis on the basis of the directed response locus is relatively easy to carry out, however, the directed response locus is valid for limited cutting conditions only. Another decisive disadvantage is, that the approximation of the milling process by this so-called single-tooth model yields the more incorrect results the greater the arc of contact is.

For this reason the multi-tooth model has been developed [8,9,10,11-14] , whereby the orientation of the chip thickness - and cutting force variation is not taken into account already during the measurement of the response loci, but by additional direction coefficients in the following stability calculation. By this the dynamic measurement can be conducted completely independent from a given machining configuration. Usually the excitation and the measurement are performed in the three directions of a rectangular carthesian coordinate system, of which the axes correlate with the feed directions of the machine. By introducing the direction coefficients now the angular-position of each tooth and the amount and the direction of the cutting forces acting at each tooth can be

considered. Thus the parameters enclosed in the block "cutting process" can be represented by two single blocks"chip thickness coefficient" and "direction coefficient" as shown in Figure 1.3.

Based upon the theory of regenerative chatter in the following at first the system equationswill be formulated and the stability analysis will be explained. Hereby the heavy duty machining of Fe-materials with carbide tools shall mainly be considered.

1.1 Control Loop Representation of the Dynamic Machining Process

As already shown, the relationships being valid in regenerative chatter, can be represented by a closed control loop. The applicability of the stability criteria, well known from the control engineering, depends on the question, in what mathematical form the blocks can be described. Therefore it seems reasonable to discuss at first the different blocks of the control loop.

1.1.1 Discussion of the Blocks of the Control Loop

For the description of the machine tool properties with regard to a chatter investigation it is sufficient to have knowledge about the machine dynamics at the cutting point only. Supposing, that in a dynamic machining operation dynamic forces are acting relatively between workpiece and tool, which can be represented by their components F_x, F_y, F_z in three directions of a cartesian co-ordinate system, the dynamic behavior at the cutting point can be described by nine response loci

$$G_{xx}(i\omega) = \frac{x}{F_x}(i\omega) \qquad G_{xy}(i\omega) = \frac{x}{F_y}(i\omega) \qquad G_{xz}(i\omega) = \frac{x}{F_z}(i\omega)$$

$$G_{yx}(i\omega) = \frac{y}{F_x}(i\omega) \qquad G_{yy}(i\omega) = \frac{y}{F_y}(i\omega) \qquad G_{yz}(i\omega) = \frac{y}{F_z}(i\omega) \qquad (1.1)$$

$$G_{zx}(i\omega) = \frac{z}{F_x}(i\omega) \qquad G_{zy}(i\omega) = \frac{z}{F_y}(i\omega) \qquad G_{zz}(i\omega) = \frac{z}{F_z}(i\omega)$$

where x, y, z are the components of the relative displacement between workpiece and tool.

The response loci are usually measured at the machine itself, because up to this time no sufficiently exact results can be obtained using digital computation methods. For this purpose in most of the cases exciter tests are carried out at the machine standing still, whereby static and dynamic forces are applied between workpiece and tool by means of special exciters. The relative displacements caused by the dynamic forces are related to these forces and plotted in the form of response loci. If an automatic transfer function analyzer in connection with an analog-digital-converter and a tape or card punch is used for this purpose, the data are available for the stability analysis on the digital computer immediately after the dynamic measurement.

Under Contract AF 61 (052)-906 on the basis of the random noise theory a measuring procedure has been developed, by means of which the dynamic measurement can be performed at the running machine and even under actual machining conditions [19] . Good simulation of the machining conditions is possible in many cases - especially where the spindle is the critical structural element - using the contactless electro-magnetic exciter, developed under this contract (see [17]).

From the properties of the machine the data characterizing the cutting process block are completely independent. The function of the so-called direction coefficients can be ex-

plained looking at the schematic drawing of a face milling operation given in Figure 1.4. The relationships derived here for milling operations are also valid for turning operations, however the equations describing the turning process are in general more simple.

Assuming at first a dynamic system with only one degree of freedom in x-direction the relation between a relative displacement x and the cutting force variation F_{ix} at the i-th edge of the cutter, caused by this displacement can be represented by the diagram in Figure 1.5. The cutting force variation can be formulated as

$$F_{ix}(x) = x\,(e^{-i\omega T} - 1)\,k_c \cdot \sin\varkappa \cdot \sin\varphi_i \cdot \cos\lambda \cdot \sin(\varphi_i + \beta) \qquad (1.2)$$

with k_c = chip thickness coefficient
T = rotational time for one tooth pitch

or

$$F_{ix}(x) = k_c \cdot u_x \cdot R_{ixx} \qquad (1.3)$$

with the direction coefficient

$$R_{ixx} = \sin\varkappa \cdot \sin\varphi_i \cdot \cos\lambda \cdot \sin(\varphi_i + \beta) \qquad (1.4)$$

Hereby the influence of the inclination angle λ shall be neglected, because this angle is practically only small.

In the general case of a system with three degrees of freedom the total chip thickness variation u_i at one edge results from three parts $u_i(x)$, $u_i(y)$, $u_i(z)$. These parts are caused by relative movements in x-, y-, and z-direction, which are produced by the components F_{ix}, F_{iy}, F_{iz} of a dynamic cutting force. The relationships between the force components and the components of the chip thickness variation can be derived in analogue manner as the equations (1.2), (1.3), (1.4). Thus the direction coefficient are obtained:

$$R_{ixx} = \frac{F_{ix}}{k_c \cdot u_x} = \sin\varphi_i \cdot \sin(\varphi_i + \beta) \cdot \cos\alpha \cdot \sin\varkappa$$

$$R_{ixy} = \frac{F_{ix}}{k_c \cdot u_y} = \cos\varphi_i \cdot \sin(\varphi_i + \beta) \cdot \cos\alpha \cdot \sin\varkappa$$

$$R_{ixz} = \frac{F_{ix}}{k_c \cdot u_z} = \sin(\varphi_i + \beta) \cdot \cos\alpha \cdot \cos\varkappa$$

$$R_{iyx} = \frac{F_{iy}}{k_c \cdot u_x} = \sin\varphi_i \cdot \cos(\varphi_i + \beta) \cdot \cos\alpha \cdot \sin\varkappa$$

$$R_{iyy} = \frac{F_{iy}}{k_c \cdot u_y} = \cos\varphi_i \cdot \cos(\varphi_i + \beta) \cdot \cos\alpha \cdot \sin\varkappa \qquad (1.5)$$

$$R_{iyz} = \frac{F_{iy}}{k_c \cdot u_z} = \cos(\varphi_i + \beta) \cdot \cos\alpha \cdot \cos\varkappa$$

$$R_{izx} = \frac{F_{iz}}{k_c \cdot u_x} = \sin\varphi_i \cdot \sin\alpha \cdot \sin\varkappa$$

$$R_{izy} = \frac{F_{iz}}{k_c \cdot u_y} = \cos\varphi_i \cdot \sin\alpha \cdot \sin\varkappa$$

$$R_{izz} = \frac{F_{iz}}{k_c \cdot u_z} = \sin\alpha \cdot \cos\varkappa$$

It can be seen, that the direction coefficients depend on the cutting force direction, given by the angles α and β, on the side cutting edge angle $\varkappa$ and on the angular position φ_i of the tooth. As the angle φ_i varies continuously against the arc of contact, the direction coefficients are periodic time-variant functions, as shown in Figure 1.6. In milling operations several teeth are normally in contact with the workpiece; thus the direction coefficients actually are the sum of the values being valid for all teeth:

$$R_{jk} = \sum_{i=1}^{z_c} R_{ijk} \qquad (1.6)$$

Form (1,5) and (1,6) yields the equation system for the resultant forces

$$F_x = k_c \, (R_{xx} u_x + R_{xy} u_y + R_{xz} u_z)$$

$$F_y = k_c \, (R_{yx} u_x + R_{yy} u_y + R_{yz} u_z) \qquad (1.7)$$

$$F_z = k_c \, (R_{zx} u_x + R_{zy} u_y + R_{zz} u_z)$$

If one considers, that a chip thickness variation can actually occur at those teeth only, which are instantaneously in contact with the workpiece, the direction coefficients are only existing in the range between the entrance angle φ_E and the exit angle φ_A that means the validity of the equations (1.5) is limited following the condition

$$\begin{aligned} R_{ixx} \cdots R_{izz} &\neq 0 \quad \text{for} \quad \varphi_E \leq \varphi_i \leq \varphi_A \\ R_{ixx} \cdots R_{izz} &= 0 \quad \text{for} \quad \varphi_A \leq \varphi_i \leq \varphi_E \end{aligned} \qquad (1.8)$$

Because of the Limitation (1.8) the functions of the direction coefficients are discontinuous at the angles of tooth entrance and tooth exit. An example for these discontinuous functions, calculated for a given milling process, is shown in Figure. 1.7.

If the stability analysis shall be performed applying one of the stability criteria well known from the control engineering technique, it is very time-consuming and there with not economical to take into account the time-dependence of the direction coefficients. Therefore extensive fundamental investigations have been carried out [11,12,13] , in order to determine the conditions, under which the timevariant coefficients can be replaced by their timeaveraged values. The result is, that this approximation is justified from the practical point of view for all machining operations, where the borderline of stability is low, that means especially for those cases being practically critical and interesting. With regard to the stability analysis

to be performed quickly and economically, in the following only the time-averaged values $R_{xxm} \ldots R_{zzm}$ of the direction coefficients shall be considered. These values can easyly be calculated by integration of the direction functions between the limits entrance angle and exit angle.

$$R_{xxm} = \frac{z}{8\pi} \cdot \cos\alpha \cdot \sin\varkappa \{ -\sin\beta (\cos 2\varphi_A - \cos 2\varphi_E) + \cos\beta [2(\hat{\varphi}_A - \hat{\varphi}_E) - (\sin 2\varphi_A - \sin 2\varphi_E)]\}$$

$$R_{xym} = \frac{z}{8\pi} \cdot \cos\alpha \cdot \sin\varkappa \{ -\cos\beta (\cos 2\varphi_A - \cos 2\varphi_E) + \sin\beta [2(\hat{\varphi}_A - \hat{\varphi}_E) + (\sin 2\varphi_A - \sin 2\varphi_E)]\}$$

$$R_{xzm} = \frac{z}{2\pi} \cdot \cos\alpha \cdot \cos\varkappa [-\cos\beta (\cos\varphi_A - \cos\varphi_E) + \sin\beta (\sin\varphi_A - \sin\varphi_E)]$$

$$R_{yxm} = \frac{z}{8\pi} \cdot \cos\alpha \cdot \sin\varkappa \{ -\cos\beta (\cos 2\varphi_A - \cos 2\varphi_E) - \sin\beta [2(\hat{\varphi}_A - \varphi_E) \cdot\cdot (\sin 2\varphi_A - \sin 2\varphi_E)]\} \qquad (1.9)$$

$$R_{yym} = \frac{z}{8\pi} \cdot \cos\alpha \cdot \sin\varkappa \{ \sin\beta (\cos 2\varphi_A - \cos 2\varphi_E) + \cos\beta [2(\hat{\varphi}_A - \hat{\varphi}_E) + (\sin 2\varphi_A - \sin 2\varphi_E)]\}$$

$$R_{yzm} = \frac{z}{2\pi} \cdot \cos\alpha \cdot \cos\varkappa [\sin\beta (\cos\varphi_A - \cos\varphi_E) + \cos\beta (\sin\varphi_A - \sin\varphi_E)]$$

$$R_{zxm} = \frac{z}{2\pi} \cdot \sin\alpha \cdot \sin\varkappa [-(\cos\varphi_A - \cos\varphi_E)]$$

$$R_{zym} = \frac{z}{2\pi} \cdot \sin\alpha \cdot \sin\varkappa (\sin\varphi_A - \sin\varphi_E)$$

$$R_{zzm} = \frac{z}{2\pi} \cdot \cos\varkappa \cdot \sin\alpha (\hat{\varphi}_A - \hat{\varphi}_E)$$

On principle the same relationships can be derived for the turning process as for the milling process, if the components of the cutting force variation and of the chip thickness variation are defined as shown in Figure 1.8. However, different simplifications concerning the direction coefficients can be observed

for the turning process. The most important difference is, that they are now constant values, because the angle φ is constant. Supposing

$$\varphi = 90^{\circ}$$

which can always be satisfied by the reasonable definition of the co-ordinate axes, R_{xy}, R_{yy}, R_{zy} are zero and equations (1,5) became

$$\begin{aligned} R_{xx} &= \cos\beta \cdot \cos\alpha \cdot \sin\varkappa \\ &\text{---} \\ R_{xz} &= \cos\beta \cdot \cos\alpha \cdot \cos\varkappa \\ R_{yx} &= -\sin\beta \cdot \cos\alpha \cdot \sin\varkappa \\ &\text{---} \\ R_{yz} &= -\sin\beta \cdot \cos\alpha \cdot \cos\varkappa \\ R_{zx} &= \sin\alpha \cdot \sin\varkappa \\ &\text{---} \\ R_{zz} &= \sin\alpha \cdot \cos\varkappa \end{aligned} \qquad (1.5a)$$

For the orthogonal turning process, given in Figure 1.9, where

$$\begin{aligned} \alpha &= 0^{\circ} \\ \varkappa &= 90^{\circ} \end{aligned}$$

only

$$\begin{aligned} R_{xx} &= \cos\beta \\ R_{yx} &= -\sin\beta \end{aligned} \qquad (1.5b)$$

have to be taken into account in the chatter investigation.

As already mentioned the transfer behavior of the cutting process is described by the so-called chip thickness coefficient k_c, which represents the relationship between a chip thickness variation and the corresponding dynamic cutting force. Various efforts to determine this coefficient theoretically taking into account tool geometry, cutting speed, feed rate, properties of tool and workpiece material did not succeed until now. However, the experimental determination of the k_c-values is extremely difficult too, whereby the greatest problem is

to simulate as well as possible the socalled "wave on wave cutting" which is existing in a chattering machining process. Therefore the initial dynamic cutting force measurements under this contract have been conducted for wave cutting and wave removing only, which are in general simplifications of the actually existing conditions [12,13] . Under Contract AF 61(052)-966 [19] a test rig to be used on a lathe was developed, by means of which also wave on wave cutting tests could be performed. The most important result of the first measurements was, that the phase angle between the two wavy surface contours is of high influence upon the picked up values. Because of this fact the test rig had to be altered in such a manner, that the phase angle could be varied easyly and kept constant for each cutting test respectively. These alterations required such a time delay, that no reliable and valid results could be obtained until now.

The applicability of the random noise theory in dynamic cutting tests proved also impossible until now due to the effect of the phase angle [19] .

However, from the cutting tests carried out up to this time [12,13,19,9] some important results could be obtained. The most interesting fact is, that the generally used equation

$$k_c = \frac{F}{u} \tag{1.10}$$

where the cutting force variation is regarded as directly proportional to the chip thickness variation, is an approximation, which is permissible under certain conditions only. This equation is mainly valid for relatively low chatter frequencies. For higher frequencies it must be considered, that k_c is dependent on the frequency with respect to amplitude and phase angle. Thus follows

$$k_c(i\omega) = \frac{F}{u}(i\omega) = \left|\frac{F}{u}\right|(\omega) \cdot e^{i\Psi(\omega)} \tag{1.11}$$

Equation (1.11) related to the width of cut w yields

$$k_{cw}(i\omega) = \frac{k_c}{w}(i\omega) = \frac{F}{w \cdot u}(i\omega) \qquad (1.12)$$

Herein the related chip thickness coefficient $k_{cw}(i\omega)$ represents a special property of material, characteristic for the chosen cutting conditions. As already pointed out, the investigations performed in this program, are primaryly directed at the heavy duty machining of the usual Fe-materials with cutting speeds in the range of about 70 ... 200 m/min. Due to this the so-called low speed stability, which is preferably interesting in the machining of high strength and hard materials [9], can be let out of consideration. Over the cited speed range the chip thickness coefficient is therefore taken as independent from the cutting speed.

The chip thickness coefficients determined in an orthogonal plunge turning test, can be applied to face milling according to Figure 1.8. From several results of dynamic cutting tests it can be seen, that the spatial components of the cutting force - especially at higher frequencies - have distinguished phase shifting to the chip thickness variation, thim means, that the direction of the resultant dynamic cutting force is time-variant in space. With

F_H = main cutting force and

F_A = thrust force consisting of a radial and an axial component,

the transfer behavior of the cutting process can be described by the equations

$$k_{cH}(i\omega) = \frac{F_H}{u}(i\omega) = \left|\frac{F_H}{u}\right|(\omega) \cdot e^{i\,\varphi_H(\omega)}$$

$$k_{cA}(i\omega) = \frac{F_A}{u}(i\omega) = \left|\frac{F_A}{u}\right|(\omega) \cdot e^{i\,\varphi_A(\omega)} \qquad (1.13)$$

and related to the width of cut

$$k_{cwH}(i\omega) = \frac{k_{cH}}{w}(i\omega) = \frac{F_H}{w \cdot u}(i\omega) \qquad (1.14)$$

$$k_{cwA}(i\omega) = \frac{k_{cA}}{w}(i\omega) = \frac{F_A}{w \cdot u}(i\omega) \qquad (1.14)$$

According to the equations (1,13) and (1.14) in Figure 1,10 the transfer behavior of the cutting process is represented by each two blocks - phasefree blocks $w \cdot k_{cwH}(\omega)$, $w \cdot k_{cwA}(\omega)$ and phase shifting blocks

$$e^{i\Psi_H(\omega)} = (\cos\Psi_H(\omega) + i\sin\Psi_H(\omega))$$

$$e^{i\Psi_A(\omega)} = (\cos\Psi_A(\omega) + i\sin\Psi_A(\omega))$$

for the two components F_H and F_A. Projecting these components into the direction of the resultant cutting force by the angular functions

$$R_H(\omega) = \sin\beta(\omega) \cdot \cos\alpha(\omega) \qquad (1.15)$$

$$R_A(\omega) = \sin\alpha \cdot \cos\beta(\omega) \cdot \cos\alpha(\omega) \qquad (1.16)$$

which can be derived from Figure 1,9, and summation yield the cutting force $F(i\omega)$, which reacts upon the vibration system of the machine. As it can be seen on Figure 1,10, in an actual cutting process the width of cut w is the gain factor, by which the amount of the dynamic cutting force and therewith the stability is directly influenced. The definitions of w in turning and milling is given by, Figure 1,11.

If the direction of the dynamic cutting force is timevariant, the ratio of the measured cutting force components and therewith the angle β and all values connected with β are also timevariant. Taking into account this time variant behavior in the stability analysis would make the calculation difficult and very time consumptive. With regard to an economical performance of the chatter investigation it shall therefore be assumed in the following, that the cutting force direction may be dependent from the frequency but time invariant for each discrete frequency. This assumption may cause slightly incorrect results; however, as demonstrated in the chapters 1,3,1 and 1,3,2, the ob-

tained results are satisfactorily exact for the practical use. The chip thickness coefficients used in the following calculations, show by far time-invariant cutting force directions within the interesting frequency range [12,13,9] . Here the maximum phase angles between the force components come up to about 10^{0}. This result correlates quite well to the results of dynamic cutting tests conducted by Polacek, of which some data were discussed at the C.I.R.P.-Meeting of Working Group "Ma" on 1 February 1969 in Paris (France). Figure 1,12 shows a schematical drawing of an orthogonal plunge turning process. Due to the chip thickness u(i ω) the static cutting force F_o is superimposed by a dynamic cutting force F(t), of which the direction must not correlate to the direction of F_o. In the given example the ratio of the force components shall be $F_H/F_A = 2$. In the case $\psi_A - \psi_H = 0^{0}$, that means no phase shifting between the components, the direction of the cutting force and thus the angle β are constant. It follows

$$\beta = arc\,tg\ \frac{F_H}{F_A} \tag{1,17}$$

Is there any phase difference of for instance $\psi_A - \psi_H = 10^{0}$ (interrupted curve of F_H), the end of the dynamic cutting force vector follows an elliptical curve. However, as it can be seen from the drawing, for a small phase difference the deviation of the cutting force direction from the time invariant direction is only small, when the cutting force vector itself is great. This means, that in the cases of small phase differences equ. (1,17) is valid with good approximation. For tools with $\varkappa \leq 90^{0}$ one obtaines according to Figure 1.9

$$\beta = arc\,tg\ \frac{F_H}{F_A \cdot \sin\varkappa} \tag{1,18}$$

$$\alpha = arc\,tg\ \frac{\cos\beta}{tg\,\varkappa} \tag{1,19}$$

1.1.2 Block Diagrams of Closed Control Loops for Systems with One and Several Degrees of Freedom

In connection with the derivation of the direction coefficients the relationship between a relative displacement at the cutting point and the corresponding cutting force was detailed. In machining processes this force reacts upon the machine structure, so that the process can be represented by the closed control loop in Figure 1.13, if a vibration system with one degree of freedom and real behavior of the cutting process are supposed. Hereby the transfer behavior of the cutting process is represented by the material characteristic value k_{cw} and the gain factor, the deapth of cut w. Assuming real behavior of the cutting process, equ. (1.19) yields

$$k_c = w \cdot k_{cw} \tag{1.20}$$

For a system with three degrees of freedom the block-diagram in Figure 1.14 is obtained. Here the total chip thickness variation u_i at the i-th tooth results from the components $u_i(x)$, $u_i(y)$, $u_i(z)$, which are caused by the displacements x, y, z. By $(w \cdot k_{cw})$ the chip thickness variation u_i produces a cutting force variation F_i. The components F_{ix}, F_{iy}, F_{iz} of F_i act upon the machine structure again. By reasonably combining the blocks of the control loop and considering (1.6) the diagram in Figure 1.15 is obtained.

With

$$A_o = R_{xx} \cdot G_{xx} + R_{yx} \cdot G_{xy} + \cdots + R_{zz} \cdot G_{zz} \tag{1.21}$$

and

$$K_o = \frac{1}{w \cdot k_{cw}(e^{-i\omega T} - 1)} \tag{1.22}$$

the very simple control loop in Figure 1.16 results.
Here the index O indicates, that the additional phase shifting due to the complex behavior of the cutting process is not yet taken into account. The influence of this complex behavior is detailed in chapter 1.2.3.

1.2 Stability Analysis by Means of the Nyquist-Criterion

As it was found out, the dynamic machining process can always - even for systems with several degrees of freedom - be reduced to a nonintermeshed closed control loop. This fact is very interesting and of high importance for the stability analysis. As the transfer behavior of the machine and the cutting process is available in the form of experimentally measured response loci only, the stability analysis is suitably performed applying the well-known Nyquist-Criterion. By means of this criterion the stability of the closed loop is analyzed on the basis of the response locus $F_o(i\omega)$ of the open loop, given in Figure 1.17.

1.2.1 Control Loop Equation

With z_e = input
z_a = output

the equation of the open loop response locus is obtained

$$F_o(i\omega) = \frac{z_a}{z_e} = A_o \cdot \frac{1}{K_o} \qquad (1.23)$$

For the chatter analysis the total response locus must not be known, because it is only important to determine those conditions, where the border of stability is reached. At the stability border the output z_a is identical to the input z_e concerning phase and amplitude:

$$\frac{z_a}{z_e} = 1 \qquad (1.24)$$

Thus the crosspoint of the response locus F_o with the real axis is the point (+ 1,0), the so-called critical point. As to the chatter this means, that vibrations once excited dont neither increase nor decrease. With a crosspoint below (+ 1) the system is absolutly stable, a crosspoint above (1,0) means instability of the system. Equ. (1.23) and (1.24) yield the condition for the

border of stability:

$$A_o - K_o = 0 \qquad (1.25)$$

1.2.2 Determination of the Stability Borderline

By means of this equation for each frequency the value K_o can be calculated, for which the control loop reaches the stability border. The value K_o includes the chip thickness coefficient, on which the deapth of cut is immediately dependent (1.22 and 1.20), as well as the delay time T, which is used for determining the corresponding rotational speeds of the workpiece (in turning) and of the cutter (in milling):

$$T = \frac{T}{Z} \qquad (1.26)$$

where T = time for one revolution of the workpiece (turning) and the cutter respectively (milling)

Z = total number of teeth on the cutter

The values A_o and K_o are complex magnitudes, which can be written as

$$A_o = (A_{or} + i\, A_{oi}) \qquad (1.27)$$

$$K_o = (K_{or} + i\, K_{oi}) \qquad (1.28)$$

with $A_{or} = Re\{A_o\}$ $\quad A_{oi} = Jm\{A_o\}$

$K_{or} = Re\{K_o\}$ $\quad K_{oi} = Jm\{K_o\}$

Equ. (1.28) compared to (1.22) yields

$$(K_{or} + i\, K_{oi}) = \frac{1}{w \cdot k_{cw} \cdot (e^{-i\omega T} - 1)} \qquad (1.29)$$

and with

$$e^{-i\omega T} = \cos \omega T - i \sin \omega T$$

$$(K_{or} + i\,K_{oi}) = \frac{1}{w \cdot k_{cw}} \cdot \frac{1}{(\cos \omega\tau - 1 - i \sin \omega\tau)} \qquad (1.30)$$

By this equation $(w \cdot k_{ow})$ and τ can be determined for a given frequency ω . For this purpose equ. (1.30) is expanded and arranged to

$$\frac{K_{or} - i\,K_{oi}}{(K_{or}^2 + K_{oi}^2)} = w \cdot k_{cw} (\cos \omega\tau - 1 - i \sin \omega\tau)$$

From this equation the real- and imaginary parts of K_o are obtained:

$$K_{or} = w \cdot k_{cw} (K_{or}^2 + K_{oi}^2) (\cos \omega\tau - 1)$$
$$K_{oi} = w \cdot k_{cw} (K_{or}^2 + K_{oi}^2) (\sin \omega\tau)$$

$(w \cdot k_{cw})$ assumed to be real, as mentioned above, yields by division

$$\frac{K_{oi}}{K_{or}} = \frac{\sin \omega\tau}{\cos \omega\tau - 1} \qquad (1.31)$$

and with

$$\operatorname{ctg} \frac{\omega\tau}{2} = \frac{\sin \omega\tau}{1 - \cos \omega\tau}$$

and considering (1.23)

$$\omega\tau = 2 \operatorname{arc\,ctg} \left(-\frac{A_{oi}}{A_{or}}\right) \qquad (1.32)$$

This equation describes an inverse trigonometric function, of which the main values are limited by

$$0 \leq \omega\tau_o \leq 2\pi$$

Considering the ambiguity of equ. (1.32) the general solution can be formulated as

$$\omega\tau = \omega\tau_o + 2\pi m$$
$$(m = 0, 1, 2, 3 \cdots)$$

or

$$\tau = \tau_o + \frac{2\pi m}{\omega} \qquad (1.33)$$

With $n = \frac{60}{T \cdot z}$

the well known relation

$$n = \frac{60\,\omega}{z \cdot (\omega \cdot \tau_o + 2\pi m)} \tag{1.34}$$

is obtained, by means of which the rotational speed corresponding to the frequencies in the response locus can be calculated.

Corresponding to the pair of values τ and $(w \cdot k_{ow})$ which satisfies equ. (1.22), the value $(w \cdot k_{ow})$ can be determined.
Equ. (1.22) expanded by K_{or} yields after some arranging

$$\frac{1}{w \cdot k_{cw} \cdot K_{or}} = (1 + i\,\frac{K_{oi}}{K_{or}})(\cos\omega\tau - 1 - i \sin\omega\tau)$$

and with (1.31) after suitable expanding and arranging the relation

$$w \cdot k_{cw} = -\frac{1}{2\,K_{or}} \tag{1.35}$$

is obtained. As detailed above, the system can only became unstable, if the response locus of the open loop crosses the real axis at a point $> (+1)$. Considering (1.35) it follows from this fact, that K_{or} must be negative, because only a positive chip thickness coefficient and a positive deapth of cut respectively have a practically reasonable meaning. Otherwise the system is stable.

With (1.27) and (1.28) equ. (1.25) becomes

$$(A_{or} + i\,A_{oi}) - (K_{or} + i \cdot K_{oi}) = 0 \tag{1.36}$$

This means

$$A_{or} - K_{or} = 0 \tag{1.36a}$$
$$A_{oi} - K_{oi} = 0 \tag{1.36b}$$

Considering (1.21) it follows from (1.36a)

$$K_{or} = Re\{R_{xx} \cdot G_{xx} + \cdots + R_{zz} \cdot G_{zz}\} \tag{1.37}$$

and with (1.35)

$$w = -\frac{1}{2\,k_{cw}\cdot Re\,\{R_{xx}\cdot G_{xx}+\cdots+R_{zz}\cdot G_{zz}\}} \qquad (1.38)$$

the relation for the calculation of the actual critical deapth of cut results. As it can be seen, therewith the stability analysis of machining operations can in every case be reduced to an equation, which is easily to be solved by hand.

1.2.3 Complex Transfer Function of the Cutting Process

As detailed in chapter 1.1.2, with regard to easy performance of the stability analysis the direction of the cutting force in space is assumed to be time-invariant, that means

$$\Psi_H(\omega) = \Psi_A(\omega) = \Psi(\omega)$$

Thus the complex transfer behavior of the cutting process can be represented by the block diagram in Figure 1.18 a. From the diagram the relationship between the chip thickness variation u and the cutting force variation F can directly be derived:

$$\frac{F}{u}(i\omega) = w\left|k_{cwH}\right|(\omega)\cdot\left[R_H(\omega)+\left|\frac{k_{cwA}}{k_{cwH}}\right|(\omega)\cdot R_A(\omega)\right]\cdot\left(\cos\Psi(\omega)+i\sin\Psi(\omega)\right) \qquad (1.39)$$

With

$$R = \left[R_H(\omega)+\left|\frac{k_{cwA}}{k_{cwH}}\right|(\omega)\cdot R_A(\omega)\right]$$

the diagram is simplified to the one on Figure 1.18 b. As it can be seen here, the transfer function of the cutting process includes proportional factors $w\cdot|k_{cwH}|(\omega)$, $R(\omega)$ and a phase shifting block $(\cos\Psi(\omega)+i\sin\Psi(\omega))$. Considering this behavior in the block diagram of the machining operation yields Figure 1.19 a. If the phase shifting block is combined to the block A_o - as shown in Figure 1.19 b - it follows

$$A(i\omega) = A_0(i\omega) \cdot (\cos\varphi(\omega) + i\sin\varphi(\omega)) \qquad (1.40)$$

This equation can be interpreted in such a way, that each vector of the machine response loci rotates against the coordinate system by that phase angle φ_i , which is valid at the concerned frequency ω_i. In the machine response loci $G(i\omega)$ the angle $(-\varphi_i)$ means a phase lag of the displacement against the force. Now an angle $(-\varphi_i)$ increases this phase lag, as shown in Fig. 1.20. The other blocks of the loop can be written in shorthand notation, analogly to (1.22)

$$\frac{1}{K} = R \cdot w \cdot k_{cwH} \cdot (e^{-i\omega\tau} - 1) \qquad (1.41)$$

so that the control loop in Figure 1.19 c results.

The stability analysis is now carried out in the same manner as shown above for the case of a real chip thickness coefficient. With the control loop equation

$$A - K = 0 \qquad (1.42)$$

the equation for calculating the critical deapth of cut is obtained:

$$w = -\frac{1}{2 \cdot R \cdot k_{cwH} \cdot Re\{R_{xx} \cdot G_{xx} + \cdots + R_{zz} G_{zz}\}} \qquad (1.43)$$

The rotational speeds of the workpiece and the cutter respectively can be determined by means of equ. (1.34) again.

1.3 Practical Chatter Investigations

By the above described relationships it is now possible to perform the theoretical stability analysis, if the characteristic values and the transfer behaviour of the cutting process and the machine are known. As already mentioned, the cutting process data are only dependent on the cutting

conditions; thus they can be determined in separate cutting force measurements and are then available for further stability investigations. Against that the machine response loci are characteristic data, which are in general specific for each machine. Because of this the response loci must be picked up at each machine to be investigated with regard to machining stability.

During the time covered by this contract, 17 lathes of different types and manufacturers and altogether 9 milling machines - of which two medium sized vertical milling machines, four single column boring and milling machines and three large portal milling machines - have extensively been investigated. The most important results of these investigations have been published in the Quarterly Technical Reports under this contract (see [11 - 18]). The general purpose of these machine investigations was to verify the validity of the theoretical research work by means of experimental machining tests on the one hand and on the other hand to find out, how the chatter analysis can be performed under consideration of the different machining problems existing in practice. Some representative investigations and results shall be detailed in the following.

At first it will be shown, how the stability borderline can easely be determined by hand especially for turning processes. Hereby the performance of the calculation can considerably be simplified by means of graphical illustrations. For extensive and complete chatter investigations in general the following parameters have to be taken into account:

a) concerning the machine:

working range
range of rotational speed
installed power
maximum torsional moment

b) concerning the machining process:

workpiece material - tool material
milling breadth
diameter of the cutter
number of teeth on the tool
tool geometry
configuration workpiece - tool

Considering these numerous parameters the chatter investigation cannot be performed with economic calculation effort without using electronical computers. Therefore with regard to the rational calculation of stability charts digital computer programmes have been developed, the application of which is demonstrated by an example of chatter investigations on a vertical milling machine.

1.3.1 Chatter Investigations on a Lathe

These chatter investigations, which included the dynamic measurements, the calculation of the critical width of cut as well as for comparison experimental cutting tests, have been conducted at a medium-sized lathe (30 kW). The calculations shall be limited to the orthogonal plunge cut, because hereby very easily understandable geometrical conditions are existing.

1.3.1.1 Dynamic Behaviour of the Investigated Lathe

For the dynamic investigation of the machine the contactless electro-magnetic exciter was applied, which has been developed under this contract (see [17]). The required response loci, picked up for a rotational speed of the spindle of $n = 140\ min^{-1}$, are plotted in Figure 1.21. It can be stated, that the machine has two main vibration modes: a bending mode of the spindle at 116 and a rocking mode of the tool head at 170 cps.

for the stability analysis it is of high importance, that the compliance in the bending mode at 116 cps with the rotating spindle overcomes the value for the stand still spindle by about 100 %. The mode at 170 cps is naturally not influenced by the spindle rotation.

1.3.1.2 Determination of the Critical Width of Cut

When manually performing the stability analysis, the calculation effort is considerably dependent on the transfer behaviour of the cutting process. If there is a frequency-dependent phase shift existing between the chip thickness - and the cutting force variation, then each vector in the response loci has to be turned by the corresponding angle ψ. As shown in Figure 1.20 a negative angle ψ means a phaseing of the cutting force - against the chip thickness variation, i.e. the compliance vectors have to be turned clockwise against the coordinate system.

This procedure on principle being simple but in practice being relatively time consumptive, can considerably be simplified if the phase shift is constant within the interesting frequency range. In such cases the phase angle is identical for all vectors of the response loci, so that only the coordinate system must be turned - counter clockwise for $\psi < 0^{\circ}$. The chip thickness coefficient used in the following example, has only negligible phase shift in the interesting frequency range. It was determined in [13] .

$$k_{cw} = 3{,}0 \cdot 10^{4} \text{ kp/cm}^2$$
$$\beta = 67^{\circ}$$

Thus equ. (1.38) can be used for the determination of the critical width of cut. As already mentioned, chatter can only occur, if $\mathrm{Re}\left\{ R_{xx} \cdot G_{xx} + R_{yx} \cdot G_{xy} \right\} (i\omega) < 0$ at one or more frequencies.

If this is not satisfied, the system will be stable for whatever high widths of cut. The above summation is reasonably be performed graphically. Figure 1.22 shows the run of the functions $Re\{R_{xx} \cdot G_{xx}\}$ and $Re\{R_{yx} \cdot G_{xy}\}$ as well as the resultant curve versus the frequency. The resultant curve shows three minima with negative sign, the absolutely greatest of which with (-0,2) $\mu m/kp$ occurs at 123 cps. For this the minimum critical width of cut is calculated:

$$w = 8,4 \text{ mm}$$

For the two other minima at 150 cps and 200 cps widths of cut of 21mm and 24 mm respectively are obtained, which however are not interesting from the practical point of view. The borderlines of stability are plotted in Figure 1.23. As it can be seen, the theoretical value of 8,4 mm is quite well verified by the additionally plotted experimental results:

If the stability calculation would be performed using the equations (1.38) and (1.34), the theoretical stability chart would show the characteristical unstable lobes, the so called "chatter lobes." The minimum of these lobes is identical to the above calculated critical width of cut of 8,4 mm. However in turning operations these lobes overlap so far in general, that the rotational speeds, where the minimum width of cut is reached lie very closely to one another in the usual range of rotational speed. Thus in practice the width of cut to be reached is equal to the minimum critical width of cut. For this reason the calculation of the - theoretically - critical rotational speeds can be given up in general for turning operations.

1.3.2 Chatter Investigations on a Milling Machine Using the Digital Computer

1.3.2.1 Dynamic Behaviour of the Investigated Milling Machine

The investigations were carried out on a medium-sized vertical

milling machine (11kW). The determination of the response loci required for the stability analysis, was performed by conventional exciter tests at the standing still machine. In Figure 1.24 the response loci for the following working position are plotted:

quill: out
spindle: above the table centre
cutter: 70 mm above the table

As it can be seen in the figure the machine shows mainly four vibration modes in the tested frequency range, namely at 57 cps, 63 cps, 65 cps and 138 cps. These are illustrated in Figure 1.25. The vibration modes excited in y-direction at 65 cps and 138 cps are also excited by F_z at the same frequencies. As it was stated, the vibration modes depend considerably on the position of the travelling machine elements concerning the compliance and the natural frequency. By the position of the table and the cross slide respectively in the xy-plane expecially the vibration modes at 57 cps and 65 cps are influenced. As shown in the following, preferably these modes are decisive for the chatter behaviour. The variation of the machine dynamics due to the position of the elements has extensively been discussed in [17].

1.3.2.2 Development and Application of the Computer Programmes RATTER 1 and RATTER 2

Corresponding to the theoretical derivations in chapter 1.2 the calculation of a stability chart includes the following steps:

1. Calculation of the cutting force angles $\alpha(i\omega)$ and $\beta(i\omega)$;
2. Calculation of time-invariant direction coefficients $R_{xx} \ldots R_{zz}$ and of the coefficients R_{II}, R_A;
3. Calculation of the products $R_{xx} \cdot G_{xx}(i\omega) \ldots R_{zz} \cdot G_{zz}(i\omega)$ and summation at each frequency; the results can be plotted as the response locus $A_o(i\omega)$;

4. Multiplication of Λ_0 $(i\omega)$ by the phase shifting block Ψ $(i\omega)$; this yields the response locus Λ $(i\omega)$;
5. Calculation of the chip thickness coefficient k_{dif} and of the critical deapth of cut at all frequencies, where Λ $(i\omega)$ has a negative real part;
6. Calculation of the rotational speeds of the cutter within an interesting range of the cutting speed;
7. Plot the stability chart and / or store the results.

By means of the computer program RATTER 1, the flow chart of which is given in Figure 1.26, the above listed steps can be carried out. In the given form by this program one complete stability chart for the parameters in the hand of the program is obtained by each calculation run. The investigations detailed here, were directed to the

left end position
middle position
right end position

of the table for constant positions of the quill and the knee. In these three positions stability charts have been calculated for the four milling configurations shown in Figure 1.27. As it can be seen, these four configurations represent four different possibilities to perform one given milling operation at the workpiece.

In Figure 1.28 the stability charts for the four configurations in the three table positions are plotted. Comparing the stability charts it can be stated, that considerable differences in the critical deapth of cut occur on the one hand for different configurations in one table position and on the other hand also for the same configuration in different table positions. The last comparison is practically interesting, when the given machining operation requires a long travel of the table. Here the minimum stability is then decisive for the maximally

possible deapth of cut. For instance with an entrance angle of 160° a chatterfree deapth of cut of only 1,6 mm can be reached, although 0,6 mm chatterfree deapth of cut is possible in the left end position. For all table positions the most favourable configuration is given for an entrance angle of 95°, because chatter must be exspected here not below 0,6 mm. In the theoretical calculations a chip thickness coefficient determined in [13] was used:

$$k_{cw} = 3,8 \cdot 10^4 \quad kp/cm^2$$
$$\beta = 67°$$
$$\alpha = 24°$$

This coefficient shows only real behaviour over the interesting frequency range.

For the verification of the theoretical results in some cases exporimental chatter testshave been carried out, the results of which are additionally plotted in the stability chart. It can be stated, that the correlation between the theoretical and experimental results is good as to the deapth of cut and as to the rotational speeds and the chatter frequencies respectively.

In order to make obvious, in how far the installed power of the machine is actually turned to profit and therewith to get a criterion for the economy of machining, it is reasonable to plot the limitation of the deapth of cut due to the installed power and due to the maximum torsional moment additionally in the stability charts. The deapth of cut limited by the installed power can be calculated for a given feed rate per tooth by the equation

$$w\,[mm] = \frac{N_e[kW] \cdot \varepsilon \cdot \sin\kappa \cdot 6,12 \cdot 10^6}{z_c \cdot h_m^{1-x}\,(mm)\; k_{s1,1}\,[\frac{kp}{mm^2}] \cdot \pi \cdot D\,(mm) \cdot n\,(min^{-1})} \qquad (1.44)$$

where N_o = installed power

η = total efficiency

$k_{s\,1.1}$ = specific cutting force

h_m = averaged chip thickness

$h_m = \frac{360^0}{\pi} \frac{B \cdot s_z \cdot \sin\varkappa}{D \cdot (\varphi_A - \varphi_E)}$

$1 - z$ = cutting forceexponent

z_c = number of teeth being in contact

$z_c = \frac{z \cdot (\varphi_A - \varphi_E)^0}{360^0}$

From tabulas

$(1 - z) = 0,88$

$k_{s\,1.1} = 185\ kp/mm^2$

are taken.

The officiendy η was determined in the tests:

$\eta = 0,55$

In the range of low spindle speeds the limitation is not given by the power but by the maximally admissible torsional moment. Assuming that the tangential force on the cutter is quite independent on the cutting speed, the deapth of cut limitation due to the torsional moment can be calculated by

$$w\,[mm] = \frac{Md\,[mkp] \cdot 1000 \cdot \eta \cdot \sin\varkappa}{z_c \cdot h_m^{1-z}\,[mm] \cdot k_{s\,1.1}\,[kp/mm^2] \cdot q\,[mm]} \qquad (1.45)$$

The calculation of these limitations can also be performed by the computer program RATTER 1 as shown in the flow chart. By means of the formulas

$$w \sim \frac{Ne}{s_z \cdot n} \qquad (1.46)$$

and

$$w \sim \frac{Md}{s_z} \qquad (1.47)$$

the power - and the moment limitation can easily be determined for whatever feed rates.

As already mentioned the program RATTER 1 is able to produce one stability chart for a given parameter combination by each run. If more than one combination are interesting, the program can easily be completed, so that the corresponding parameters can be varied automatically. The results of such an extensive stability analysis in certain circumstances is a great number of stability charts, which characterize the chatter behaviour of the machine under the interesting conditions. For the organization of work such data may be very useful, however as to the application in the workshop this great number of stability charts is only difficultly to survey and to handle.

Thus it raises the problem to reduce the number of data, but without leaving out and neglecting the practically required information. This could be realized by altering and further developing the program RATTER 1, as detailed in the following.

The program RATTER 2 (Fig. 1.29) was established on the basis of the problem being often existing in practice, that for a given machining operation at the workpiece the optimum conditions must be determined. Apart from special cases, as for instance machining with boring bars, rough machining operations are in general critical with regard to the chatter behaviour. Here one reduction is already possible due to the fact, that for given workpiece materials certain tools have been proved. Thus for turning tools and cutters the tool material and the tool geometry are given. By the workpiece - tool combination also the cutting speed range and the feed rate per tooth are limited. If a certain machine and a tool are chosen for the given machining operation, at last the most favourable position in the working range as well as the optimum configuration workpiece - tool must be determined by means of the

computer program.

Further considerable reduction of the data will be possible due to the fact, that it is preferably of interest in practice, which lowest chatterfree deapth of cut can surely be realized. This question can be answered by specifying only one value namely the minimum deapth of cut in the stability chart.

In Figure 1.30 some results of the stability calculation by means of the computer program RATTER 2 are given. Here the run of the minimum stability of all possible milling configurations for a given B/D-ratio and a cutter with given tool geometry is plotted against the entrance angle φ_E . With

$$W \sim \frac{1}{z} \tag{1.48}$$

which follows from (1.38) and (1.9), the borderline of stability can be related to the number of teeth on the cutter z, so that the chart is valid for cutters with a whatever number of teeth. The figure describes the behaviour for the middle position of the table. As it can be seen, the stability minima in the stability charts in Figure 1.28 e-h occur at 0°, 90°, 180° and 270° respectively. At these entrance angles it is equivalent for the stability, whether the table is moved in x- or y-direction, because for B/D = 0,5 the angle of contact is just 90°.

Considering the stability charts in Figure 1.28 it could already be expected, that considerable differences occured in the chatterfree deapth of cut versus the entrance angle. However in practice a high stability is only important and useful, if it can be reached with the installed driving power and if the maximum torsional moment must not be exceeded. In the program RATTER 2 these limitations can be calculated too.

When calculating and plotting only the minimum stability as performed by the program RATTER 2, the higher stability which

in milling operations exists in general between the unstable lobes, is not taken into account and thus cannot turned to profit. This possible increased stability is preferably interesting in those cases, where the machining operation - for example at a workpiece already mounted - must be performed in an unfavourable configuration. As the evaluation of numerous stability charts for face milling processes showed the stability between the unstable lobes can amount up to about 200 % of the minimum value, if the ratio of tooth mesh frequency f_z and chatter frequency f_R satisfies the condition

$$\frac{f_z}{f_R} = \frac{n \cdot z}{60 f_R} > 0{,}25 \qquad (1.49)$$

Considering the chatter frequency f_R and the value $\frac{\omega \tau_0}{2\pi}$, which are additionally put out and plotted in Figure 1.30, the most unfavourable rotational speeds can easily be calculated by means of the equation derived from equ. (1.34)

$$n = \frac{60 f_R}{z\left(\frac{\omega \tau_0}{2\pi} + m\right)} \qquad (1.50)$$

In practice the increased stability can be turned to profit by chosing rotational speeds between each two of the most unfavourable speeds. As it can be seen in the given stability charts, this improvement of the cutting performance is specially possible in those cases, where only one vibration mode is preferably decisive for the chatter behaviour. If the frequency ratio is $f_z / f_R < 0{,}25$ or if more than one vibration mode influence the chatter behaviour, in most cases the unstable lobes overlap in such a manner, that the increased stability can not be realized.

In Figure 1.30 a and c the minimum critical depth of cut is plotted against the entrance angle for $D/D = 0{,}3$ and $D/D = 0{,}7$, respectively. For $D/D = 0{,}3$ and generally for all $D/D \leq 0{,}5$ it is possible to machine the workpiece with table travel in x- as well as in y-direction. For $D/D = 0{,}7$ and generally for all

B/D > 0,5 the curve cuts off at a certain entrance angle, since the given breadth of the workpiece can no more be machined when exceeding this angle.

Comparing the stability charts in Figure 1.30 a,b,c makes obvious, that the critical deapth of cut is only slightly effected by the B/D - ratio over wide ranges of the entrance angle for instance for $0^{\circ} \leq \varphi_E \leq 90^{\circ}$ and $270^{\circ} \leq \varphi_E \leq 360^{\circ}$. This result means, that the utilization of the installed power becomes relatively better with an increasing B/D-ratio in those ranges, where the borderline of stability lies below the limitation due to the installed power.

In the shop by means of such representations of the stability behaviour the critical deapth of cut to be reached can easily be predetermined for given positions in the working range, given tool geometry and workpiece material. In addition to this the operation personnel can get a good qualitative survey over the chatterfree performance of the machine. Finally it may be stated that the detailed procedures will enable the machine tool users to improve the utilization of the machines considerably in many cases.

2. Chatter Specifications

As mentioned above the purpose of the research work performed on the section "Chatter Specifications" was to complete the geometrical acceptance tests (after Schlesinger) used until now since over 30 years, by suitable investigation procedures and specification data by means of which also the dynamic - preferably the chatter-behaviour of machine tools can be tested and judged respectively. The necessity of dynamic acceptance tests of machine tools results from the customers demand for minimum cost and minimum machining time at prescribed accuracy and surface quality of the workpieces. The machine tool user is therefore only interested in a procedure by which the cutting performance can be determined as perfectly as possible under consideration of the relative displacements between workpiece and tool.

At the Werkzeugmaschinenlabor in Aachen extensive investigations aimed to acceptance tests and specifications have been carried out especially with regard to the chatter behaviour of large and heavy machine tools. Prior conditions for this were analytical investigations into the chatter fundamentals. It was at first necessary to clarify the causes for the observed chatter phenomena and secondly to work out methods for the measurement and the calculation respectively of the necessary data.

As to the question, which data or values should be used and defined for specifying and judging the chatter behaviour, when initiating this program all participating research groups agreed, that the most suitable solution was to take the actual critical depth or width of cut, because this is the value only being interesting in practice. Thus the main research effort was at first directed at the problem to develop the necessary techniques for determining these values.

Hereby the following points of view had to be considered:

1. A minimum number of values should be sufficient for the judgement;
2. The measurement procedure and the calculation method should not be too sophisticated but easy to understand;
3. The required effort of measuring and calculation time and the test- and evaluation equipment should be as minimum as possible.

In the following different possibilities resulting from the performed research work, shall be detailed in short and discussed with regard to the reliability and reproducibility of the obtained results. When initiating this research program only few of the parameters having influence on the chatter behaviour were known. However during the investigations many further parameters have been found out of partly high importance. The influencing parameters for one part already quantitatively for the other part qualitatively known until now, are altogether given with the block diagram of the dynamic machining process in Figure 2.1. Some of them, especially those concerning the machine dynamics, as for instance clamping and moving of the machine elements and the travel speed, could not be investigated before the development of the measuring procedure based on the random noise theory. (see [19]). As to these effects only few measurements could be performed till now, so that quantitative relationships being generally valid are not yet available. Examples for the influence of the changed position of the machine elements have extensively been discussed in [17, 18] . Investigations detailed in [18] showed the considerable effect of the workpiece mounting . The dynamics of the workpiece itself are preferably decisive in the higher working positions of the machines. Corresponding results of investigations into large portal milling machines are given in [10].

Mainly three procedures seem to be possible, which will provide the necessary data for judging and specifying the chatter behaviour of machine tools. Two of them provide to determine the

practically interesting cutting conditions, these procedures are

Experimental Chatter Tests
Theoretical Chatter Analysis

The third possibility is to look at the

Dynamic Compliance of the Machine

at the cutting point because there is a close - at least qualitative - relationship between the dynamic compliances and the chatter behaviour.

2.1 Experimental Chatter Tests

Considering that the critical deapth or width of cut is mostly interesting for the machine user, the method of the direct measurement of the stability border by means of experimental cutting tests is suggesting itself. The main advantage of machining experiments for chatter analysis of machine tools is the simple performance of the tests. The stability border can be determined by altering the deapth of cut and observing the noise or the workpiece surface. More comfortable is the use of a vibration pick-up and a recorder or an oscilloscope. This procedure is easy to understand for the manufacturer as well as for the user. This may be an important argument under certain circumstances, if trouble raises between manufacturer and user. Further important advantages are, that no special measuring device and qualified personnel are required for performing the tests.

One significant disadvantage is the fact, that the investigation requires extremely high time consumption, if numerous combinations of the influencing parameters must be taken into account. This time consumption whereby the machine must be taken out of production is considerable especially at large and expensive machine tools.

Additionally several problems in performing the tests must be mentioned. One main difficulty of chatter experiments is the fact, that the stability border is dependent on an external disturbance force. This results in a certain hysteresis of the stability border. Going from the stable region to the unstable yields a greater critical doapth of cut than coming from the unstable region. This is caused by the fact that near the stability border the raise time of the selfexcited vibrations depends on external forces, which are present in machining a workpiece surface which is already wavy.

Another influence factor is the workpiece material. In [16] results of experimental chatter tests are given, where the stability border is plotted versus the diameter of a turning workpiece. Here considerable differences of about 100 % in the critical width of cut were found out for different workpiece diameters. Besides to this the influence of the cutting edge wear must be observed carefully. Results of experimental chatter tests on a milling machine [18] showed, that the chatter tests can carried out only in a certain stage of tool wear.

Finally the determination of the critical cutting conditions by means of experimental chatter tests can be regarded as the most simple procedure, the reliability of which however is limited if only normal time consumption shall be admitted. The application of this procedure seems to be reasonable, if only small spectra of working conditions shall be taken into account, for instance at special or single purpose machine tools.

Considering, that in the case of large machine tools the influence of the workpiece upon the chatter behavior can not at all be neglected, the difficulty in specifying the above mentioned cutting tests is considerably increased. Thus it can be understood, that there are many objections against the general application of cutting tests for specifying the chatter behavior of

large machine tools, though the procedure itself is very simple to apply.

2.2 Theoretical Chatter Analysis

The fundamentals as well as the performance of the theoretical chatter analysis have been detailed in the Quarterly Technical Reports Nr. I, II, III [11, 12, 13] and in chapter I of this report. The most important advantage is, that by means of the developed computer programs the stability behavior under all interesting conditions can theoretically be determined with practically satisfactorily accuracy rationally and economically, if the characteristic properties of the machine and the cutting process are known. From the practical point of view it is advantageous, that the machine must only be available for the dynamic investigation whereas the evaluation and calculation can be carried out apart from the machine. The necessary measuring time at the machine itself will furthermore considerably be reduced by applying the recently developed spectral density measurement technique developed under a closely related contract at the Werkzeugmaschinenlabor der TH Aachen too [19]. By means of this measuring technique it will additionally be possible to take the machining parameters rotational speed, feed rate, moving of elements, clamping a.s.o into account during the dynamic investigation. When representing the chatter behavior in the form of stability charts it is also possible to calculate and to plot the limitation of the cutting performance due to the installed power and due to the maximum torsional moment. By means of these additional values it is easily possible to compare the chatter-free performance with that performance which the machine is designed for, and therewith got a good and clear judgement of the practical utilization of the machine.

Different disadvantages cannot be let out of consideration. The first one is due to the highly sophisticated and thus not

large machine tools, though the procedure itself is very simple to apply.

2.2 Theoretical Chatter Analysis

The fundamentals as well as the performance of the theoretical chatter analysis have been detailed in the Quarterly Technical Reports Nr. I, II, III [11, 12, 13] and in chapter I of this report. The most important advantage is, that by means of the developed computer programs the stability behavior under all interesting conditions can theoretically be determined with practically satisfactorily accuracy rationally and economically, if the characteristic properties of the machine and the cutting process are known. From the practical point of view it is advantageous, that the machine must only be available for the dynamic investigation whereas the evaluation and calculation can be carried out apart from the machine. The necessary measuring time at the machine itself will furthermore considerably be reduced by applying the recently developed spectral density measurement technique developed under a closely related contract at the Werkzeugmaschinenlabor der TH Aachen too [19]. By means of this measuring technique it will additionally be possible to take the machining parameters rotational speed, feed rate, moving of elements, clamping a.s.o into account during the dynamic investigation. When representing the chatter behavior in the form of stability charts it is also possible to calculate and to plot the limitation of the cutting performance due to the installed power and due to the maximum torsional moment. By means of these additional values it is easily possible to compare the chatter-free performance with that performance which the machine is designed for, and therewith get a good and clear judgement of the practical utilization of the machine.

Different disadvantages cannot be let out of consideration. The first one is due to the highly sophisticated and thus not

generally understandable theory the whole procedure is based upon. Another fact is the complicated measuring and evaluation procedure as well as the very expensive test equipment, of which the operation requires still qualified personnel up to now. Besides to this other difficulties are produced by the parameters - already discussed in connection with the cutting tests - influencing the chatter border during machining.

However the decisive reason which is opposed to a general application of the theoretical chatter analysis is the fact, that no sufficiently reliable data concerning the transfer behavior of the cutting process are available at this time.

Considering the advantages and disadvantages the above detailed procedure seems to be the optimum possibility for future time, if the chatter behavior of machine tools shall be judged by specifying the actual deapth or width of cut for a large spectrum of machining conditions.

There is absolutely no doubt, that for judging machine tool chatter behavior the actual critical width or deapth of cut are the most suitable and interesting values from the practical point of view. However when considering all the mentioned parameters (see Figure 2.1), there raises the question, whether it is reasonable at all to take the width or deapth of cut as criterion for the chatter specifications of machine tools.

In order to provide a test as simple as possible it seems to be advantageous, to let the parameters of the cutting process out of consideration. In this case no longer the borderline of stability is the basis for the judgement, but, as can be seen in the block-diagram, the dynamic properties of the system machine-workpiece. If the compliance of the workpiece is let out of consideration too, at last only the dynamic properties of the machine itself must be regarded.

2.3 Dynamic Compliance of the Machine

The fundamental idea when taking only the dynamic compliance of the machine as criterion for the chatterfree performance is the fact, that there is a close-at least qualitative-relationship between the chatter behaviour and the mere dynamic compliance of the machine. To test these properties is relatively simple, but it must be verified, what judgement about the chatter behavior can be made by considering only the dynamics of the machine. As it is simple to understand this test provides not at all an absolute judgement of the machine tool. However as to the large machine tools it seems to be highly questionable, whether such a test is still reasonable, after the investigations performed till now, have shown, what decisive influence upon the chatter behavior is often caused by the compliance of the workpiece (see [10, 15]). To this it must be replied, that first of all the machine itself must fulfill certain prior conditions concerning the dynamic stiffness in the critical vibration modes.

Considering for instance a portal milling machine the most critical vibration modes are the bending modes of the portal. Presuming now the workpiece to be rigid, it can be stated, that the chatter behavior of a machine A, which in the two vibration directions of the portal has by far higher stiffness as a machine B, will be better than the chatter behavior of machine B. By this simple example it shall only be demonstrated, that by means of the dynamic properties of a machine a relative judgement between machines of the same type is possible at all.

On the other hand it must be noticed, that considerable uncertainty may be exist, when applying this method. It will not at all be possible, to find out differences of 20 to 30 % between machines, however it should be possible to ascertain for example a machine, which is about 300 % worse than other ones.

Thus it can be said, that this method will provide a good engineering judgement about the dynamic behavior and therewith about the chatterfree performance. However before generally applying this method extensive dynamic and chatter tests will still be necessary into the problems, what vibration modes are decisive for the chatter behavior at the different types of machine tools and in howfar the dynamic and the chatter behavior vary due to the changing machining parameters as for instance the position of the elements within the working range, the movement of the elements and the clamping conditions.

Summarizing the considerations concerning the chatter specifications it can be stated, that now after having systematically investigated and clarified the fundamental relationships being valid in machine tool chatter three procedures to test and specify respectively the chatter behavior of machine tools are now available on principle. However the above discussion of these procedures showed, that further practical cutting tests as well as dynamic investigations are necessary before one of these procedures can be proposed to be the most suitable one in general and before general purpose machine tool chatter specifications can be established respectively.

3. Structure Analysis

3.1 Digital Computation of Machine Tool Elements and Structures

For the improvement of the dynamic behaviour of machine tools it is an important point of view to develop analytical methods for the calculation of the dynamic properties already in the status of design. As the mathematical treatment of a complete machine tools system is an extremely complex problem, due to the influence of joints and the interdependence of the single elements, these investigations must start from a separate analysis of the different components. The next step will then be the connection of these elements.

All the analytical methods being developed have been programmed and tested by comparing measured an computed results. The methods are described in a form which makes it possible to reproduce them, easily on any computer.

3.1.1 Computation of Spindle Systems

Several investigations of heavy machine tools have shown that the characteristics of the working spindle are of great importance for the working accuracy and the chatter behaviour. It was stated that under certain conditions up to one third of the total deflection is given due to spindle bending. (Fig. 3.1)

The computation techniques for spindle systems known from the literature so far usually require considerable simplifications concerning the geometrical shape or the boundary conditions e.g. the arrangement of the bearings. In the following a method will be presented, which is applicable to spindles with any arrangement and number of bearings.

Usually the cross-sections of a spindle and with this the moment of inertia I (x) and the mass m(x) will vary along the spindle-axis. According to Timoshenko the behaviour of a spindle element as shown in Figure 3.2 is described by the partial differential

equation

$$\frac{\partial^2}{\partial x^2}\left[E \cdot J_x \cdot \frac{\partial^2 y(x,t)}{\partial x^2}\right] = q(x,t) \qquad (3.1)$$

A complete solution of equation (3.1) is generally impossible. But under certain conditions a sufficiently correct approximation can be obtained when using electronic computers. For the solution of the problem by means of a digital computer the temporal deviation is made equal to zero. Then equation (3.1) is transformed into an ordinary differential equation

$$\frac{d^2}{dx^2}\left[E \cdot J_x \cdot \frac{d^2 y(x)}{dx^2}\right] = q(x) \qquad (3.2)$$

This can be solved for an elastic beam with many different cross-sections and several flexible supports by a method using matrix algebra. The following results can be obtained.

a) static behaviour of the system spindle-bearing,
b) natural frequencies of the systems.

For the computation the spindle is divided into separate sections which may have different lenghts. In order to achieve a high accuracy as many sections as possible should be chosen. The state of forces M_i; Q_i and deformation γ_i; y_i is described by the vector

$$z = \begin{vmatrix} y \\ \gamma \\ M \\ Q \end{vmatrix}$$

The general solution of equation (3.2) for a ny section "k" of the spindle (see Fig. 3.2) is obtained by four fold integration for the region $0 \leq x_k \leq l_k$ [11].

After that the relationship between any two interesting points of the spindle may be expressed in matrix-notation.

$$\begin{vmatrix} y_{i+1} \\ \gamma_{i+1} \\ M_{i+1} \\ Q_{i+1} \\ q_{i+1} \end{vmatrix} = \begin{vmatrix} 1 & -l_k & \frac{l_k^2}{2EJ_k} & \frac{l_k^3}{6EJ_k} & \frac{l_k^4}{24EJ_k} \\ & 1 & -\frac{l_k}{EJ_k} & -\frac{l_k^2}{2EJ_k} & -\frac{l_k^3}{6EJ_k} \\ & & 1 & l_k & \frac{l_k^2}{2} \\ & & & 1 & l_k \\ & & & & 1 \end{vmatrix} \cdot \begin{vmatrix} y_i \\ \gamma_i \\ M_i \\ Q_i \\ q_i + g_k \end{vmatrix} \qquad (3.3)$$

Additional influences, such as flexible bearings, are taken into consideration by a so-called point-matrix p_k. This operation can be explained by means of Figure 3.3. The status directly on the left side of the point b, which is called b_L starting from the status on the right side b_R is obtained by the calculation

$$z_{bL} = (P_k \cdot F_k) \cdot z_a \qquad (3.4)$$

or

$$z_{bL} = \mathcal{L}_k \cdot z_a$$

respectively, where L_k is the so-called transfer matrix.

External forces Q or moment M and alterations of the diameter, which cause an alteration of the load q, are taken into account by defining the vector z_L in a more general form

$$z_L = \begin{vmatrix} y_R \\ \gamma_R \\ M_R \pm M \\ Q_R \pm Q \\ q_R \text{ or } q_L \end{vmatrix} \qquad (3.5)$$

The values y_1 and γ_1 of point 1, which are unknown so far, are obtained from a linear system of two equations in dependence on the coundary conditions, $M_n = 0$ and $Q_n = 0$ [11].

If the initial status vector z_1 is known the vector z_n for a given point can be determined in the following way.

$$\begin{aligned} z_1 \cdot \mathcal{L}_2 &= z_{2R} \rightarrow z_{2L} \\ z_{2L} \cdot \mathcal{L}_3 &= z_{3R} \rightarrow z_{3L} \\ &\vdots \\ z_{(n-1)L} \cdot \mathcal{L}_n &= z_n \end{aligned} \qquad (3.6)$$

In Figure 3.4 the measured and the calculated bending lines of a lathe-spindle loaded at the spindel-nose by a static force of 2200 lb (1000 kp) are compared. The correspondence between the measured and calculated deflections is quite good.

In order to determine the natural frequencies a mass-matrix, similar to the point-matrix, is introduced into the program for the static bending line [13]. Assuming an arbitrary deflection of the spindle-nose the solution is found in an iterative computation process. In the natural modes both the force Q_n and the moment M_n at the end of the spindle must be equal to zero. The frequencies where this condition is fulfilled are calculated.

By aid of this method given in form of a block diagram in Fig. 3.5 the natural frequencies and according mode shapes may be found. If there are only the natural frequencies of interest the effort can be decreased rapidly. [13]

Figure 3.6 shows the resonance frequency of a lathe-spindle with a workpiece clamped in the three-jaw-chuck as a function of the front bearing stiffness. It can be seen that the dynamic behaviour of the system is described quite exactly by the chosen method.
Furthermore in a test series the natural frequencies of five machine tools of the same type and the same type of spindle systems have been measured. A remarkable scattering of the natural frequencies has to be stated which cannot be explained completely. The age differences of the single machines do not show a definite influence. Using the digital computer program and the mathematical model of the spindle-bearing system shown in Fig. 3.7 the natural frequencies have been calculated. A comparison between theoretical and experimental results - see Fig. 3.8 - yields deviations between 0 and -16,5 %. On the

average a difference of - 7,25 % is found. If this is compared to the scattering of the actual natural frequencies, ± 11,1 %, the usefulness of the computation method, even if so complex structures as the working spindle of a boring mill are concerned, becomes evident.

When applying the chosen procedure of computation the accuracy of the results is the higher the better the mass distribution is approximated within the mathematical model. However, from this fact it cannot be concluded, that the accuracy could be improved at any rate by increasing the number of mass elements as at the same time the effect of rounding-errors become more significant. Due to these opposed influences an optimum for the number of mass elements will exist. In the present case the computer program is suitable for a separation into 28 mass elements and no detrimental effect due to rounding errors was observed.

3.1.2 A numerical method for calculating cross section values

In this chapter a numerical method will be described to calculate the cross section values of an arbitrary given polygonal figure. By help of this method the following values can be calculated:

Shear Area,
Neutral Axis,
Area Moments about given axis,
Inertia Moments about given axis,
Inertia Moments about Neutral axis,
Counter clockwise angle of rotation of principle axis,
Inertia Moments about principle axis,
Polar Mass Moment of Inertia,
Transverse Mass Moments,
Weight of element.

All these values are needed as inputdata for the programs to calculate the static and dynamic behaviour of columns and frames of machine tools as described in chapter 3.1.3.

The calculation of shear area values of single or inerrupted areas as shown in Fig. 3.9can be done by the Gauss Integral Law for areas, called Green's-Law as well.
In the most general form this law may be written

$$A = \iint_B F_x(x,y)\, dx\, dy = \oint_C F(x,y)\, dy \qquad (3.7)$$

On the other hand for a given area in the x-y-plane the shear area value can be calculated by the following formula too:

$$A = \iint_B dx\, dy \qquad (3.8)$$

From this formula it can easily be obtained that F_x (x,y) in formula 3.7 has to be equal to 1 in this case. Thus F (x,y) in the right hand part has to be equal to x:

$$F(x,y) = x \qquad (3.9)$$
$$F_x(x,y) = \frac{\partial F(x,y)}{\partial x} = 1$$

Now formula (3.7) may also be written

$$A = \iint_B dx\, dy = \oint_C x\, dy \qquad (3.10)$$

Taking into account that

$$\oint_C x\, dy = -\oint_C y\, dx$$

it can be written

$$A = \tfrac{1}{2} \oint_C (x\, dy - y\, dx) \qquad (3.11)$$

This equation can be splitted in general. Presuming all the areas to be calculated being given as polygonal figures this formula can be subdevided into a lot of segments where each of them is set up along the straight line between any two given polygon points. Thus for equation 3.11 the following numerical

formula may be written

$$A = \tfrac{1}{2} \sum_{i=1}^{n} [x_i (y_{i+1} - y_i) - y_i (x_{i+1} - x_i)] \qquad (3.12)$$

or in a more compact form

$$A = \tfrac{1}{2} \sum_{i=1}^{n} [x_i y_{i+1} - y_i x_{i+1}] \qquad (3.12a)$$

In this formula the index i is following the curve C in mathematical positive way as shown in figure 3.10 and for i = n point (n + 1) is equal to the starting point.

The formula as given in 3.12 a can easily be programmed to calculate the value of the cross section area.

The next step is to calculate the areamoments and the neutral axis.

Therefore always two neighbourpoints with the subscripts i and i + 1 and the starting point of the system of coordinates are assumed to be the three corner pointsof a triangle. For each of the n triangles which are possible the neutral y-axis for example can be given as

$$y_s = \frac{y_{i+1} + y_i}{3}$$

The area of each of them can be calculated as

$$\alpha = \tfrac{1}{2} (x_i y_{i+1} - y_i x_{i+1})$$

Thus the area moment of such a triangle becomes

$$s_x = \alpha \cdot y_s = \tfrac{1}{2} (x_i y_{i+1} - y_i x_{i+1}) \cdot \tfrac{1}{3} \cdot (y_{i+1} + y_i)$$

As long as it is possible to surround these triangles in a mathematical positive way with respect to the ascending numbered points the values for s become positive otherwise negative (Fig. 3.10). The sum of all of them is equal to the area moment of the whole cross section. About the x-axis it can be written

$$S_x = \tfrac{1}{2} \sum_{i=1}^{n} [(x_i y_{i+1} - x_{i+1} y_i)(y_i + y_{i+1})] \qquad (3.13)$$

and about the y-axis in the same way

$$S_y = \tfrac{1}{6} \sum_{i=1}^{n} \left[(x_i y_{i+1} - x_{i+1} y_i)(x_i + x_{i+1}) \right] \qquad (3.14)$$

From these equations now the distances between the given x-y axis and the neutral ones can be calculated:

$$x_s = \frac{S_y}{A}$$

$$y_s = \frac{S_x}{A} \qquad (3.15)$$

Quite similar to the results as shown until now the formulas for the moments of inertia about given x- and y-axis can be found

$$J_x = \tfrac{1}{12} \sum_{i=1}^{n} \left[(x_i y_{i+1} - x_{i+1} y_i) \cdot \left[(y_i + y_{i+1})^2 - y_i \cdot y_{i+1} \right] \right] \qquad (3.16)$$

and

$$J_y = \tfrac{1}{12} \sum_{i=1}^{n} \left[(x_i y_{i+1} - x_{i+1} y_i) \left[(x_i + x_{i+1})^2 - x_i \cdot x_{i+1} \right] \right] \qquad (3.17)$$

For the moment of deviation I_{xy} about the given axis it can be written

$$J_{xy} = \tfrac{1}{12} \sum_{i=1}^{n} \left\{ (x_i y_{i+1} - x_{i+1} y_i) \left[(x_i + x_{i+1})(y_i + y_{i+1}) - \tfrac{1}{2} (x_i y_{i+1} + x_{i+1} \cdot y_i) \right] \right\} \qquad (3.18)$$

All these formulas are easily to be programmed and the further existing characteristics of any given polygonal cross section can be calculated on the basis of those values.

The moments of inertia being calculated about the given coordinates can be expressed about the neutral axes by help of Steiner's Law.

$$\begin{aligned} I_{xs} &= I_x - A \cdot y_s^2 \\ I_{ys} &= I_y - A \cdot x_s^2 \\ I_{xys} &= I_{xy} - A \cdot x_s \cdot y_s \end{aligned} \qquad (3.19)$$

Using these expressions the angle of rotation between the neutral axis system and the system of principle axes (Fig. 3.11) can

be calculated

$$\tan(2\varphi) = \frac{2\,J_{xys}}{J_{ys} - J_{xs}} \qquad (3.20)$$

Furthermore the principle moments of inertia about the ξ- and η-axis are given by the following formulas

$$J_\xi = \frac{J_{xs}+J_{ys}}{2} + \left[\frac{J_{xs}-J_{ys}}{2}\cos(2\varphi) - J_{xys}\cdot\sin(2\varphi)\right]$$

$$J_\eta = \frac{J_{xs}+J_{ys}}{2} - \left[\frac{J_{xs}-J_{ys}}{2}\cos(2\varphi) - J_{xys}\cdot\sin(2\varphi)\right] \qquad (3.21)$$

On the basis of the cross section values as described above it is easy to obtain the values for the weight of an element of the lenght L (Fig. 3.12) and the polar- and transverse mass moments of inertia.

In Fig. 3.13 a block diagram of the program is given for calculating all the values mentioned above. The applicability of the method is shown for the cross section of a machine tool column as given in Fig. 3.14. The results of calculation as they are put out from the computer are shown on Fig. 3.15.

3.1.3 Calculation of the Static and Dynamic Behaviour of Machine Tool Elements and Frames

In Fig. 3.1 the flux-of-force-analysis for a heavy boring- and milling-machine is shown. The result of this analysis is typical for most of these machines. It can be seen that about 1/3 of the total deflection results form the spindle-system.

Methods for calculating the static and dynamic behaviour of this part have been presented and applied to some spindle systems. As the next step a method for calculating the static deflection of a machine structure - reduced to a three-dimensional beam-system - will be described.

3.1.3.1 Calculation of Static Deflections

The method described here is based upon the possibility to re-

duce a machine-tool-structure to a three-dimensional system of uniform beams. This is possible in the very most cases. Another limitation is Hooke's Law.

After the machine-tool-structure has been reduced, the different elements have to be named. The denomination can be seen in Fig. 3.16. All the elements are marked by the letters of the alphabet beginning with "a".

Internally the beginning of each element is called "1", the end "2". The ends "2" of each element, which are the connecting-joints between two elements at the same time, are indicated with the capital-letters of the element's names. The deflection of a point A, for instance in the x-direction due to a load applied at point B, will be called $x_{A,B}$. The rotations are indicated in the same way.

In the following two systems of coordinates are used. One is a right handed general-system for coordinating all the members; the axis are x', y' and z'. On the other hand each of the elements has its own system, the member-system, which is a right handed one too. The axis of the member-system of an element i are called x_i, y_i, and z_i where x_i is always the lenght-axis.

The sign-declaration (Fig. 3.17) is the one of a right handed system of coordinates for the deformations as well as for the loadings.
Each of the elements is regarded to be rigidly supported at point "1". The real boundary-conditions will be introduced later. For such an element, loaded at "2" the deflections and distorsions may be expressed with respect to Hookes's - Law as:

$$\begin{vmatrix} \delta_x \\ \delta_y \\ \delta_z \\ \phi_x \\ \phi_y \\ \phi_z \end{vmatrix} = \begin{vmatrix} l/AE & 0 & 0 & 0 & 0 & 0 \\ 0 & l^3/3EJ_z & 0 & 0 & 0 & l^2/2EJ_z \\ 0 & 0 & l^3/3EJ_y & 0 & -l^2/2EJ_y & 0 \\ 0 & 0 & 0 & l/GJ_x & 0 & 0 \\ 0 & 0 & -l^2/2EJ_y & 0 & l/EJ_y & 0 \\ 0 & l^2/2EJ_z & 0 & 0 & 0 & l/EJ_z \end{vmatrix} \cdot \begin{vmatrix} P_x \\ P_y \\ P_z \\ m_x \\ m_y \\ m_z \end{vmatrix} \qquad (3.22)$$

or

$$\bar{d} = F \cdot \bar{p} \tag{3.22a}$$

The F-matrix is symmetrical (Maxwell-Betty reciprocal theorem).

Alter the relationship between force and deflection has been demonstrated for one arbitrary element of a system, the transition to a complete system will be explained. The main-problem in a complex system in space is the so-called shifting of forces and moments from the acting point into all the other ones for computation.

By looking at the compatibility-conditions between the ends "1" and "2" of an arbitrary placed and formed element (Fig. 3.18) therefore the following relationship can be obtained.

$$\begin{vmatrix} p_{x1} \\ p_{y1} \\ p_{z1} \\ m_{x1} \\ m_{y1} \\ m_{z1} \end{vmatrix} + \begin{vmatrix} 1 & 0 & 0 & 0 & 0 & 0 \\ 0 & 1 & 0 & 0 & 0 & 0 \\ 0 & 0 & 1 & 0 & 0 & 0 \\ 0 & -L_z & L_y & 1 & 0 & 0 \\ L_z & 0 & -L_x & 0 & 1 & 0 \\ -L_y & L_x & 0 & 0 & 0 & 1 \end{vmatrix} \cdot \begin{vmatrix} p_{x2} \\ p_{y2} \\ p_{z2} \\ m_{x2} \\ m_{y2} \\ m_{z2} \end{vmatrix} = 0 \tag{3.23}$$

By this equation a force can be shifted in the most general case within a system and the ends "1" and "2" may be any two point I and S:

$$\bar{p}_1 + H_{12} \cdot \bar{p}_2 = 0 \quad (3.23a); \quad \bar{p}_I + H_{IS} \cdot \bar{p}_S = 0 \tag{3.23b}$$

or

$$\bar{p}_I = -H_{IS} \cdot \bar{p}_S \tag{3.24}$$

The total deflection as well as the torsion of any system joint can be subdivided into two components:

a) the part due to the elastic deformation of the regarded ele-

ment itself, caused by a load acting anywhere, called member deformation $\bar{e}$ and

b) the part due to the deformation of the other elements (in accordance to the general denomination, which is called rigid body displacement $\bar{d}^*$.

Thus for the total deflection and trosion it may be written

$$\begin{vmatrix} \delta_x \\ \delta_y \\ \delta_z \\ \cdot \\ \cdot \\ \varphi_z \end{vmatrix} = \begin{vmatrix} e_x \\ e_y \\ e_z \\ \cdot \\ \cdot \\ \widehat{e_z} \end{vmatrix} + \begin{vmatrix} \delta_x^* \\ \delta_y^* \\ \delta_z^* \\ \cdot \\ \cdot \\ \varphi_z^* \end{vmatrix} \quad \text{or} \quad \bar{d} = \bar{e} + \bar{d}^* \tag{3.25}$$

For the member deformation may be written

$$\bar{e} = F \cdot \bar{p} \tag{3.26}$$

To find $\bar{d}^*$ we have to consider a completely rigid member without any elastic deformation. Its end-deformations shall be $\bar{d}_1$ and $\bar{d}_2$ due to the forces $\bar{p}_1$ and $\bar{p}_2$. For the total virtual work being done by the applied forces it may be wrtitten

$$\bar{p}_1^{\,t} \cdot \bar{d}_1 + \bar{p}_2^{\,t} \cdot d_2 = 0 \tag{3.27}$$

and substituting $\bar{p}_1^{\,t}$ from equation (3.4)

$$-\bar{p}_2^{\,t} \cdot H^t \cdot \bar{d}_1 + \bar{p}_2^{\,t} \cdot \bar{d}_2 = 0 \tag{3.27a}$$

it follows

$$\bar{d}_2 = H^t \cdot \bar{d}_1 \tag{3.28}$$

With equation 3.28 any existing deformation at point 1 can be related to point 2 and particularly the rigid body deformation

$$\bar{d}_2^{\,*} = H^t \cdot \bar{d}_1^{\,*} \tag{3.28a}$$

Substituting $\bar{e}$ from equ. 3.26 and $\bar{d}^*$ from 3.28a the total deformation can be expressos for any given element k between

the joints I and K:

$$\bar{d}_K = F_K \cdot \bar{P}_K + H_K^t \cdot \bar{d}_I^* \tag{3.29}$$

In the previous chapters only systems consisting of elements without any relativ angles between them were discussed. To handle systems where arbitrary angles between the members may occur two possibilities exist:

a) The forces and deformations can be transformed from one member-coordinate-system into another one at each joint or

b) all the forces and deformations of any element are transformed into a general coordinate-system.

The last possibility is chosen for the following investigations. For all the acting forces and moments the general transormation matrix T can be obtained:

$$T = \left|\begin{array}{cccccc} \cos(x,'x_K) & \cos(x,'y_K) & \cos(x,'z_K) & 0 & 0 & 0 \\ \cos(y,'x_K) & \cos(y,'y_K) & \cos(y,'z_K) & 0 & 0 & 0 \\ \cos(z,'x_K) & \cos(z,'y_K) & \cos(z,'z_K) & 0 & 0 & 0 \\ 0 & 0 & 0 & \cos(x,'x_K) & \cos(x,'y_K) & \cos(x,'z_K) \\ 0 & 0 & 0 & \cos(y,'x_K) & \cos(y,'y_K) & \cos(y,'z_K) \\ 0 & 0 & 0 & \cos(z,'x_K) & \cos(z,'y_K) & \cos(z,'z_K) \end{array}\right| \tag{3.30}$$

The transformation matrix T is orthogonal. Thus it may be written:

$$T^t = T^{-1} \tag{3.31}$$

The relationship between the deformations in the member system and the general system can be found in the same way as shown for the loadings

$$\bar{d}' = T \cdot \bar{d} \tag{3.32}$$

Substituting $\bar{d}$ by means of equations (3.22a) it can be written

$$\bar{\alpha}' = T \cdot F \cdot \bar{p}_0$$

The H-matrix, which allows to shift loadings within the system can be transformed in the same way:

$$H' = T \cdot H \cdot T^t$$

A vector $\bar{p}_m$ will be introduced which yields all the forces at the ends "2" of the elements in member-coordinates

$$\bar{p}_m = \begin{vmatrix} p_{2a} \\ p_{2b} \\ p_{2c} \\ \cdot \\ \cdot \\ p_{2n} \end{vmatrix} \quad \text{with} \quad p_{2i} = \begin{vmatrix} p_{2x} \\ p_{2y} \\ \cdot \\ \cdot \\ m_{2z} \end{vmatrix}_i$$

In the same manner a vector $\bar{e}_m$ is defined which contains all the member deformations at the ends "2" of the whole system

$$\bar{e}_m = \begin{vmatrix} e_{2a} \\ e_{2b} \\ \cdot \\ \cdot \\ e_{2n} \end{vmatrix}$$

Now the relationship between $\bar{e}_m$ and $\bar{p}_m$ due to the elasticity of the elements can be written in accordance with equation (3.26)

$$\bar{e}_m = \begin{vmatrix} F_a & 0 & 0 & 0 & \cdot \\ 0 & F_b & 0 & \cdot & \cdot \\ 0 & 0 & F_c & & \\ \cdot & & & & F_n \end{vmatrix} \cdot \bar{p}_m \qquad (3.27)$$

Before the rigid body deformation or boundary conditions will be included the formulas obtained so far will be transformed into the general coordinate system.

It may be written:

$$\bar{p}_a' = T \cdot \bar{p}_a = -T \cdot H \cdot \bar{p}_2$$

and

$$\bar{p}_2' = T \cdot \bar{p}_2 \qquad (3.19)$$

The equilibrium conditions of the joints in Fig. 3.19 can now be formulated in general coordinates:

$$\begin{aligned} \bar{P}_A' &= T_a \cdot \bar{P}_{a_a} - T_b \cdot H_b \cdot \bar{P}_{a_b} \\ \bar{P}_B' &= T_b \cdot \bar{P}_{a_b} - T_c \cdot H_c \cdot \bar{P}_{a_c} \\ \bar{P}_C' &= T_c \cdot \bar{P}_{a_c} \end{aligned} \qquad (3.28)$$

or in matrix notation

$$\begin{vmatrix} \bar{P}_A' \\ \bar{P}_B' \\ \bar{P}_C' \end{vmatrix} = \begin{vmatrix} T_a & -T_b \cdot H_b & 0 \\ 0 & T_b & -T_c \cdot H_c \\ 0 & 0 & T_c \end{vmatrix} \cdot \begin{vmatrix} \bar{P}_{a_a} \\ \bar{P}_{a_b} \\ \bar{P}_{a_c} \end{vmatrix} \qquad (3.28a)$$

or $$\bar{P}' = C \cdot \bar{P}_m \qquad (3.28b)$$

The matrix C is called connection matrix.

In addition the following relationship between the member- and total-deformation can be obtained

$$\bar{e}_m = C^t \cdot D' \qquad (3.29)$$

Substituting $\bar{p}_m$ in equations 3.28b by the formulas 3.26 and 3.29 it may be written

$$\bar{P}' = C \cdot K_m \cdot \bar{e}_m = C \cdot K_m \cdot C^t \cdot D' \qquad (3.30)$$

or

$$D' = [\, C^{-1\,t} \cdot F_m \cdot C^{-1} \,] \cdot \bar{P}' \qquad (3.31)$$

This equation represents the relationship between loadings and deformations of an arbitrary system in the most general case. In equation 3.31 the H-matrix occur in member coordinates. Usually it is easier to take the length-elements for the H-matrix directly out of a drawing in general coordinates. In order to introduce these values into the C-matrix the H-matrices have to be substituted by the H'-matrices.

Another simplification is to indicate the H-matrices by means of the joint names as for instance

$$H_b = H_{nB}$$

Furthermore H_{ii}-matrices are introduced, which are equal to the unit matrix, in order to get more systematology.

Now for the final matrix, given in equation 3.31 it can be written

$$((C^{-1})^t \cdot F_m \cdot C^{-1}) =$$

$$\begin{bmatrix}
H'^t_{aa}\cdot T_a\cdot F_a\cdot T_a^t H'_{aa} & H'^t_{aa}\cdot T_a F_a T_a^t H'_{aB} & H'^t_{aa}\cdot T_a F_a T_a^t H'_{ac} & \cdots & H'^t_{aa} T_a F_a T_a^t H_{av} \\
H'^t_{aB}\, T_a F_a T_a^t H'_{aa} & H'^t_{aB}\cdot T_a F_a T_a^t H'_{aB} + H'^t_{BB}\cdot T_b\cdot F_b\cdot T_b^t H'_{Bb} & H'^t_{aB}\cdot T_a F_a\cdot T_a^t H'_{ac} + H'^t_{BB}\cdot T_b\cdot F_b\cdot T_b^t H'_{Bc} & \cdots & H'^t_{aB}\cdot T_a F_a T_a^t H'_{av} + H'^t_{BB}\, T_b F_b T_b^t H'_{Bv} \\
H'^t_{ac}\, T_a F_a T_a^t H'_{aa} & H'^t_{ac}\cdot T_a F_a T_a^t H'_{aB} + H'^t_{Bc}\cdot T_b\cdot F_b\cdot T_b^t H'_{Bb} + H'^t_{cc}\cdot T_c\cdot F_c\cdot T_c^t H'_{cB} & H'^t_{ac}\cdot T_a F_a\cdot T_a^t H'_{ac} + H'^t_{Bc}\cdot T_b\cdot F_b\cdot T_b^t H'_{Bc} + H'^t_{cc}\cdot T_c\cdot F_c\cdot T_c^t H'_{cc} & \cdots & H'^t_{ac}\cdot T_a F_a T_a^t H'_{av} + H'^t_{Bc}\, T_b F_b T_b^t H'_{Bv} + H'^t_{cc}\, T_c F_c T_c^t H'_{cv} \\
\cdots & \cdots & \cdots & \cdots & \cdots \\
H'^t_{av}\, T_a F_a T_a^t H'_{aa} & H'^t_{av}\, T_a F_a T_a^t H'_{aB} + H'^t_{Bv}\, T_b F_b T_b^t H'_{Bb} & H'^t_{av}\, T_a F_a T_a^t H'_{ac} + H'^t_{Bv}\, T_b F_b T_b^t H'_{Bc} + H'^t_{cv}\, T_c F_c T_c^t H'_{cc} & \cdots & H'^t_{av}\cdot T_a F_a\cdot T_a^t H'_{av} + H'^t_{Bv}\cdot T_b F_b\cdot T_b^t H'_{Bv} + \cdots + H'^t_{nv}\, T_n F_n T_n^t H'_{nv}
\end{bmatrix} \tag{3.32}$$

Substituting each element of the final-matrix (equ. 3.32) by a from like for instance

$$H'^{t}_{Ak} \cdot T_e \cdot F_a \cdot T_a' \cdot H'_{kB} \Rightarrow {}^{k}\bar{A}_{mp}$$

equation 3.24 can be simplified

$$(({}^{c}\bar{c}^{-1})^{t} F_m \, {}^{c}\bar{c}^{-1}) =$$

$$\begin{bmatrix} {}_{11}\bar{A}_{11} & {}_{11}\bar{A}_{12} & \cdots & {}_{11}\bar{A}_{1n} \\ {}_{12}\bar{A}_{11} & {}_{12}\bar{A}_{12} + {}_{13}\bar{A}_{21} & & \vdots \\ & {}_{13}\bar{A}_{12} + {}_{13}\bar{A}_{22} + {}_{33}\bar{A}_{33} & & \vdots \\ \vdots & \vdots & & \vdots \\ {}_{1n}\bar{A}_{11} & \cdots & \sum_{i=1}^{n} {}_{in}\bar{A}_{in} \end{bmatrix} \qquad (3.33)$$

The applicability of this method can be obtained from the comparison of the measured and computed deformation of a complicated machine tool column as given in Fig. 3.20. The computed results are shown in Fig. 3.21 as they were pointed out by the computer. For point 6 for a computed deflection of 7.13 /um (0.282 thou) obtaines. This results corresponds very good with the measured value of 7.25 /um (0.286 thou).
The above mentioned method can be used for calculating multiple pinned systems too. Therefore the load vector of equation

$$d = [F] \quad P$$

has to include the reaction loads at the additional pinned points. These loads can easily be found by the principle of superpositioning [16] .

3.1.3.2 The Calculation of eigenfrequencies

The differential equation for an undamped one mass system is

$$m \cdot \ddot{x} + k \cdot x = 0$$

In the same way it is possible to describe the dynamic behaviour of a system of several masses connected by springs:

$$[M] \cdot \ddot{X} + [K] \cdot X = 0 \qquad (3.34)$$

In this equation the expression [K] represents the stiffness of the whole system and [M] is the so called mass matrix. The inverse of [K] is called flexibility matrix of the system. The development of this matrix has already been described in the Quarterly Report Nr. 4 for single systems and in Quarterly Report Nr. 6 for multiple pinned ones [14,16].

The mass matrix [M] in general is a diagonal matrix of the form

$$[M] = \begin{bmatrix} m_1 & & & 0 \\ & m_2 & & \\ & & m_3 & \\ & & & m_4 \\ & & & & \ddots \\ 0 & & & & & m_n \end{bmatrix} \qquad (3.35)$$

for a given system consisting of n elements and n lumped masses. As for any element in space six degrees of freedom are taken into account each of the elements of the mass matrix consists of a diagonalmatrix itself.

To find out the eigenfrequencies and modeshapes of a given system described in short hand notation by equation 3.34 it can be assumed

$$\ddot{X}_r = -\omega_r^2 \cdot X_r \qquad (3.4)$$

Introducing this expression into equation 3.1 it can be written

$$-[M] \cdot \omega_r^2 \; X_r + [K] \; X_r = 0$$

and with $[K]^{-1} = [F]$

$[F]\,[M] = [A]$

and $\frac{1}{\omega_r^2} = \lambda_r$

this formula becomes the most general form of an eigenvalues-problem

$$([A] - \lambda_r E) \cdot X_r = 0 \qquad (3.35)$$

After the n eigenfrequencies of a system consisting of n elements and lumped masses have been found the next step is to determine the according eigenvectors X_r.

Therefore the system of equations 3.35 has to be solved for all the eigenvalues: λ_r

$$([A] - \lambda_r E) \cdot X_r = [B]_r \quad X_r = 0 \qquad (3.36)$$

After the eigenfrequencies and modeshapes have been calculated it is possible to calculate the response locus for a chosen degree of freedom [8], the damping values which are needed therefore have to be assumed previously.

To find out the correlation between computed and measured results the machine tool column of Fig. 3.22 was excited in the x- and y-direction. The test rig is shown in Fig. 3.23. The measured and computed first eigenfrequencies for both directions are

direction	measured 1 frq.	computed 1 frq.	error
x	326 Hz	335 Hz	+ 2,76 %
y	300 Hz	323 Hz	+ 7,66 %

Finally the frequency response loci for both directions were calculated as already described before on the base of the so far

computed eigenfrequencies an according modes shapes.

The results for both directions are shown in fig. 3.24 und 3.25 as they were printed out from the computer for exciting and picking up at the top of the column. The correlation between the measured and computed amplitude for the above mentioned first frequencies can be obtained from the following table:

direction	aplitude for the first bending eigenfrequency measured	computed	error
x	3,4 /um	3,01 /um	-11,5 %
y	3,3 /um	3,33 /um	0 %

3.2 Theoretical Analysis of Loading and Deformation of Columns

For analysing the elastic deformation of columns some simplifications have to be assumed both for loading and stress distribution in the investigated structure.

3.2.1 Loading and Stress Distribution

In general the forces and moments acting on the column of a horizontal boring and milling machine can be reduced to three cases of loading shown in Figure 3.26.

a) The bending moment M_o involves bending deformations.

b) The two forces F/2 acting on the slide-ways in the same direction are directly introduced to the side walls of the column. They cause bending deformations due to the moment $F \cdot l$ and shear deformations due to the force $Q = F$.

c) The torsional moment $F \cdot b$ can be reduced to the couple of forces, which is applied at the slide-ways too. The couple of forces causes twisting of the cross-section and under certain conditions considerable distortion of the cross-section contour. This warping leads to considerable twist deformations at the front wall of the column and by this at the slide-ways for the cutter head.

Calculating the elastic behaviour of the specimen following assumptions concerning the stress distribution are made:

a) The wall thickness is small in relation to cross-section and length of the structure. Therefore normal and tangential stress can be assumed to be constant all over the wall thickness.

b) Normal stress is linear along the walls of the cross-section. Tangential stresses are distributed in the form of a parabola.

c) Along the walls of longitudinal sections tangential stresses are assumed to be constant.

The stiffness of the walls against bending can be neglected when regarding the direction of the minimum second moment of area. In the same way the stiffness of the walls against torsion can be neglected.

3.2.1.1 Bending Deformations

The bending deformation of a hollow beam, fixed at one end and loaded as shown in Figure 3.26 a) and b), can be calculated from the well known formulas:

a) loaded by a pure bending moment M_o

$$f_B = \frac{M_o}{2EI_y} l^2 \qquad (3.37)$$

b) loaded by a single force F

$$f_B = \frac{F}{3EI_y} l^3 \qquad (3.38)$$

3.2.1.2 Shear Deformations

When loading a beam by a single force F, not only normal stresses but also shear stresses occur in the cross-section. They lead to additional shear deformations. The deflection in the height l

of the loaded cross-section due to shear force can be written as:

$$f_Q = \varkappa \frac{Q \cdot l}{G \cdot A} \tag{3.39}$$

The factor $\varkappa$ takes into account the distribution of shear stress over the cross-section. Föppl [5] gives the following equation for the factor $\varkappa$:

$$\varkappa = \frac{A}{Q^2} \int_A \tau^2 \cdot dA \tag{3.40}$$

For the shear stress it can be written

$$\tau(x,z) = \frac{1}{b(x)} \int_A \frac{\partial \sigma(x,z)}{\partial z} dA \tag{3.41}$$

and

$$\frac{\partial \sigma(x,z)}{\partial z} = \frac{x}{I_y} \frac{dM(z)}{dz} = \frac{x}{I_y} Q(z) \tag{3.42}$$

For calculating a thin walled rectangular cross-section the factor $\varkappa$ (see [3,13]) can be written as

$$\varkappa' = \frac{3(\alpha+1)}{5\alpha(\alpha+3)^2} (2\alpha^2 + 10\alpha + 15) \tag{3.43}$$

In this equation the shear stresses of the unloaded walls no. 2 in Figure 3.20 b have been neglected, as the wall-thickness is small in comparison to the cross-section. However for small values of the factor $\alpha = h/b$ the shear stress in the unloaded walls have to be considered.

Considering the loaded walls no. 2 in Figure 3.20 for calculating the influence of shear force the equation to compute $\varkappa$ (see [3, 13]) becomes

$$\varkappa = \frac{3(\alpha+1)}{5\alpha^2(3+\alpha)^2} (2\alpha^3 + 10\alpha^2 + 15\alpha + 5) \tag{3.44}$$

Equ. (3.44) shows that the distribution of the shear stresses in the structure depends only on the factor α i.e. on the shape of the cross-section. The relation-ship between α and both the factors $\varkappa'$ and $\varkappa$ is plotted in Figure 3.27. The diagram shows that the influence of the shear stresses in the unloaded walls can be neglected for $\alpha \geq 1$ in practical cases as the difference between $\varkappa$ and $\varkappa'$ is small. Only in the range $\alpha < 1$ these tangential stresses have to be considered.

3.2.1. 3 Total Deflection due to a Single Force F

For a thin-walled beam loaded by a single force F the total deflection at the point of force application can be written as

$$f_{tot} = f_B + f_Q$$

With the rations $G = \frac{5}{13} \cdot E$ for steel and $G = \frac{2}{5} E$ for cast iron and using the abbreviation

$$1/h = B$$

the total deformation of the thin walled beam with rectangular cross-section becomes for

a) calculating a steel structure:

$$f_{tot} = \frac{F \cdot \beta}{2Es\alpha(3+\alpha)} \left[4\alpha^2\beta^2 + \frac{1,56}{3+\alpha}(2\alpha^3 + 10\alpha^2 + 15\alpha + 5)\right] \quad (3.45)$$

b) calculating a cast iron structure

$$f_{tot} = \frac{F \cdot \beta}{2Es\alpha(3+\alpha)} \left[4\alpha^2\beta^2 + \frac{1,5}{3+\alpha}(2\alpha^3 + 10\alpha^2 + 15\alpha + 5)\right] \quad (3.46)$$

In Figure 3.28 the deflection due to shear force is compared to the deflection due to bending. The ratio of the deflections at the point of force application is plotted over the distance of the loaded section from the fixed end of the beam, which is related to the height of the cross-section. The diagram shows that in the range of usual sizes of machine tool columns

$$- L/h = 2.5 + 4.0 \quad \text{with} \quad 1/L = 0.15 + 0.8$$

where L means the total lenght of the column -

the deflection due to the shear force has considerable significance besides the bending deflection. The influence of shear force can be neglected in comparison to bending deformation only for relatively great distances of the loaded section from the fixed end of the column.

It may be assumed for instance that deflections due to shear force can be neglected if their part of the whole deflection is less than 15 %. In this case the influence of shear remains disregarded for a column with $\alpha = 2$ for $1 > 3$ h. For a beam with square cross-section shape ($\alpha = 1$) this border is growing up to $1 \approx 4$ h. However, if the column has a small height of cross-section in comparison to its breadth b, as it is valid for values of $\alpha = 0,8$ or less, shear deformation can only be neglected for $\beta > 6$ ($1 > 6$ h).

3.2.2.1 Torsional Loading and Deformation of Columns

The torsional deformation of a column fixed at one end and loaded as shown in Figure 3.29 can be calculated by well known formulas if there is no distortion of the cross section.

$$\frac{\varphi}{l} = \frac{M_T}{G \cdot I_T} \qquad (3.47)$$

For thin walled columns the polar area moment of inertia usually is calculated from the equation known as "Bredt's"-Formula

$$I_T = \frac{4 A_m^2}{\oint \frac{dU}{s}} \qquad (3.48)$$

A_m is the area enclosed by the centre line of the walls, U is the circumference given by the center lines of the walls and s is the variable wall thickness. If the wall thickness is constant around the circumference the equation for calculating the area moment of inertia becomes

$$I_T = \frac{4 A_m^2 \cdot s}{U} \qquad (3.49)$$

The equations (3.48) and (3.49) suppose the angles remaining constant under loading and the column being able to arche freely.

These equations also do not consider arching of the outside walls and distortion of the cross-section. The torsional loading M_T has to be applied to the column with respect to the flux of shear stress being constant all over the cross section ($\tau \cdot s$ = const.).

As the deflection of a column caused by torsional loading due to a couple of forces as shown in Figure 3.29 cannot be computed by normally used equations, a method to calculate these torsional deflections has been evaluated taking into account the distribution of the shear stress. Similar to bending a factor $\varkappa$ (see [3 , 15]) is stated which considers the cross-sectional deformation. The index of $\varkappa$ corresponds with the numbers of walls in Figure 3.26

$$\varkappa_1 = \frac{1}{\alpha^3}(1{,}2\alpha^3 + 2\alpha^2 + \alpha + 0{,}2) \qquad (3.50)$$

$$\varkappa_2 = 0{,}2\,\alpha^3 + 0{,}2 \qquad (3.51)$$

3.2.2.2 Torsional Deformations with and without Warping Effects

For the pure torsion the twisting of the column in the force acting height causes a deflection of the walls which carry the slide ways. This deflection can be calculated from already presented equations

$$\frac{\varphi}{l} = \frac{M_T}{G \cdot I_T} \quad (3.47); \qquad \varphi = \frac{2 f_{1x}^*}{b}$$

The torsional moment is assumed to be

$$M_T = F \cdot b'$$

and with the area moment of inertia

$$I_T = \frac{4 A_m^2 \cdot s}{U} \approx \frac{4 b^2 h^2}{2 b (1+\alpha)} \qquad (3.49)$$

the equation to calculate the deformation becomes

$$f_{1x}^* = \frac{5 F \beta (1+\alpha)}{8 E s \alpha} \qquad (3.52)$$

For any given cross-section the relationship between the torsional deformation with distortion can be written as

$$\frac{f_{1x}}{f_{1x}^*} = \frac{8}{5(1+\alpha)^2}\left[4\left(\frac{l}{h}\right)^2 \alpha^2 + 3\alpha^2 + 2\alpha + 0{,}5\right] \qquad (3.53)$$

In the diagram of Figure 3.30 the ratio f_{1x}/f_{1x}^* is plotted to the normalized height $\beta = l/h$. The curve shows that in a height of $\beta = 2$ the torsional deformation due to a distortion of the cross-section is about 10 times higher than the corresponding torsional deformation without distortion.

3.2.3 Model Tests

To check the investigation methods on one side and prove the equations derived above on the other side experimental model tests have been carried out using welded steel models.

3.2.3.1 Tested Columns and Test Method

The dimensions of the welded steel models have been scheduled in such a way that the specimen can be handled easyly and investigated with as small expenditure as possible. The design of the tested columns and their dimensions are shown in Figure 3.31 and 3.32. The ratios of the dimensions of the model with square cross-section

$$\alpha = h/b = 1$$
$$l/h = 3,25$$
$$s/h = 0,026$$

correspond approximately to the values used at real columns of machine-tools.

The models with rectangular cross-section have the same height l = 19.7 in (500 mm), as the models with square cross-section have but the ratios

$$\alpha = 2,00 \qquad \text{or} \qquad \alpha = 0,49$$

for the dimensions of the cross-section. All models are manufactured with and without top - plate.
Figure 3.33 shows the test rigs to investigate the behaviour of the columns under bending and torsional loads. The columns are fixed by 16 screws on to a stiff intermediate-plate which itself is fastened by screws on a fixing-plate. The fixing conditions of the columns have proved very stiff. Nevertheless

a certain flexibility of the clamping causes an additional deflection of the column and therefore the vertical deflections of the flange of the column are measured to seperate the deflection of the column due to the clamping condition from the deformation of the column.

The forces are applied to the column by means of two screws which are situated in the front wall as near to the side walls as possible. For bending the columns are loaded by a single force F in a way that two forces each of the value F/2 are acting on the side walls in the same direction. The torsional moment represented by a couple of forces is symmetrically applied to the column by means of an U-iron that is loaded by two hydraulic load units which are fed with oil of the same pressure by one pump. Applying the torsional moment it is ensured that no single force occurs which could lead to additional bending and shear deformation. In three different heights the columns are loaded by bending forces, or torsional moments, the heights are:

case a:	height of loaded section	l = 17.9 in (455 mm)
case b:	" " " "	l = 14.55 in (370mm)
case c:		l = 8.3 in (210 mm)

All deformations and deflections are measured with inductive deflection pick-ups. The pick-ups are mounted on a stand which is fastened on the fixing plate in a manner that the stand does not move whilst loading the column. From this stand the absolute deformations can be measured.

3.2.3.2 Investigation of Unribbed Columns

In order to check the accuracy of the above derived methods to calculate the deformations of columns under bending and torsional loads models of unribbed columns are tested. In addi-

tion the bending stiffness obtained from these tests is chosen as a standard to relate the measured stiffness of ribbed columns.

3,2,3,3 Bending Deflections

The table in Figure 3.34 shows the calculated and measured deflections of the columns with square cross-section. The measured values given in the table are taken as the average values of the deflections which have been measured at the 4 corners of the loaded cross-section. It can be seen that there is quite a good accordance between the calculated and measured values of deformation.

The deflections of the columns with rectangular cross-section measured in the same way are compared with the calculated deflections in Figure 3.35. The column with top plate shows a little higher stiffness. The errors are less than 10 %.

The occuring errors are caused by the simplifying assumptions, which have been made for the calculation, as well as by errors, made in measurement, during running tests, and manufacturing the columns.

3.2.3.4 Torsional Deflections

The measured deformations of the columns under the applied torsional moment do not show a pure torsional deformation but a cross-sectional distortion which is drawn in Figure 3.36. For this reason a "stiffness against torsional load" is declared as the measured deformation at the point of loading devided by the force itself. In the Figures 3.37 and 3.38 the relationship between the measured deformation and that being computed neglecting the warping effects are given. Figure 3.37 describes the values obtained from the columns with square cross-section whilst Figure 3.38

shows those of the column with rectangular cross-section. The measured results agree quite well with the computed ones in the loading heights of 17.9 in and 14.56. The accordance becomes worse in a height of 8.3 in. These differences are led back on the influence of the flange diminishing the cross-sectional distortion.

3.2.3.5 Investigation of Ribbed Columns

In order to compare the influence of some kinds of internal ribbing the measured deformations of the columns loading them in a height of 17.9 in are only taken into account.

3.2.3.6 Bending stiffness

The measured bending stiffnesses of the internally ribbed columns are related on the one of the unribbed column . In Figure 3.39 the normalized bending stiffnesses are given. The listing shows that the stiffness increases by ribbing approximately in proportion to the growth of the area moment of inertia. Of all tested columns the one with double diagonal ribbing stiffens the columns best. The increase of stiffness amounts up to 32 % whilst the other tested types of vertical ribbing increase the bending stiffness between 13 % to 21 % corresponding to the kind of ribbing. When considering the amount of material in the ribs which increases the bending stiffness by relating the stiffness to the total weight of each column respectively it becomes obvious when looking at Figure 3.39 that the weight increases quicker than the stiffness. Thus the bending stiffness of the unribbed column related to the weight is higher than those of the internally ribbed columns.

3.2.3.7 Torsional Stiffness

As shown in Chapter 3.2.3.4 the symmetrically applied couple of

forces distorts the cross-section of the unribbed columns and thus a considerably lower torsional stiffness is caused. For this reason the calculated stiffness due to a pure torsional deformation of the column has been chosen as a base to relate the measured stiffnesses of the ribbed column. As it is a theoretically calculated stiffness this value is marked in Figure 3.15 as "theoretical". For comparison only the test results of the loading height of 17.9 in are taken into account.

The normalized stiffnesses against torsion are listed in Figure 3.40. In opposite to the bending stiffness the stiffness against torsion can be increased by a top-plate which becomes evident comparing the unribbed and the ribbed columns with parallel ribbing. The stiffness against torsion of these columns without top-plate varies between 6.5 % and 15 % at the maximum whilst the columns with top-plate reach 51.6 % of the theoretical stiffness. With one diagonal rib the column reaches a stiffness of 65 % and the highest stiffness is measured at the column with double diagonal ribbing, and amounts up to 115 % of the theoretical stiffness. The diagonally ribbed columns with top-plate even show a higher stiffness but the difference to the ones without top plate is not as important as at the unribbed columns or those with ribs parallel to the outer walls. Also good results show the columns with horizontal ribs, these ribs suppress the cross-sectional distortion and thus stiffen the columns up to a stiffness equal to the stiffness of pure torsion.

The torsional stiffnesses related to the total weight of the columns show a tendency similar to the one of the bending stiffnesses. Choosing the torsional stiffness without cross-sectional distortion as a base this stiffness is not reached by any of the internally ribbed columns. From Figure 3.40 can be seen that the effectiveness of the material in ribs is best when ribbing the columns

with horizontal ribs. Two horizontal ribs and a top-plate give a torsional stiffness related to the weight of 96 % of the theoretical stiffness.

3.2.4 Test Method of Dynamic Investigations

In order to obtain characteristic data determining the dynamic behaviour the columns have been dynamically tested. They are loaded by a dynamic force of ± 100 p which is generated by an electro-dynamic exciter. The experimental arrangement is shown in the blockdiagram of Figure 3.41. According to bending and torsional loads the dynamic force is applied at three different points to the column as shown in Figure 3.42. The pick-ups are mounted on the column opposite to the exciter to measure the response curves. Exciting the columns at a corner on the top the columns vibrate at different frequencies in their bending and torsional modes, a few plate vibrations are incited as well. Applying the exciter force in the centre-line on the top of the columns the bending mode and plate vibrations are incited and when exciting the columns in the centre of a side wall mainly plate vibrations occur.

In all three positions of the exciter the response curves have picked up in a frequency range between 300 cps and 3000 cps. The body modes and plate vibrations are identified by measuring the amplitudes and directions of the vibrations at many points of the column so that the modes can be plotted. Of the body modes and and of some plate vibrations the damping coefficients have been determined from the decay curves.

3.2.4.1 Response Curves and Mode Shapes of Unribbed and Internally Ribbed Columns

In Figure 3.43 the resonance curves of 8 columns without top-

plate when exciting the columns at a corner on the top are shown. The resonance curves differ in their shape except that two resonance peaks can be found at almost the same frequencies. They are the resonance frequencies of the bending mode at 450 cps and the one of the torsional mode at 1300 cps. These resonance frequencies change only very little although the stiffnesses of the columns against bending and torsional loads alter for relatively large amount corresponding to the different types of ribbing. But as the vibrating mass is changed by the ribs as well stiffness and mass are altered about the same amount and thus the resonances of the bending and torsional modes remain at their frequencies independent from the type of ribbing.

A resonance frequency which changes between 450 cps and 750 cps according to the different internal ribbing is the one of the torsional mode with cross-sectional deformation. The frequencies of this mode shape vary in such a large range because the stiffness of the cross-section against distortion alters so much.

The mode shapes of these 3 body modes of the whole column are drawn in Figure 3.44. They are the mode shapes which are of interest in a dynamic analysis of the structure.

Any resonances else which have been measured at the columns have been determined as plate vibrations of the outer walls or of the ribs respectively. But unlike to the resonances of the body modes no relationship can be found between the resonance frequencies and mode shapes of the plate vibrations in the response curves of the different columns. The plate vibrations are influenced by the internal ribbing and thus the resonance frequencies of similar shape of the plate vibrations differ between the columns.

Most resonance frequencies of plate vibrations have been determined at the unribbed and diagonally ribbed columns. Some of these mode shapes are represented in Figure 3.40. At the columns

with horizontal ribs and those with internal ribs parallel to the outer walls the number of resonances of plate vibrations is small in the frequency range up to 2000 cps. This is led back to the fact that the horizontal ribs and the ones prallel to the outer walls devide them into smaller diaphragms. Thus resonances of lower frequencies are suppressed.

Not only internal ribbing but also a top-plate which closes the column at the top diminishes the number of plate vibrations as it can be seen from a comparison of the response curves of the columns with and without top-plate. These response curves are represented in Figure 3.46. At the column with top-plate even the torsional mode with cross-sectional distortion does not appear, because the exciting force is in this case applied to the column near to the top-plate and the top-plate suppresses the cross-sectional distortion.

For two other points of force application the response curves of the C columns are shown in Figure 3.47 and 3.48. The results derived from these curves are the ones that for improving the dynamic behaviour of columns plate-vibrations must be suppressed as it is possible for example with horizontal ribs. Another way to avoid plate vibrations is to stiffen the plates by wall ribbing. In order to check the influence of wall ribbings on the dynamic behaviour of columns some types of wall ribbing have been tested. The results of these test are discussed in the following chapters.

3.2.5 Tested Columns with Wall Ribbing

The dimensions of the columns with wall ribbing are like those of the internally ribbed columns and they are tested in an equal way. In this investigation three different types of wall ribbing are tested. They are shown in Figure 3.49. The columns of type A,D have horizontal wall ribs around the column. Type B,E is derived from type A by adding a

vertical rib in the centre line of each wall from the bottom to the top of the column and type C,F is a variation of type A which is originated be dividing the fields between the horizontal ribs diagonally.

3.2.5.1 Results of Static Tests

As the wall ribs add only a little to the area moment of inertia but on the other hand the weldings weaken the structure because of the notch effect the columns with wall ribbing do not reach the bending stiffness of the unribbed column which becomes obvious by looking at the diagram in Figure 3.50. The stiffness against torsion yet has been improved a little by the wall ribs. This mainly is caused by the horizontal ribs which detain the cross-sectional distortion. The torsional stiffness of columns with wall ribs is listed in Figure 3.51. From that figure can be seen that the columns of type F with 4 horizontal and diagonal wall ribs is stiffest although there still remains a remarkable amount of cross-sectional distortion.

3.2.5.2 Results of Dynamic Tests

Figure 3.52 and 3.53. show response curves of the tested columns. In Figure 3.52 response curves of six columns are given when exciting them at a corner on the top. These response curves indicate that the wall ribs do not change the frequencies of the body modes but avoid a lot of the plate vibrations which are incited at the unribbed column (see Figure 3.40). Looking at Figure 3.53, which shows the response curves of the columns when exciting them on the top in the centre of a wall the effectiveness of the wall ribs becomes obvious. Up to frequencies near to the one of the pure torsional mode plate vibrations can be avoided by wall ribbing. In dynamic tests of large machine tools it has been proved that the frequency of the pure torsional

mode of the column can be assumed as a border up to which resonance frequencies of columns are of interest. Frequencies of a column higher than the one of the torsional mode in most cases do not influence the dynamic characteristic of the whole machine

3.2.6 Damping Coefficients and Mode Shapes

Besides the number of resonances and the resonance frequencies the damping coefficient is an important parameter which determines the dynamic characteristic of a structure. As it is necessary to know the exact damping coefficients for a calculation of cross response curves the damping coefficients in the different mode shapes of the tested columns have been measured. The results of the damping measurement are plotted in the diagram of Figure 3.54. From the diagram can be seen, that for different body mode shapes different damping coefficients exist. In the bending mode the highest damping coefficients have been measured. The coefficients vary in a large range thus no definite value can be given for a computation. For the torsional mode with cross-sectional distortion the damping coefficients lie near a mean value which amounts a quarter of the mean value of the one of the bending mode. The damping coefficient of the pure torsional mode is a little higher and varies a bit wider than the ones of the torsional mode with cross-sectional distortion.

From Fig. 3.54 can be deduced that for each body mode a damping coefficient exists in a certain range which differs definitely from the others. Although at the moment it is not possible to predict the damping coefficients of a structure it is thought possible that by systematic investigations a list of damping coefficients can be set up in order to enable more exact computations of cross-response curves.

The plate vibrations in most cases are not of interest in a dynamic analysis of a machine tool structure because in

a well designed structure plate vibrations must not occur. Thus only a few damping coefficients of different modes of plate vibrations have been measured to check the amount of these coefficients. They are all near the damping coefficients of the torsional modes.

3.2.7 Deductions from the Model Tests

From the static and dynamic investigations of the simplified models of columns a few important points of view can be derived which should be taken into account when designing columns of machine tools.

To obtain a respectable static stiffness of a column the stiffness against bending and torsional loads have to be determined independently because a structure which is stiff against bending is not necessarily stiff against torsional loads. To optimize the bending stiffness of a column the cross-section should be designed as large as possible or for given dimensions of a cross-section the outer walls should be thickened instead of adding internal ribs to stiffen the structure. Any internal ribbing will not increase the bending stiffness as much as an equal amount of material which is used to thicken the outer walls.

In Figure 3.55 a list of normalized cross-sectional values as area, area moment of inertia and area moment of inertia related to the area of unribbed and ribbed cross-sections is given. All cross-sectional values are related to the ones of an unribbed square cross-section 6.24 in by 6.24 in and 0,157 in (4mm) wall thickness. For each ribbed cross-section the afore mentioned values of two unribbed cross-sections are computed when distributing the material of the ribs evenly to the outer walls. In the first case the wall thickness is growing to the inner and in the second case it is growing to the outer of the cross-section. From Figure 3.55 can be seen that i.e.

2 diagonal ribs increase the area moment by 28 % whilst distributing the material of the ribs to the outer walls the area moment grows by 69 % or 74 % respectively.

The torsional stiffness when loading a column by a couple of forces can essentially be increased by internal ribs which suppress a cross-sectional distortion. Another way to obtain a sufficient torsional stiffness is to choose a cross-section which does not distort if the acting forces are applied properly. Such a cross-section for example is a circle.

Conclusions

With regard to optimum use of machine tools in manufacturing plants it is important and necessary to know those machining conditions definitely, where the installed machine power can be turned to profit as far as possible without chatter occuring.

After having extensively studied the fundamentals of the chatter behavior of machine tools, a procedure could be developed, and has been detailed in this report, by means of which clear and understandable diagrams of the chatter behavior of lathes and milling machines can be produced theoretically. Based upon the theory of regenerative chatter a mathematical model of the system machine tool - cutting process has been established, of which the stability analysis can easily be carried out by applying the Nyquist-Criterion.

In practice numerous parameters and machining conditions must be taken into account, when carrying out a complete stability analysis of a machine. Because of this fact different digital computer programs have been developed for the quick and economical performance of extensive chatter investigations in consideration of the practically interesting conditions. Some results of chatter investigations on a lathe and a milling machine have been discussed as characteristic examples.

From theoretical and practical studies into the chatter behavior carried out so far, three test procedures result, which in the future can offer the possibility to provide the necessary data for specifying machine tool chatter behavior. However, further extensive investigations and discussions between the manufacturers and the machine tool users seem to be necessary, before one of these procedures will prove as the optimum one and before definite machine tool chatter specifications can be laid down.

The methods for precalculating the static and dynamic behavior of machine tool systems as briefly described in this Final Report and in more detail in the according Quarterly Reports are found out very helpful during the design processes. These methods developed under this contract cover a wide range of problems which could not or only unsufficiently be solved so far.

However, it should be pointed aut that still problems occur, when dealing with the static and dynamic behavior of connection points within a structuree. g. between elements or at the foundation.

If these parameters - as in several cases - may be neglected, the above mentioned methods and corresponding programs work very well. In cases of high influences due to connection - conditions between the elements of a system the overall behavior can only be determinated qualitativly so far. In this cases nevertheless the possibility to compare some given suggestions in form of different designed structures is given by eleminating the above mentioned influences.

In a theoretical analysis some equations have been derived to calculate the bending deflections of a column when taking the influence of shear force into account and moreover equations have been formulated to calculate the torsional deformation of a column loaded by a couple of forces which distort the cross-section. The influence of shear force and the one of cross-sectional distortion as a function of the loading has been pointed out.

In tests of models of unribbed columns the theoretically derived equations have been proved. In order to analyse the influence of internal ribs on the static stiffness a number of models of columns have been tested and the results presented show that for optimizing the bending stiffness the material is best used not by adding ribs to a column but in thickening

the outer walls or in enlarging the cross-section. Whilst the torsional stiffness loading a column of rectangular cross-section by a couple of forces is increased in the best way by adding diagonal or horizontal ribs or by choosing a circular cross-section. Furthermore it turned out from the static tests of columns with wall ribs that this kind of ribbing does not sufficiently stiffen the columns neither against bending nor against torsional loads.

Plate vibrations can create relatively large deformations of a column. From dynamic tests of the internally ribbed columns it turned out that plate vibrations can be avoided at lower frequencies by dividing the large areas of the side walls by for example horizontal ribs. But the best way to suppress plate vibrations is thought in stiffening the walls by types of wall ribbing which divide the walls into sufficiently small areas between the ribs. This postulation has been proved by tests of columns with different types of wall ribs. The dynamic test of these columns indicate the plate vibrations can be avoided by wall ribbing up to frequencies near to the first pure torsional mode.

References

1. Danek, O.
   Polacek, M.
   Spacek, L.
   Tlusty, J.
   Selbsterregte Schwingungen an Werkzeugmaschinen
   VEB Verlag 1962

2. Dregger, E.U.
   Roese, H.
   Möglichkeiten zur Berechnung und Erhöhung der Stabilitätsgrenze beim Fräsen
   Industrie-Anzeiger, 88 (1966), Nr. 15 und 24

3. Dreyer, W.
   Modelluntersuchungen an Werkzeugmaschinenständern
   Industrie-Anzeiger Nr. 23, 21.3.1967

4. Fishwick, W.
   Tobias, S.A.
   Eine Theorie des regenerativen Ratterns an Werkzeugmaschinen
   Maschinenmarkt 1956, Nr. 17, WP 25

5. Föppl, A.
   Vorlesungen über Technische Mechanik
   III. Band, Festigkeitslehre
   Verlag R. Oldenbourg, 1943

6. Gurney, J.P.
   Tobias, S.A.
   A Graphical Method for the Determination of the Dynamic Stability of Machine Tools
   Int. J. Machine Tool Des. Res., 1 (1961)

7. Lemon, J.
   Control of Forced Vibration in Machine Tool/Metal Cutting Systems
   Technical Report AFML-TR-67-88

8. Long, G.W.
   Kegg, R.L.
   Effect and Control of Chatter Vibrations in Machine Tool Processes
   Final Report AF ML-TR-65-177

9. Long, W.G.
   Hohn, E.
   Kegg, R.
   The Effect and Control of Chatter Vibrations in Machine Tool Processes
   Technical Report AFML-TR-68-35 Project 7-771

10. Opitz, H. — Effect and Control of Chatter Vibrations in Machine Tool Vibrations
Final Report, AF 61 (052)-713

11. Opitz, H. — Chatter Behavior of Heavy Machine Tools
Quarterly Technical Reports AF 61 (052)-916 Nr. I

12. Opitz, H. — --- Nr. II

13. Opitz, H. — --- Nr. III

14. Opitz, H. — --- Nr. IV

15. Opitz, H. — --- Nr. V

16. Opitz, H. — --- Nr. VI

17. Opitz, H. — --- Nr. VII

18. Opitz, H. — --- Nr. VIII

19. Opitz, H. — Effect and Control of Chatter Vibrations in Machine Tool Processes
Quarterly Technical Reports AF 61 (052)-966/I-VII, Final Report

20. Peters, J. Vanherck, P. — Ein Kriterium für die dynamische Stabilität von Werkzeugmaschinen
Industrie-Anzeiger 85 (1963), H. 11 und 19

21. Tobias, S.A. — Schwingungen an Werkzeugmaschinen
Carl Hanser Verlag, München 1961

22. Weck, M. — Anwendung der "Systemanalyse mit regellosen Signalen" zur theoretischen Vorherbestimmung der Rattergrenze
Industrie-Anzeiger, 90 (1968), Nr. 59

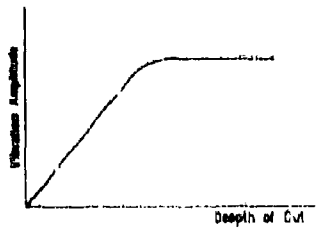

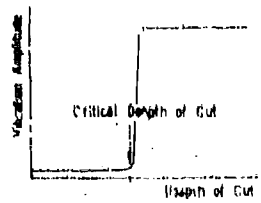

a) Forced Vibration b) Self excited Vibration

Fig. 1.1 Qualitative Dependency of the Vibration Amplitude from the Depth of Cut

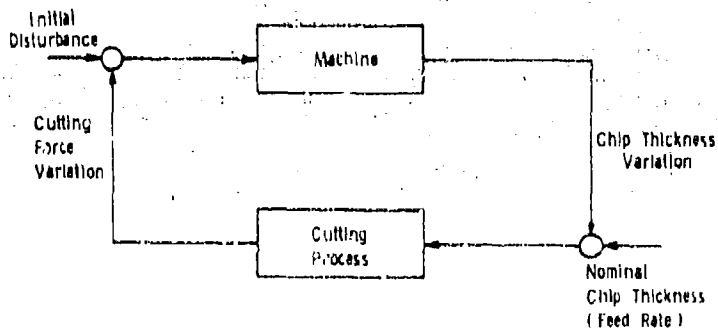

Fig. 1.2 Block Diagram of the Dynamic Machining Process

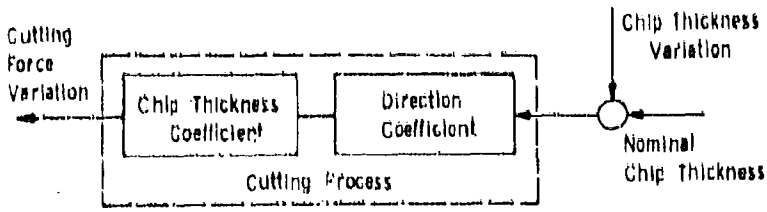

Fig. 1.3 Block Diagram of the Cutting Process

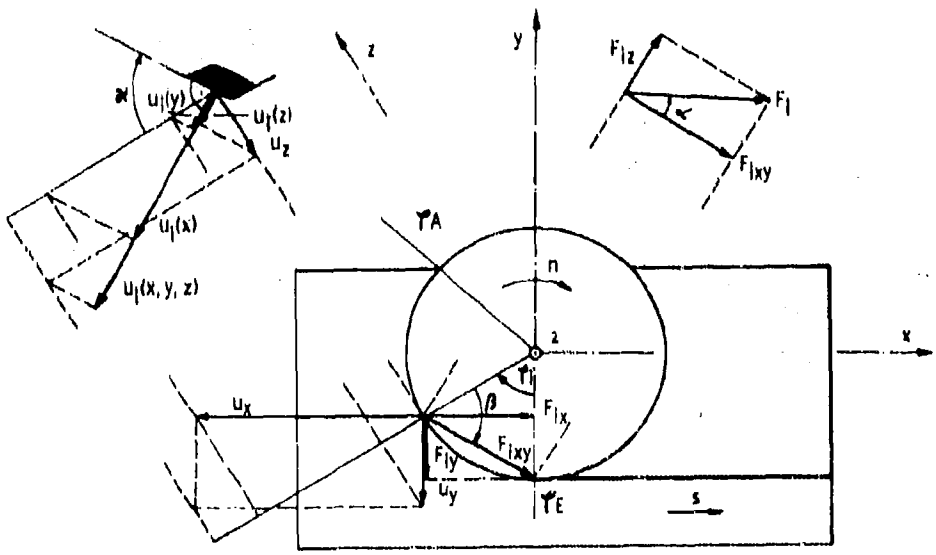

Fig. 1.4 Cutting Force and Chip Thickness Variation in Face Milling

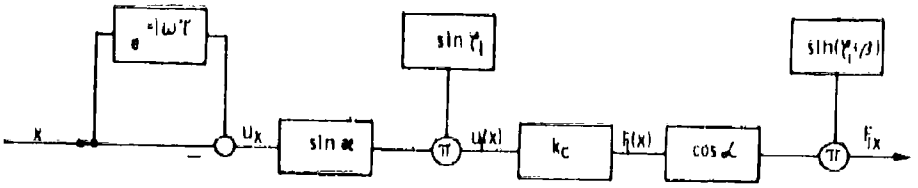

Fig. 7.5 Relationship between a Relative Displacement at the Cutting Point and the Cutting Force Variation at the i-th Tooth

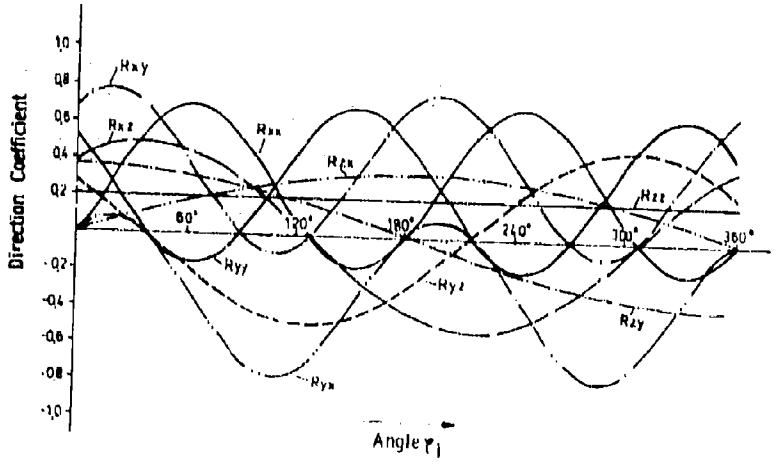

Fig. 7.6 Dependency of the Direction Coefficients from the Angle φ ; ($\alpha = 24^\circ$; $\beta = 67^\circ$; $\varkappa = 60^\circ$)

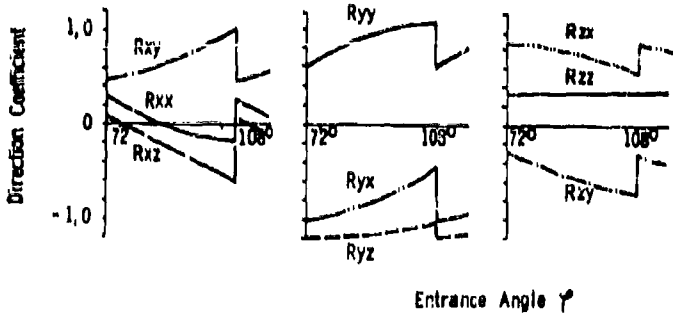

Fig. 1.7 Time-Variant Direction Coefficients of a System with Three Degrees of Freedom (α = 24°; β = 67°; $\varkappa$ = 60°; z = 10)

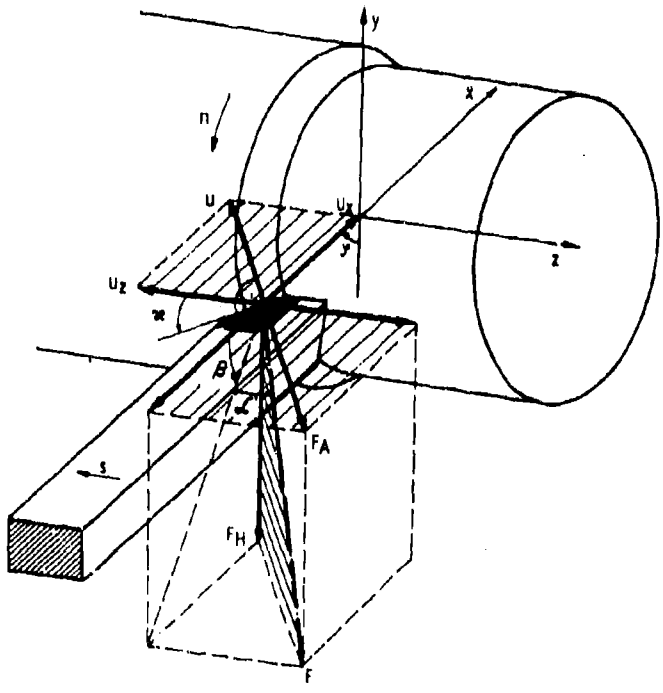

Fig. 1.8 Cutting Force and Chip Thickness Variation in a Turning Operation

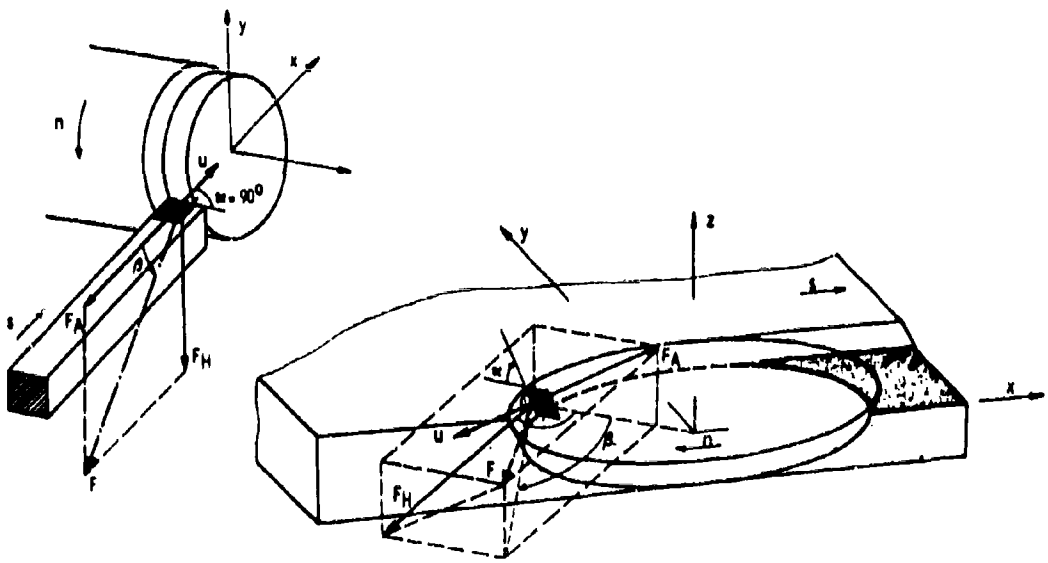

Fig. 1.9 Orthogonal Turning Process and Milling Process

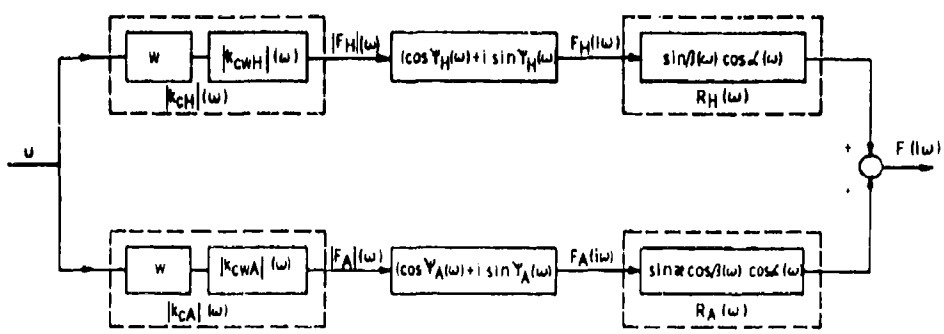

Fig. 1.10 Rolationship between Chip Thickness Variation and Cutting Force Variation for Complex Transfer Behaviour of the Cutting Process ($\Psi_{II}(\omega) \neq \Psi_A(\omega)$)

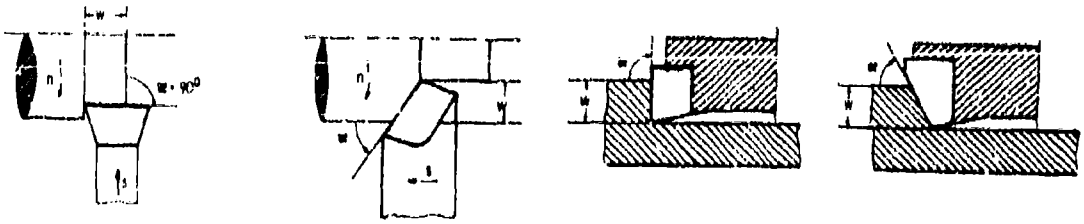

Orthogonal Turning | General Turning | Milling $\kappa = 90^{\circ}$ | Milling $\kappa \leq 90^{\circ}$

Fig. 1.11 Definition of the Width of Cut in Turning and of the Deapth of Cut in Milling

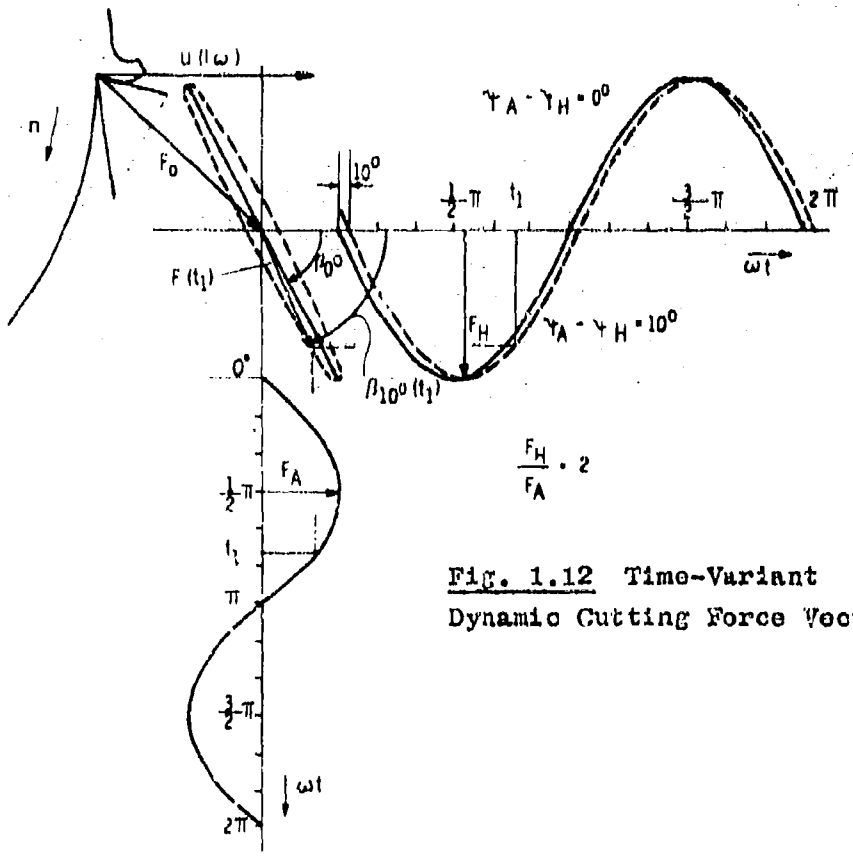

Fig. 1.12 Time-Variant Dynamic Cutting Force Vector

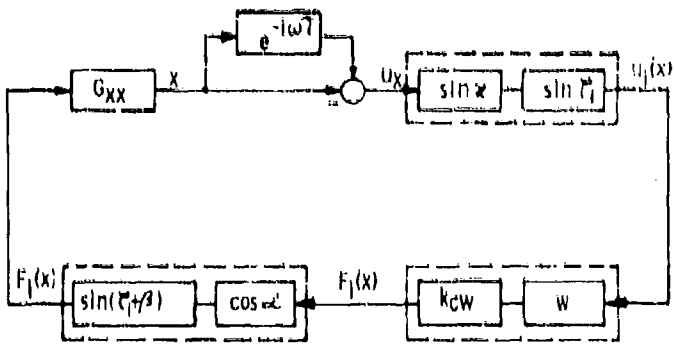

Fig. 1.13 Block Diagram of a Machining Process System with One Degree of Freedom

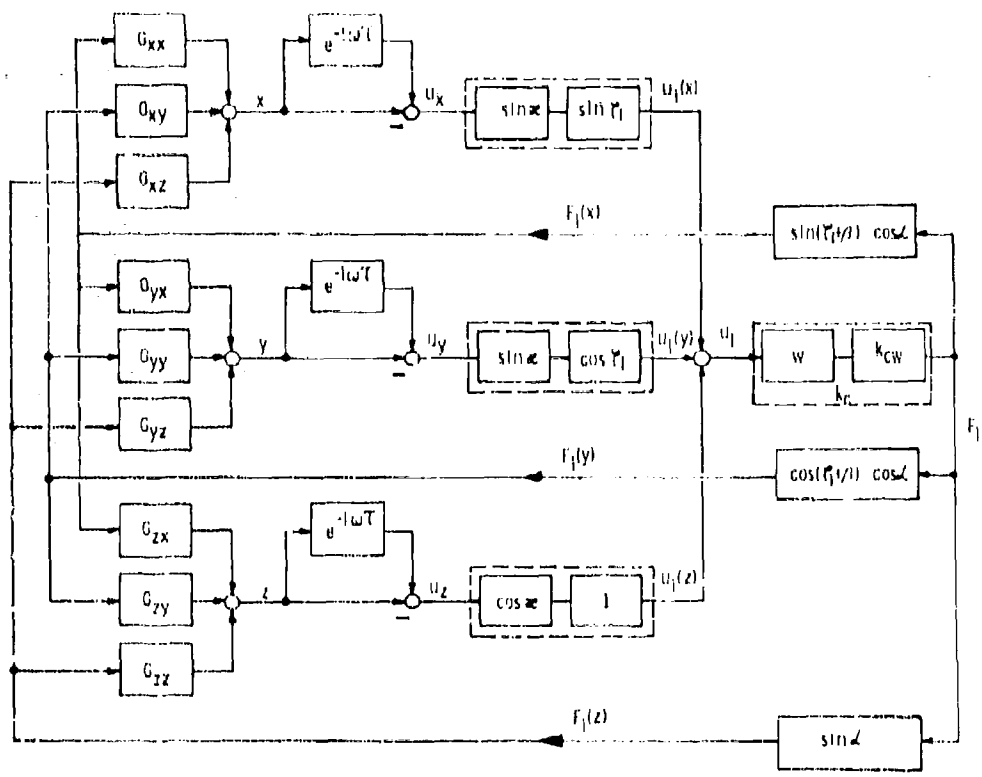

Fig. 1.14 Block Diagram of a Machining Process; System with Three Degrees of Freedom

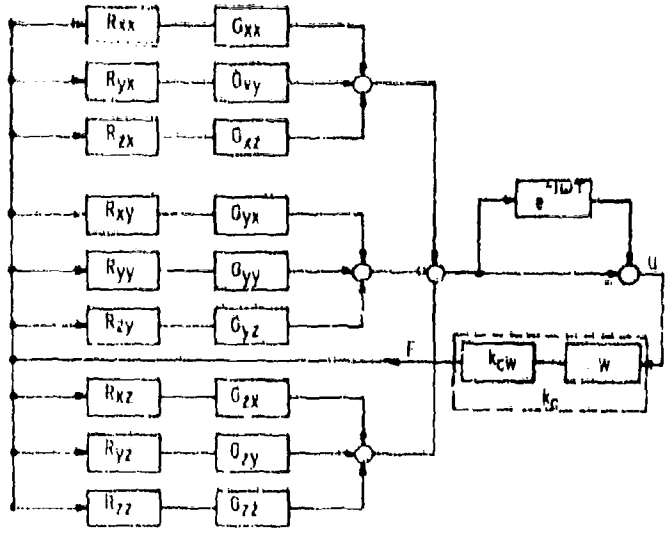

Fig. 1.15: Simplified Block Diagram of a Machining Process System with Three Degrees of Freedom

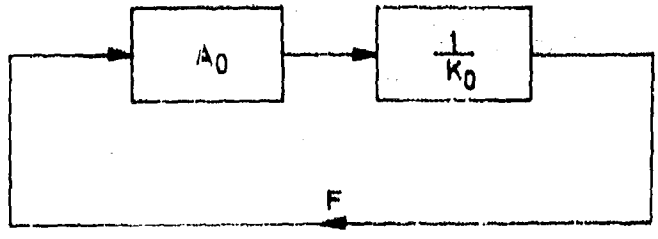

Fig. 1.16 General Block Diagram of a Machining Process

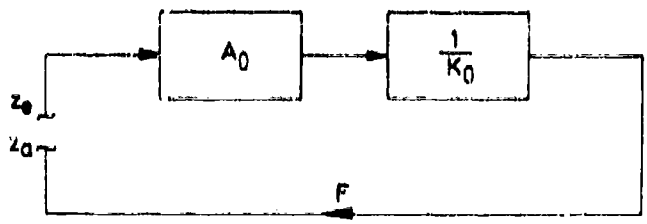

Fig. 1.17 Block Diagram of the Open Control Loop

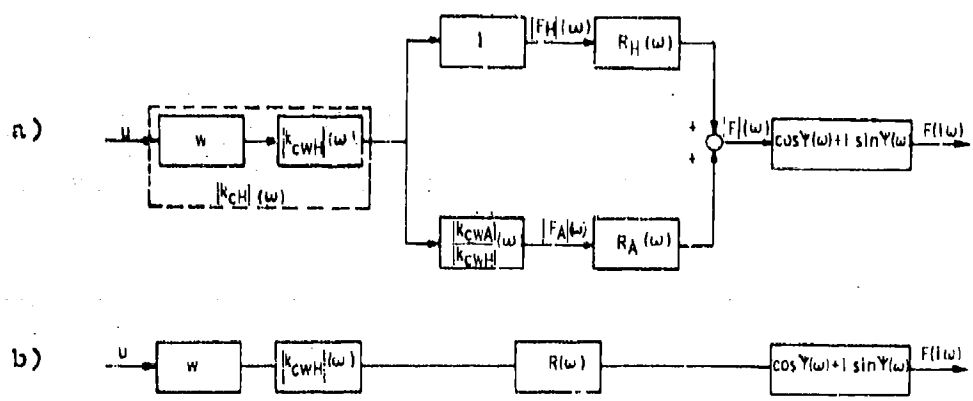

Fig. 1.18 Cutting Process with Complex Transfer Behaviour ($\Psi_H(\omega) = \Psi_A(\omega) = \Psi(\omega)$)

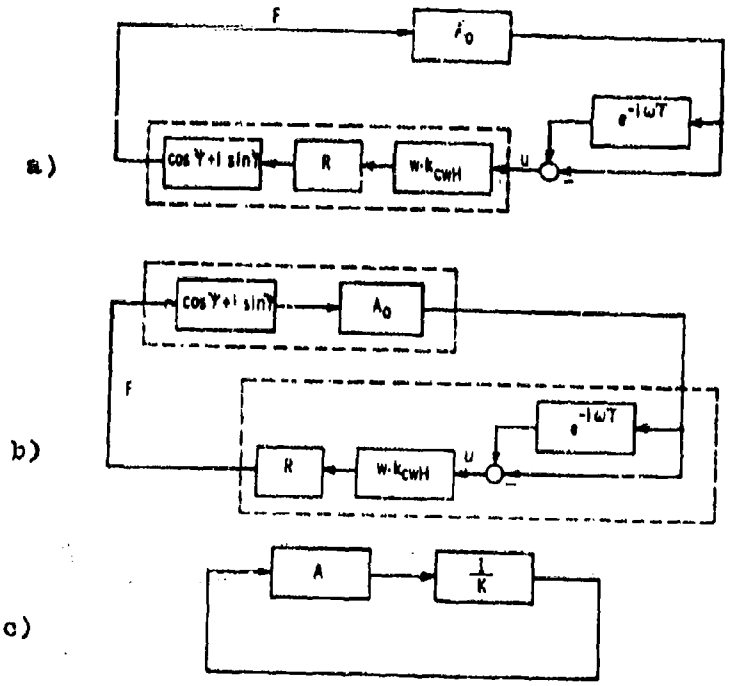

Fig. 1.19 Block Diagram of a Machining Process with Complex Transfer Behaviour of the Cutting Process

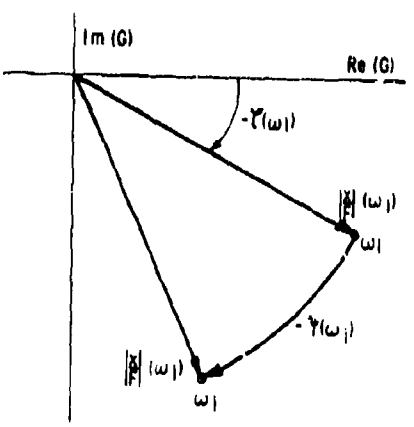

Fig. 1.20 Rotation of a Compliance Vector in the Machine Response Locus by a Complex k_c - Value

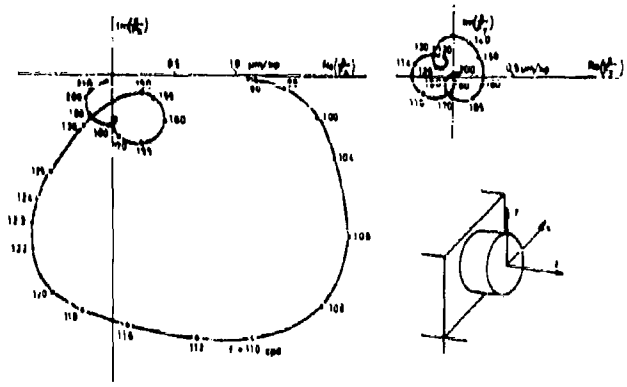

Fig. 1.21 Response Loci G_{xx} and G_{xy} of the Tested Lathe

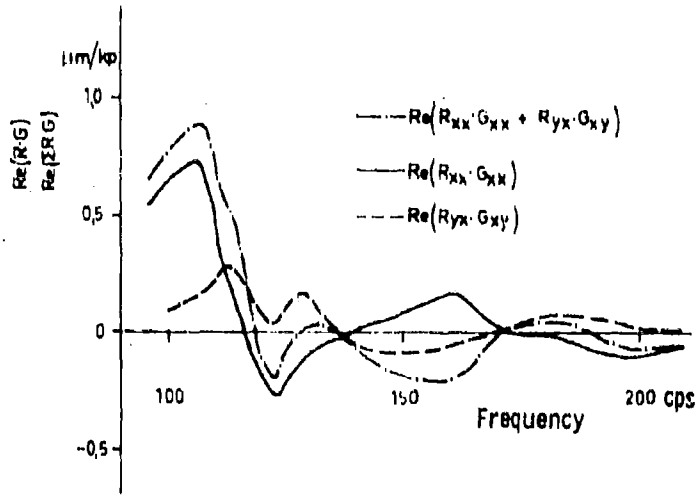

Fig. 1.22 Graphical Determination of the Greatest Negative Real Part of ($R_{xx} \cdot G_{xx} + R_{xy} \cdot G_{xy}$)

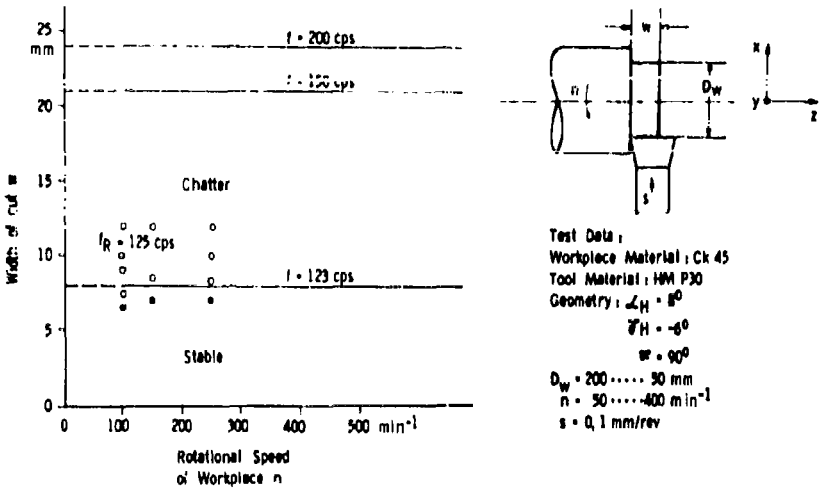

Fig. 1.23 Theoretical and Experimental Stability Chart of the Orthogonal Turning Process

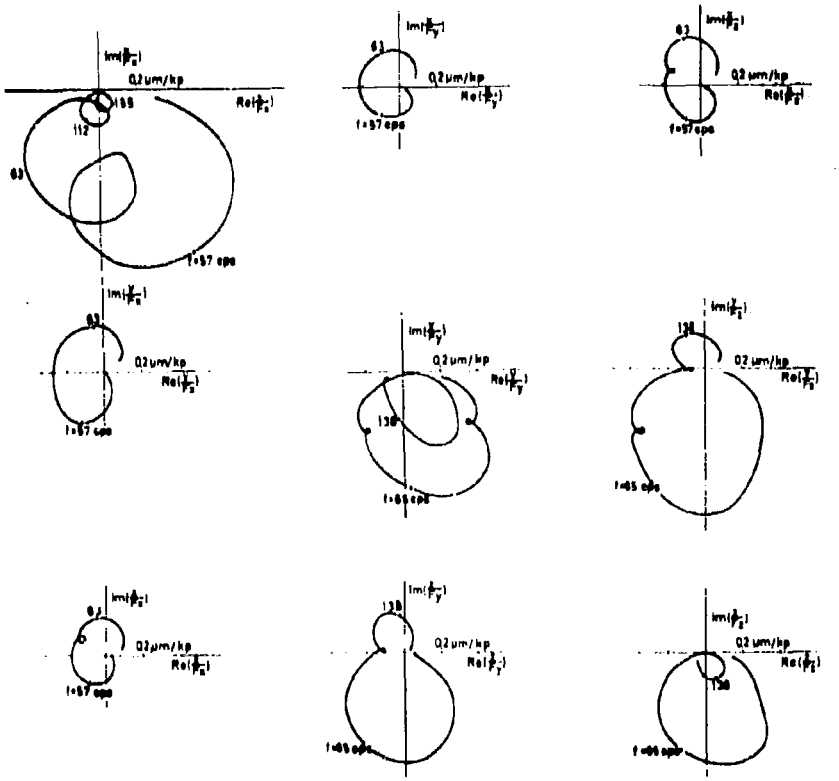

Fig. 1.24 Response Loci of the Tested Vertical Milling Machine

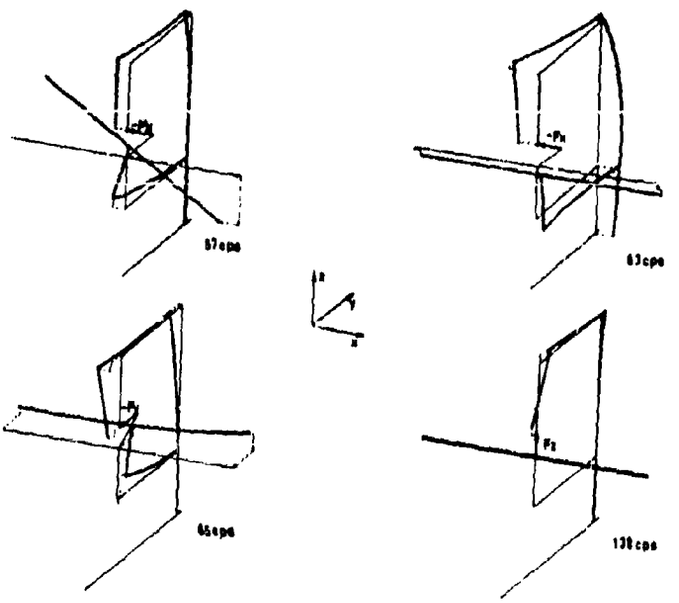

Fig. 1.25 Vibration Modes of the Tested Vertical Milling Machine

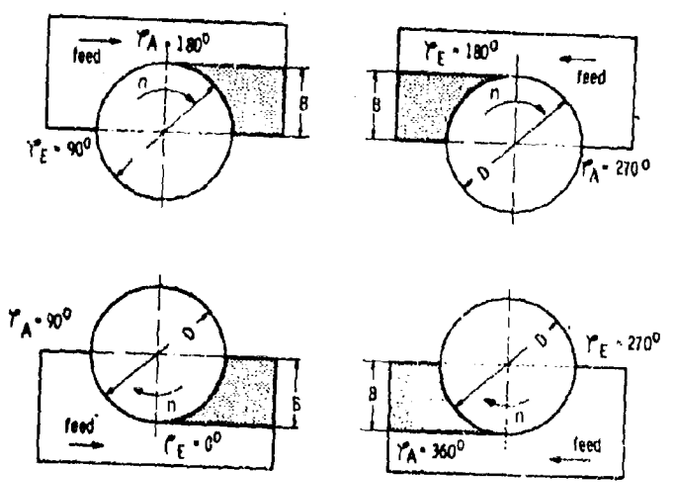

Fig. 1.27 Tested Milling Configurations

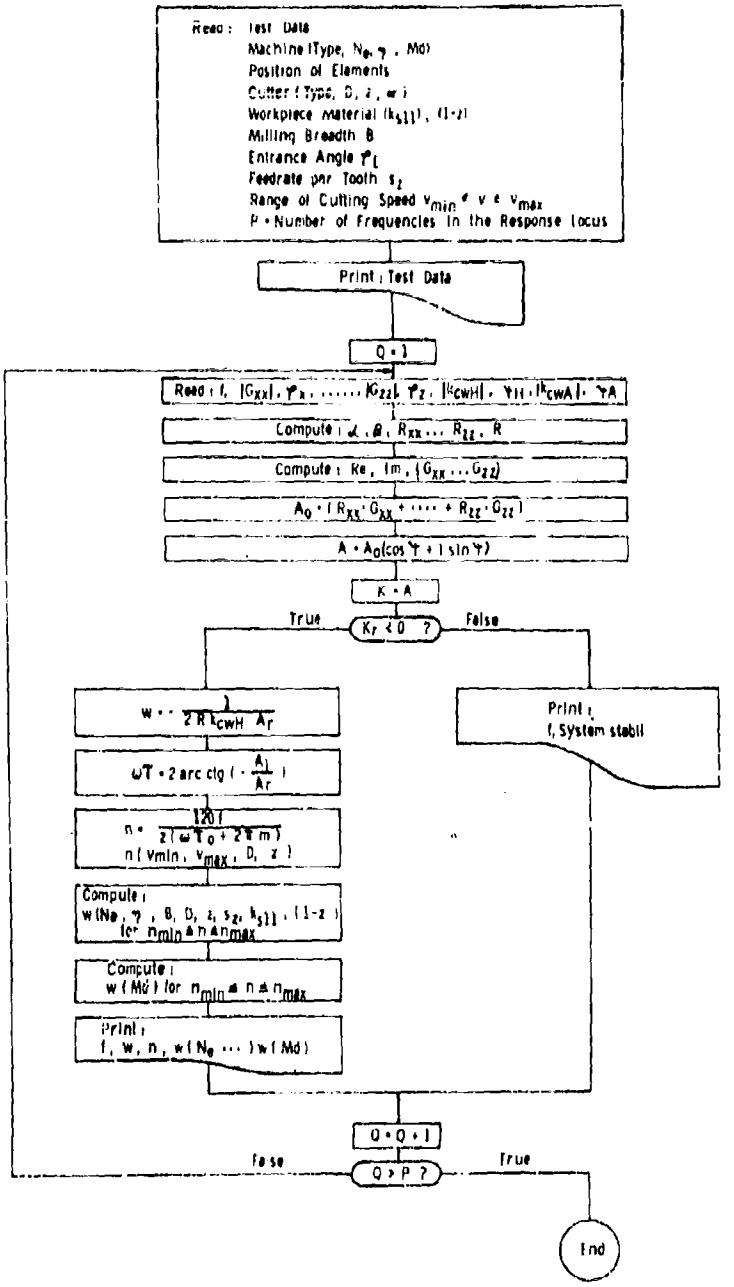

Fig. 1.26 Flow Chart of the Computor Program RATTER 1

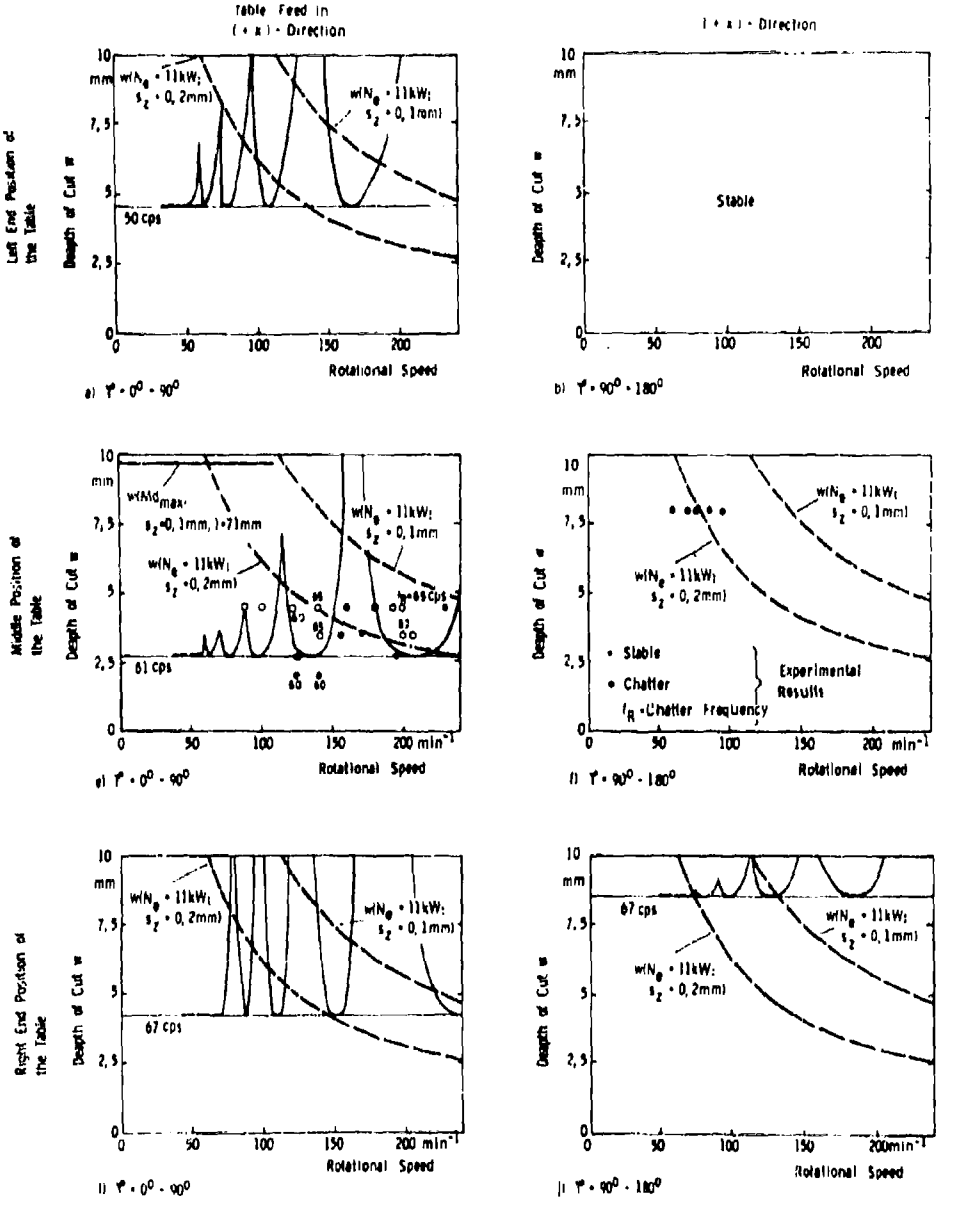

Fig. 1.28 Theoretical and Experimental Stability Charts of the Vertical Milling Machine

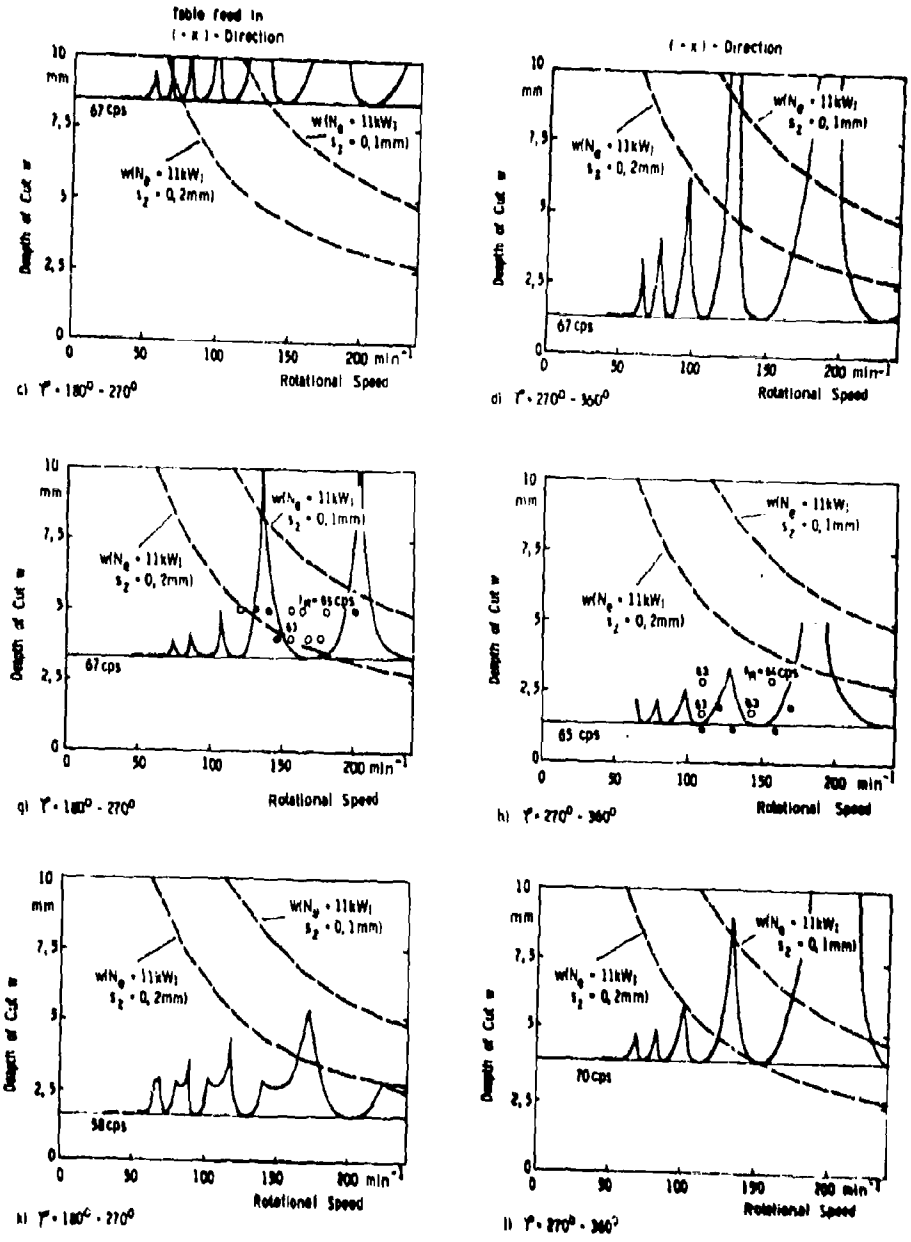

Fig. 1.28 Theoretical and Experimental Stability Charts of the Vertical Milling Machine (Continued)

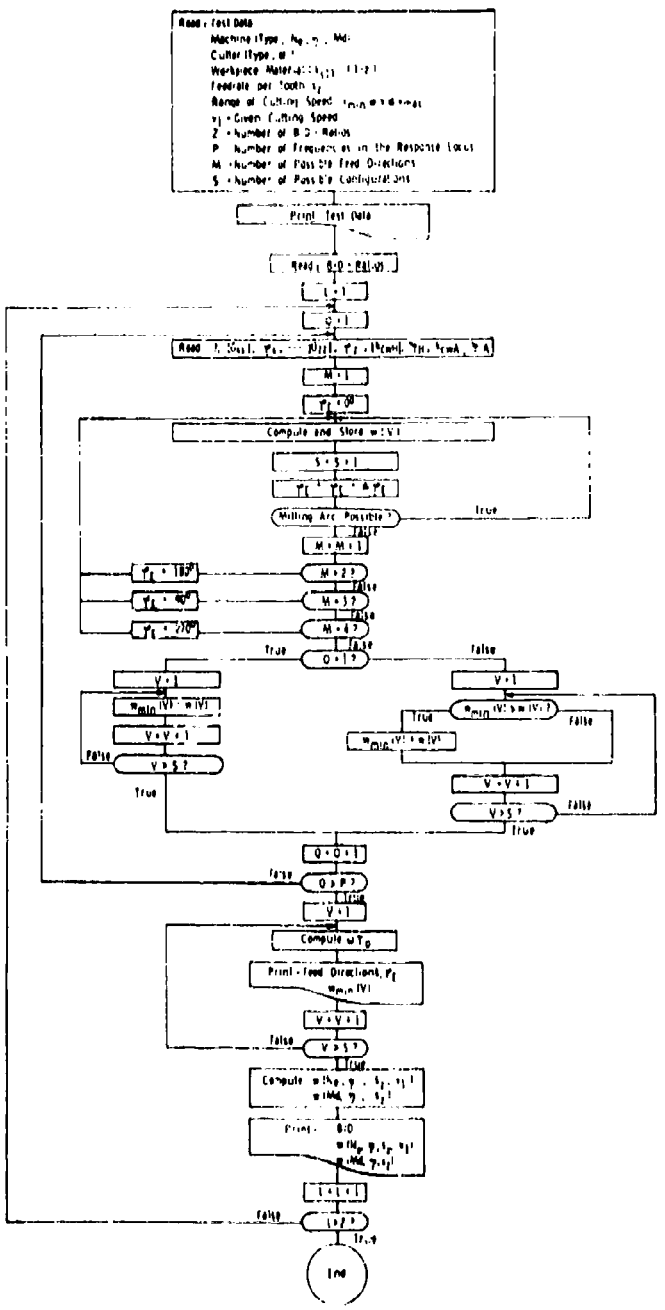

Fig. 1.20 Flow Chart of the Computer Program RATTER 2

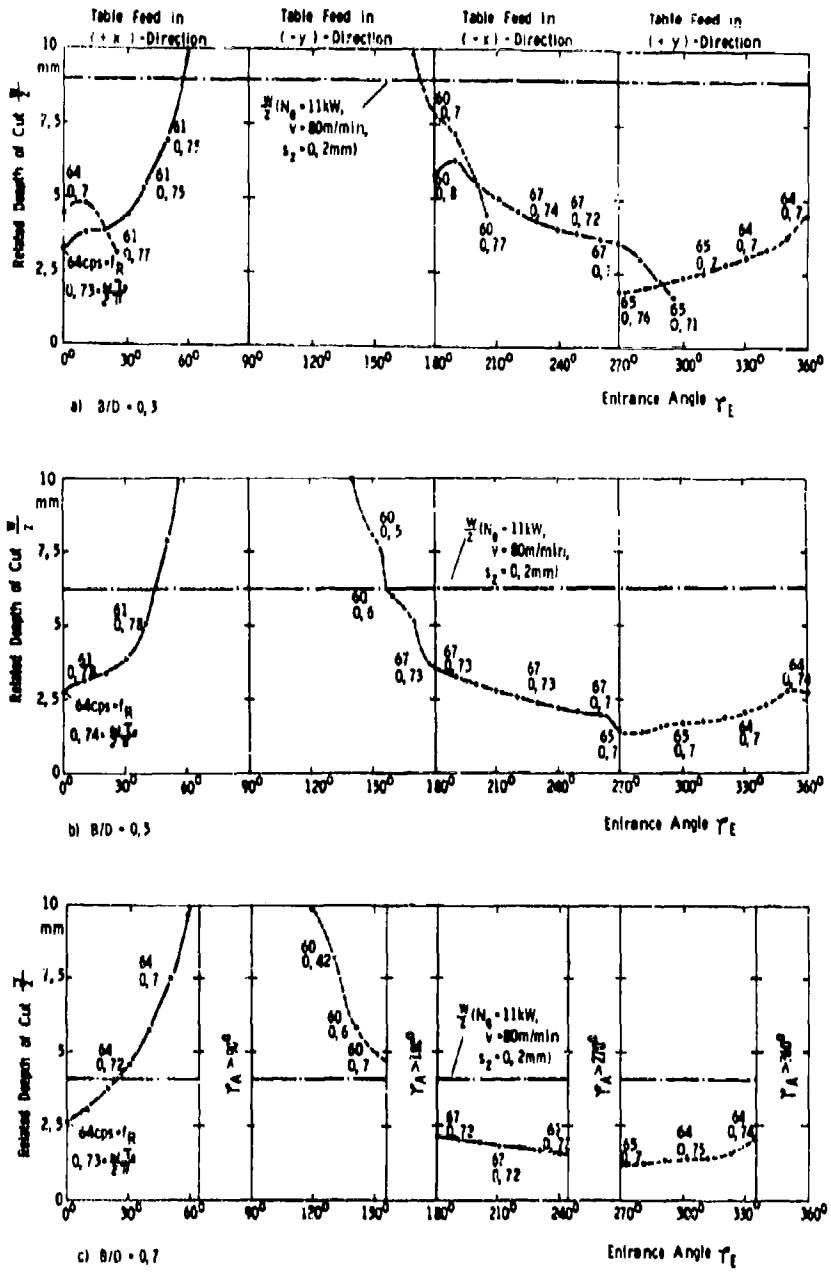

Fig. 1.30 Dependency of the Critical Deapth of Cut from the Entrance Angle φ_E

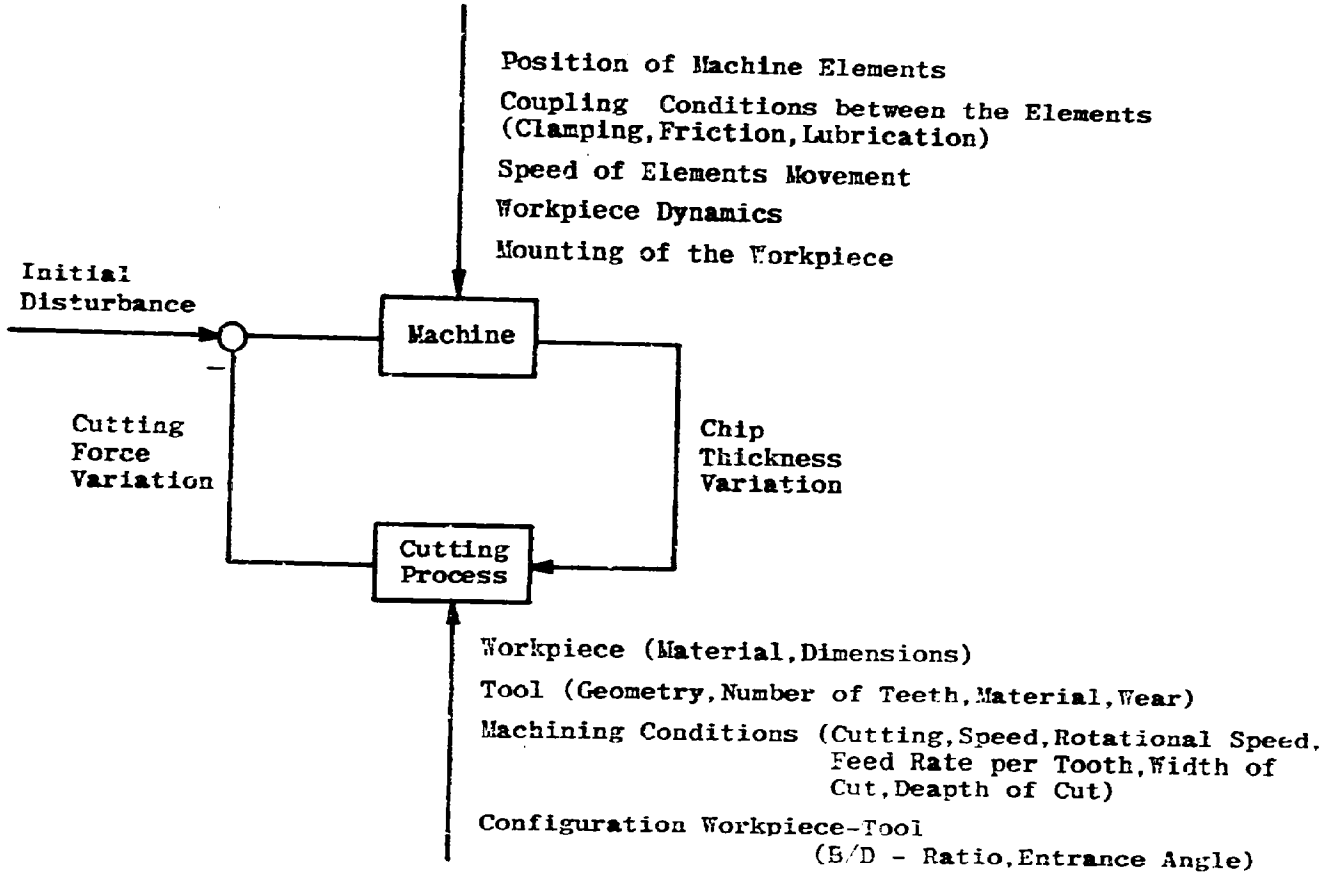

Figure 2.1 : Influences upon the Chatter Behavior of Machine Tools.

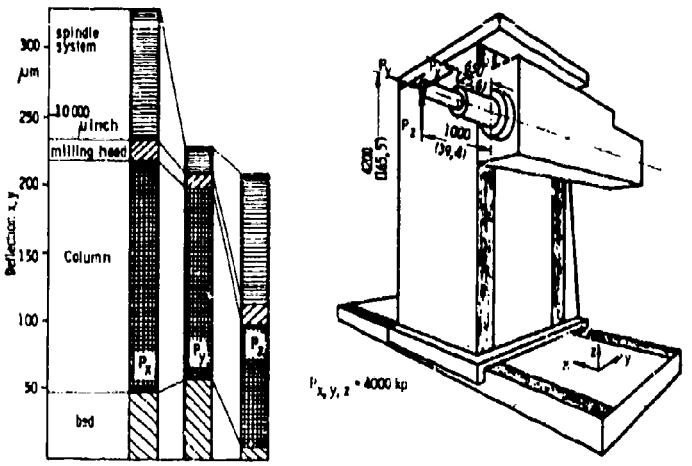

Fig. 3.1 Flux of Force Analysis

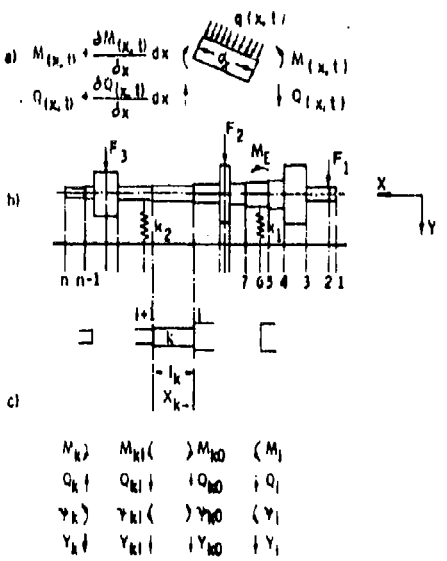

Fig. 3.2 Force and Deformation Qualities on a Spindle Section

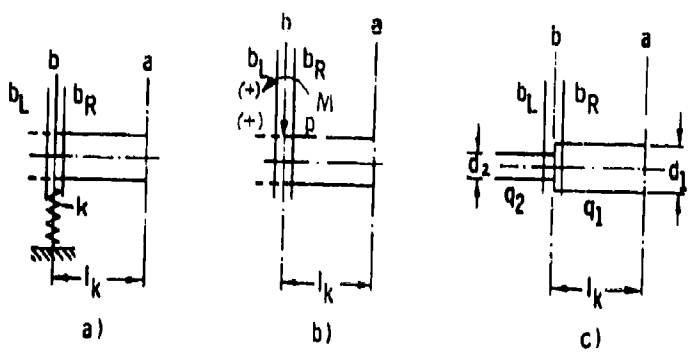

Fig. 3.3 Special Effects at Section Ends

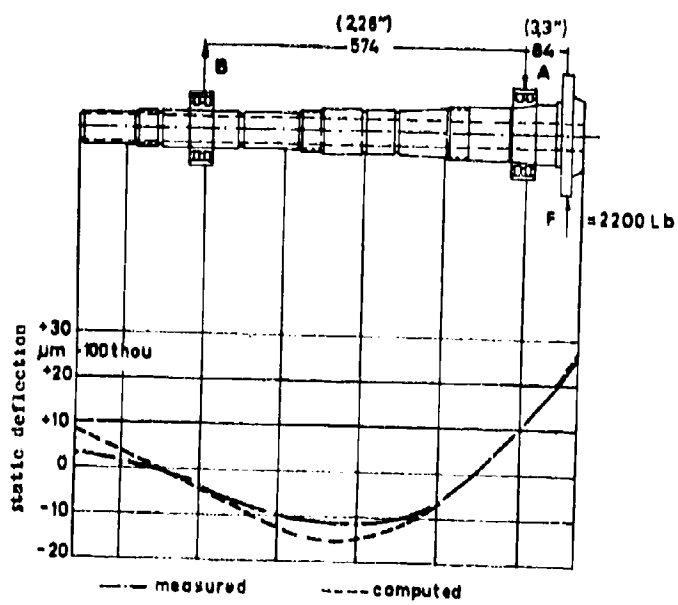

Fig. 3.4 Static Bending Line

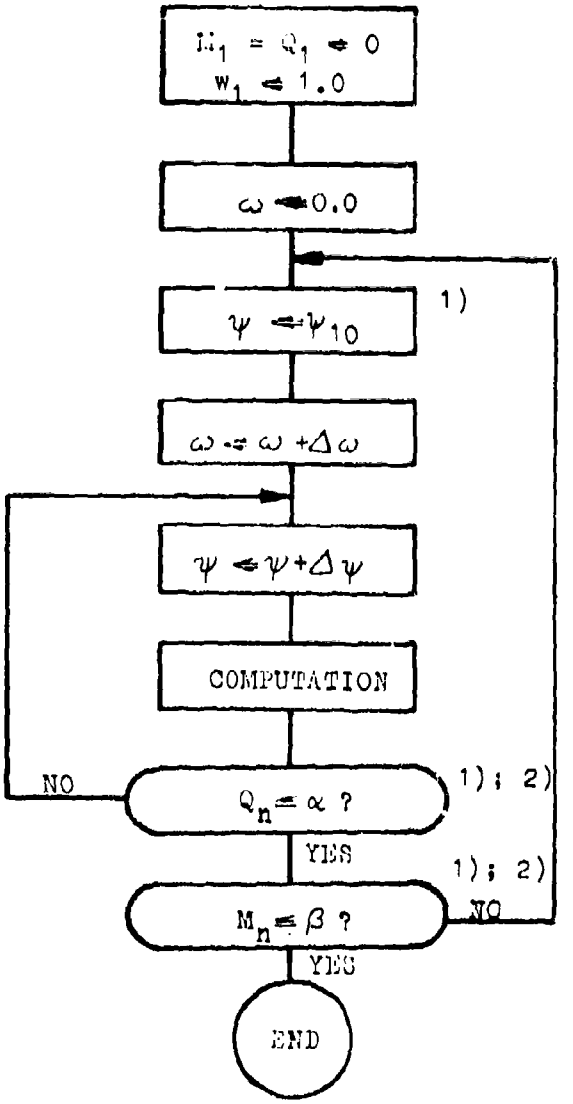

1): α, β and ψ_{10} are discrete values
2): criterion can be realized by an iteration

Fig. 3.5 Block Diagram for Calculating the Natural Frequency and Mode Shape

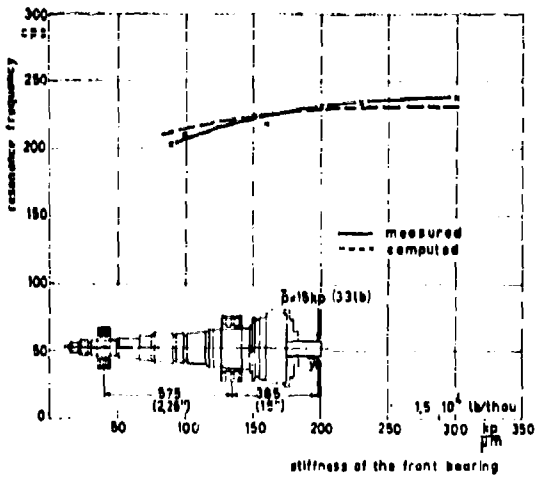

Fig. 3.6 Resonance Frequency for different Stiffnesses of the Front-Bearing

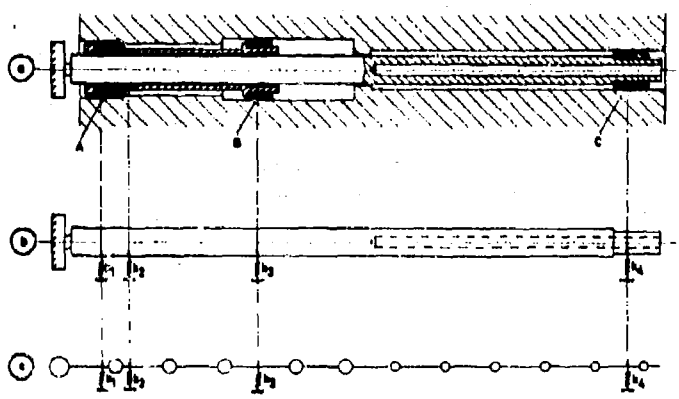

Fig. 3.7 Computer Model of a Boring Spindle System

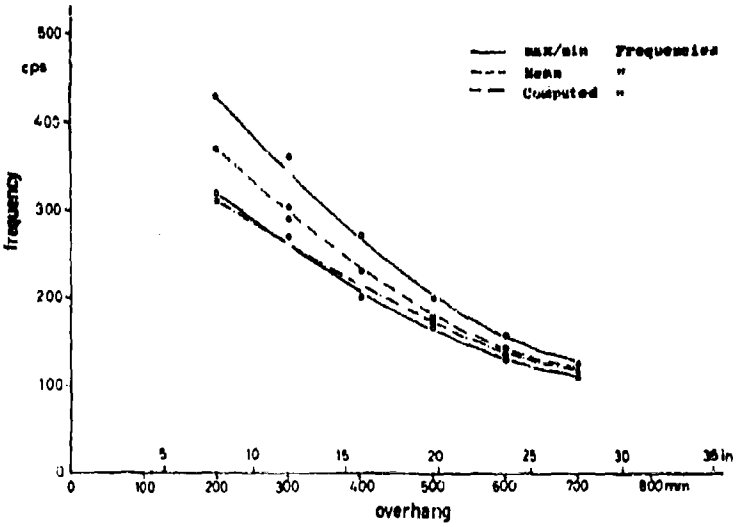

Fig. 3.8 Relationship between Natural Frequency and Overhang for a Boring Spindle System

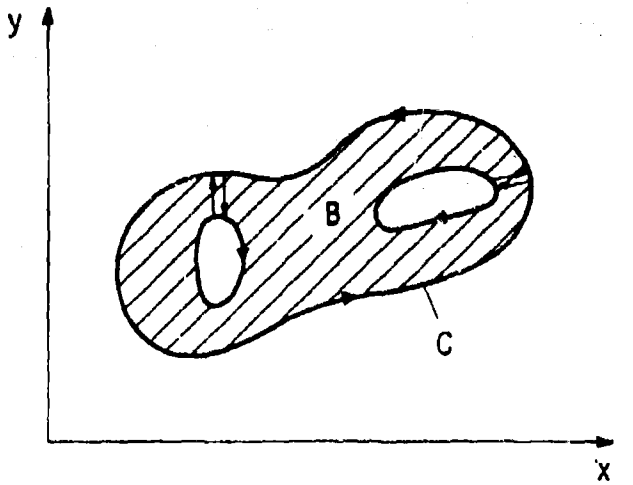

Fig. 3.9 Interrupted Cross Section

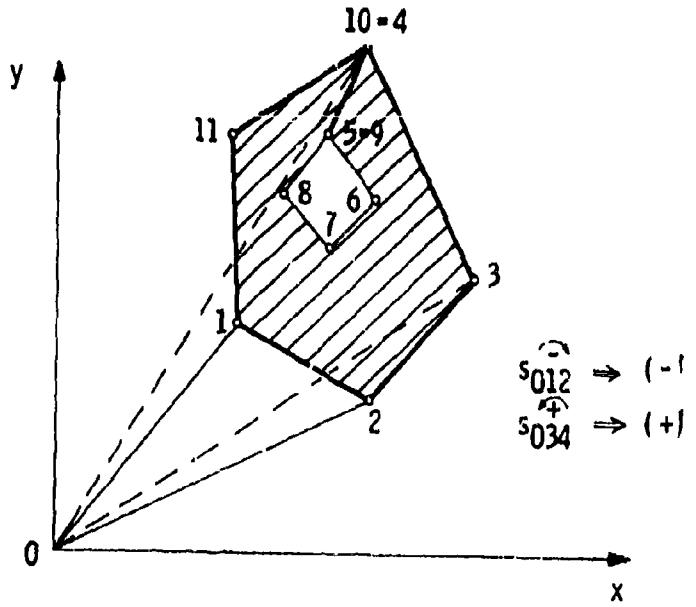

Fig. 3.10 Polygonal Cross Section

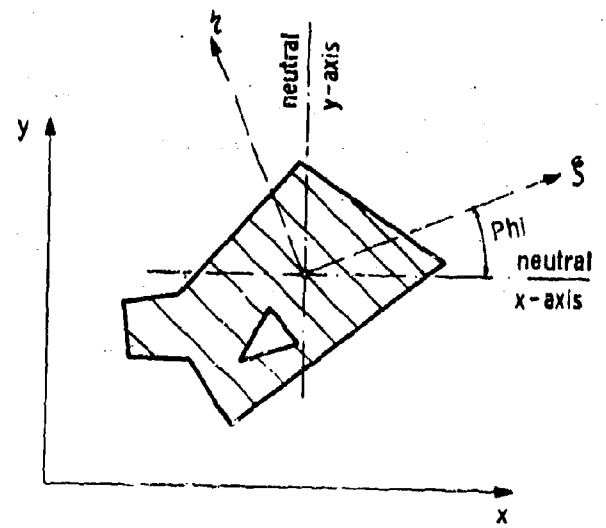

Fig. 3.11 Axis Declaration

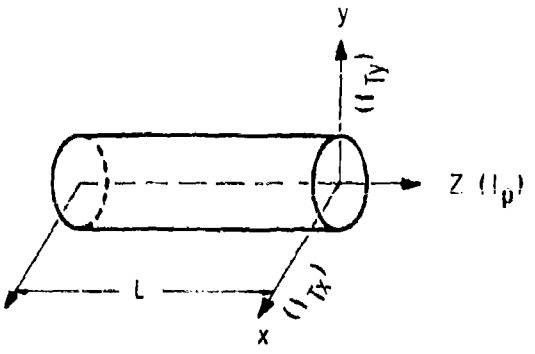

Fig. 3.12 Element in Space

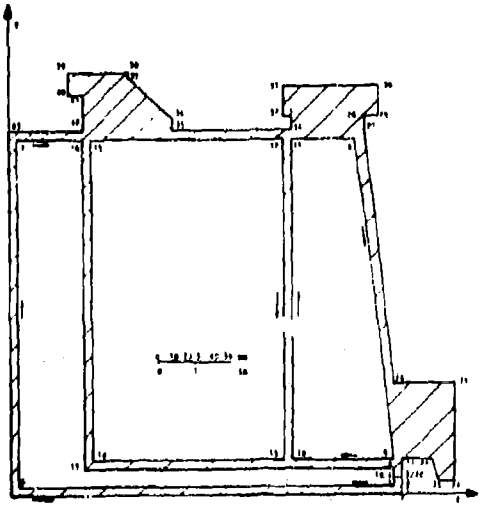

Fig. 3.14 Cross Section

RESULTS

SHEAR AREA	1.6462100000012AE+04
NEUTRAL X-AXIS	1.6975942J15980596+02
NEUTRAL Y-AXIS	1.524712716A870508E+02
X-AXIS AREA MOMENT	2.513289741868824E+06
Y-AXIS AREA MOMENT	2.728748200002416+06
X-AXIS INERTIA MOMENT	5.739666159HA94356+0A
Y-AXIS INERTIA MOMENT	6.17A074763A87B2F+0B
NEUTRAL X-AXIS INERTIA MOMENT	1.9A2594946064040E+0B
NEUTRAL Y-AXIS INERTIA MOMENT	1.65491748?AA2195E+0A
COUNTER CLOCKWISE ANGLE OF ROTATION OF PRINCIPLE AXES	3.7216622?2419167F+01
MOMENT OF INERTIA ABOUT PRINCIPLE X-AXIS	2.2191313140259421E+0B
MOMENT OF INERTIA ABOUT PRINCIPLE Y-AXIS	1.3183A1119921713E+0B
POLAR MASS MOMENT OF INERTIA	1.9AA2936999330953E+01
TRANSVERSE MOMENT ABOUT THE X-AXIS	1.2079147056338035E+01
TRANSVERSE MOMENT ABOUT THE Y-AXIS	1.0694A7A342552B1E+01
TRANSVERSE MOMENT ABOUT THE PRINCIPLE X-AXIS	1.3960049416867D9E+01
TRANSVERSE MOMENT ABOUT THE PRINCIPLE Y-AXIS	8.813976982071496E+00
WEIGHT OF ELEMENT	8.01669648500099AE+00

Fig. 3.15 Result of Computation

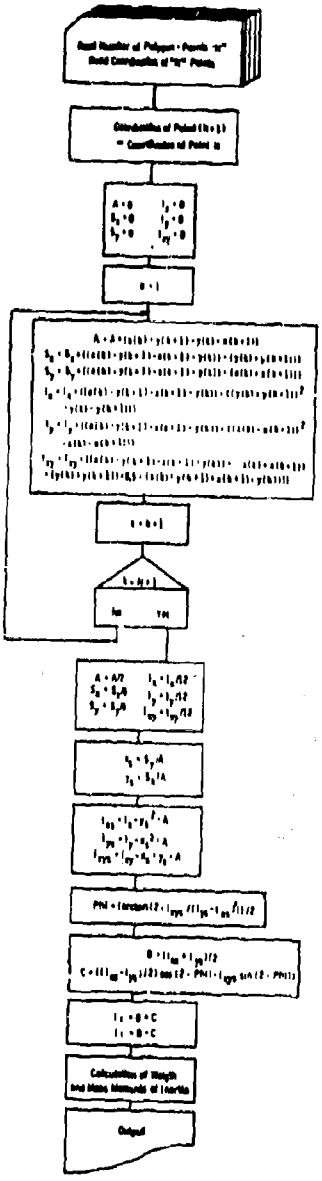

Fig. 3.13 Block Diagram for Calculating Cross Section Values

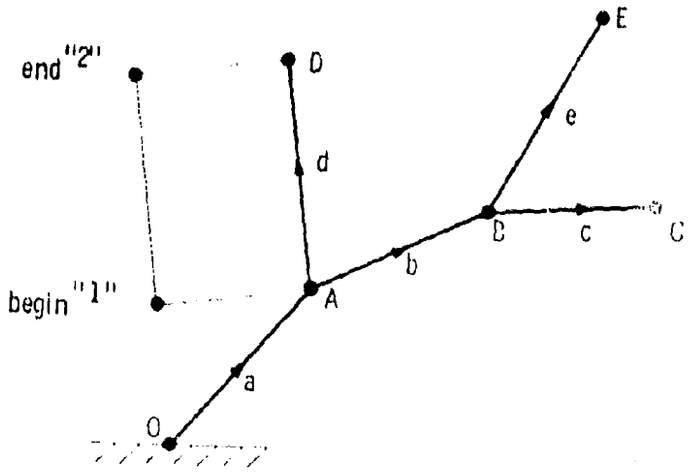

Fig. 3.16 Denomination of Elements

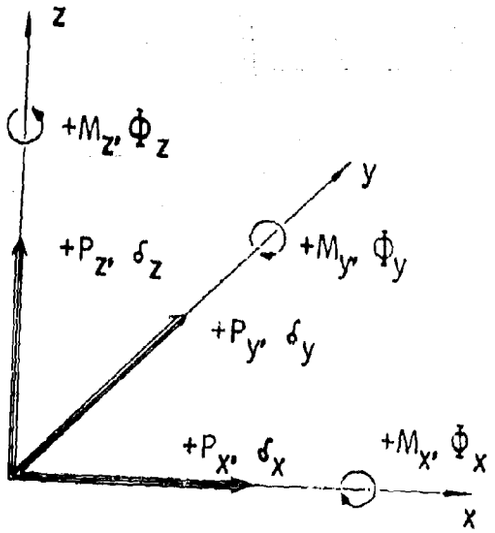

Fig. 3.17 Sign-Declaration

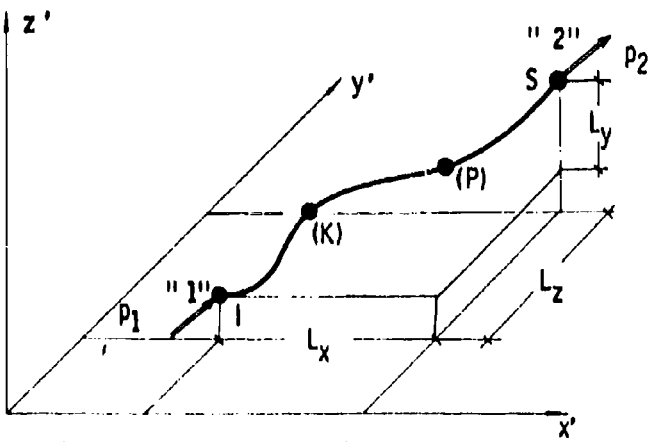

Fig. 3.18 General Element in Space

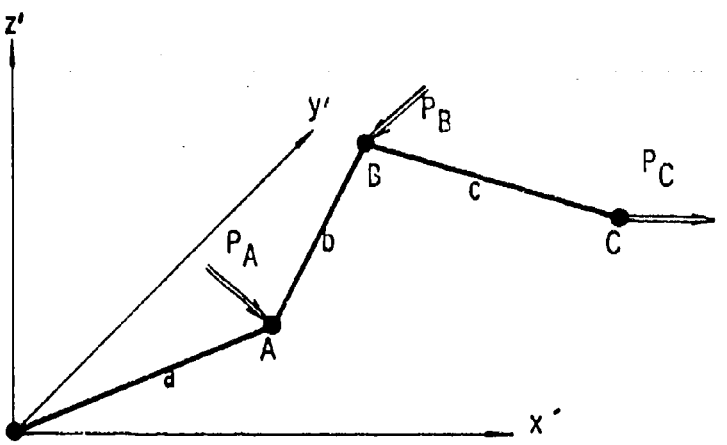

Fig. 3.19 Arbitrary System of Beams

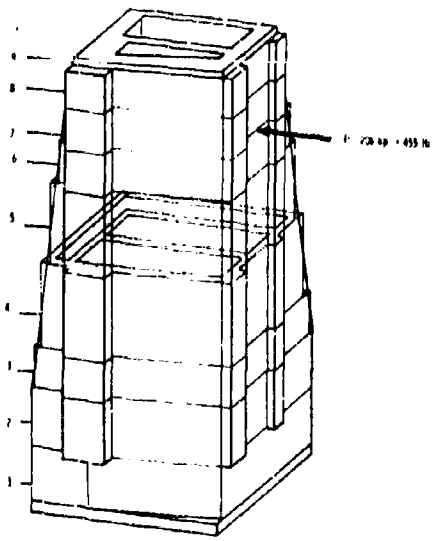

Fig. 3.2C Column of a Single-Column Machine

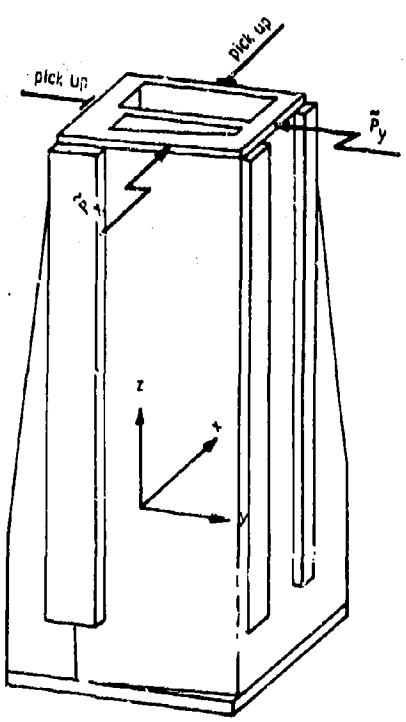

Fig. 3.22 Exciting Scheme of a Machine Tool Column

BELASTUNGSFALL

NR	PX	PY	PZ	MX	MY	MZ
1	0.	0.	0.	0.	0.	0.
2	0.	0.	0.	0.	0.	0.
3	0.	0.	0.	0.	0.	0.
4	0.	0.	0.	0.	0.	0.
5	0.	0.	0.	0.	0.	0.
6	0.	1.00000000E+00	0.	0.	0.	0.
7	0.	0.	0.	0.	0.	0.
8	0.	0.	0.	0.	0.	0.
9	0.	0.	0.	0.	0.	0.

VERFORMUNGEN

NR	SX	SY	SZ	PHIX	PHIY	PHIZ
1	0.	2.47149803E-06	0.	0.	0.	1.75664124E-08
2	0.	6.70762955E-06	0.	0.	0.	2.48311263E-08
3	0.	9.84287133E-06	0.	0.	0.	3.11128992E-08
4	0.	1.89381289E-05	0.	0.	0.	5.03433402E-08
5	0.	2.92808977E-05	0.	0.	0.	6.03259976E-08
6	0.	3.44573639E-05	0.	0.	0.	6.09875445E-08
7	0.	3.88599845E-05	0.	0.	0.	6.09875445E-08
8	0.	4.29407908E-05	0.	0.	0.	6.09875445E-08
9	0.	4.33671428E-05	0.	0.	0.	6.09875445E-08

Fig. 3.21 Results of the Static Calculation

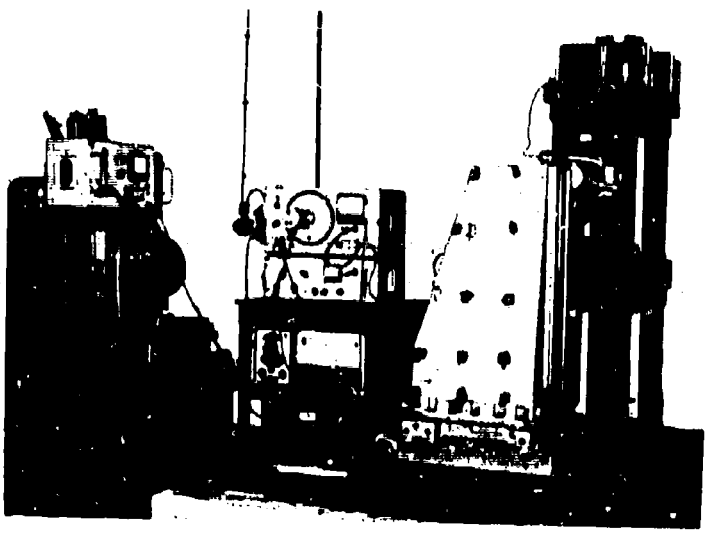

Fig. 3.23 Test Rig

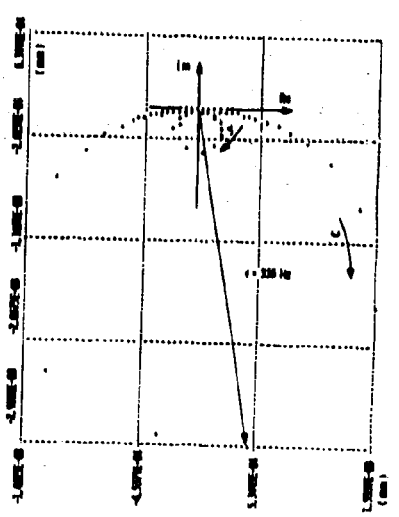

Fig. 3.24 Response Locus for the x-Direction

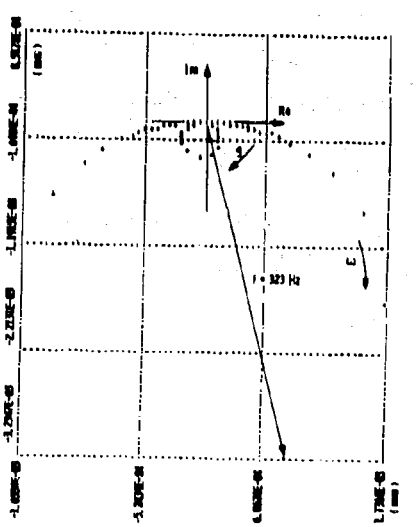

Fig. 3.25 Response Locus for the y-Direction

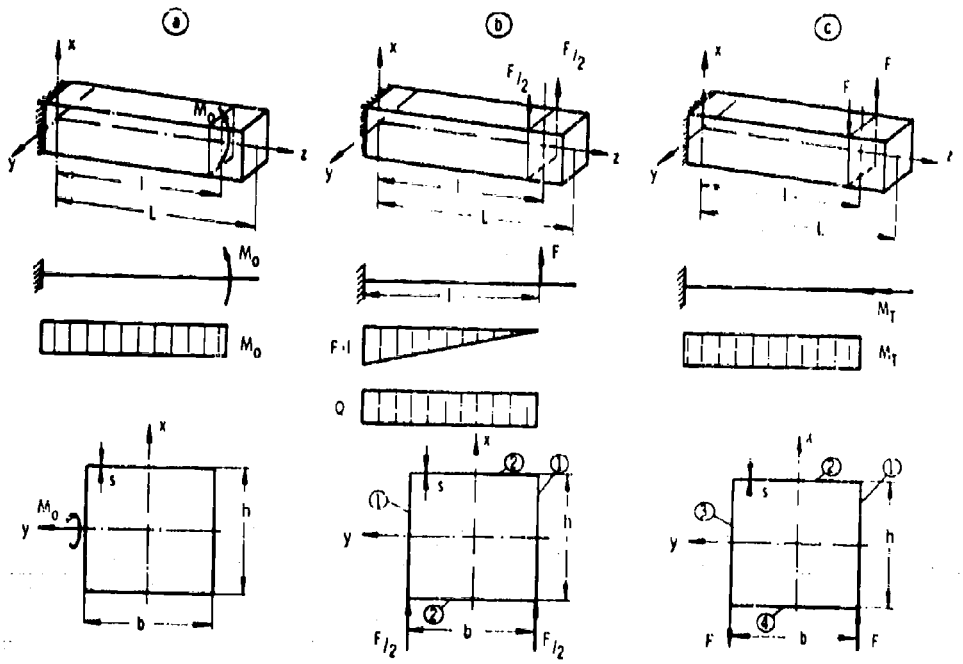

Fig. 3.26 Loading Conditions of a Column

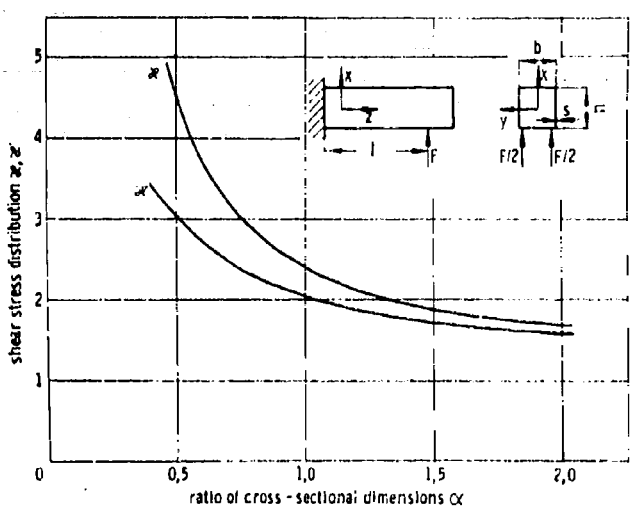

Fig. 3.27 Relationship between Factor ϰ of Shear Stress Distribution and Ratio of Cross-Sectional Dimensions

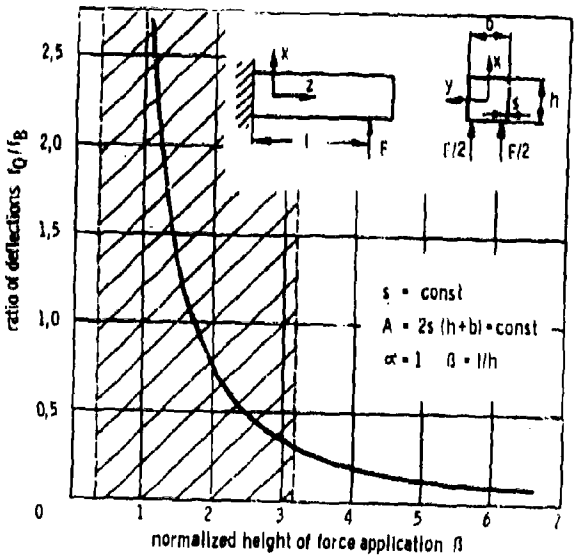

Fig. 3.28 Relation between Ratio of Deflection f_Q/f_D and Normalized Height of Force Application

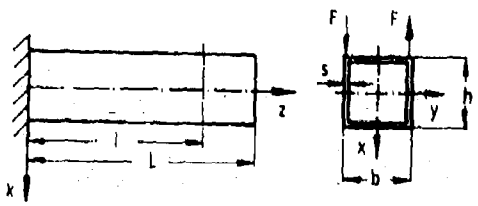

Fig. 3.29 Column Loaded by a Couple of Forces

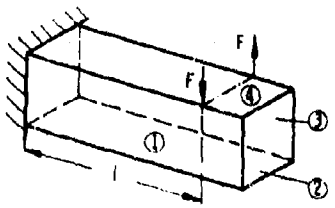

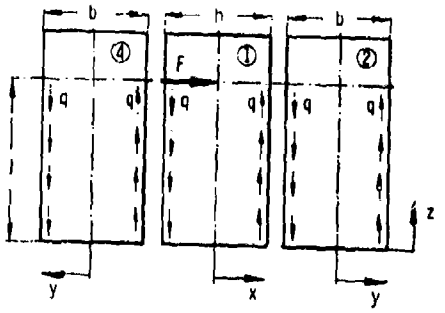

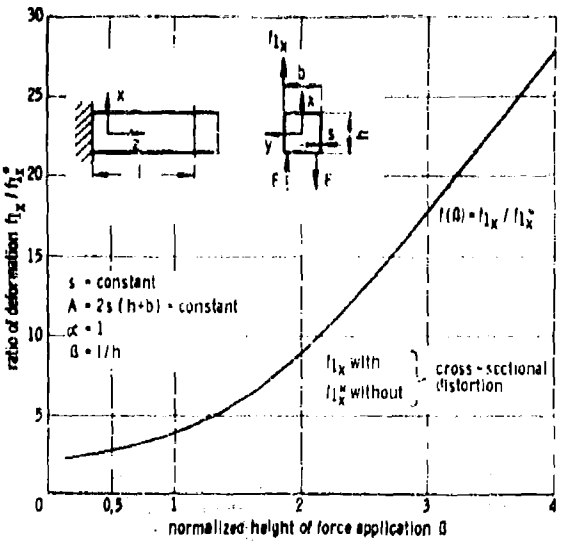

Fig. 3.30 Normalized Deformation of a Column Loaded by a Couple of Forces

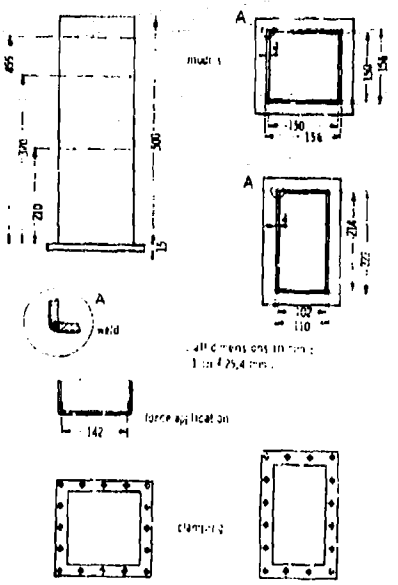

Fig. 3.31 Dimensions of Tested Columns

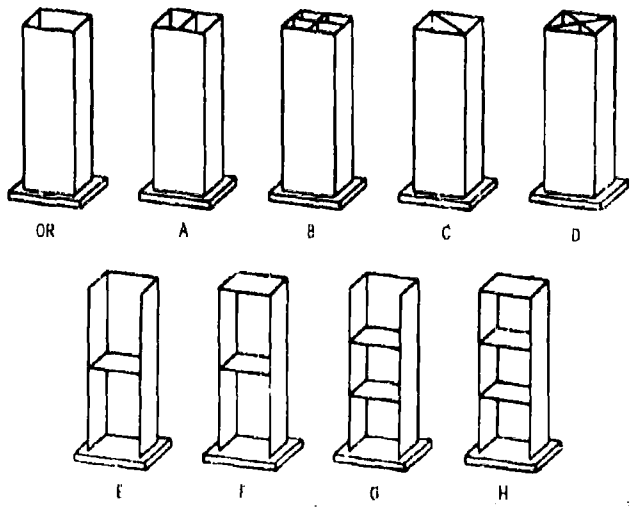

Fig. 3.32 Design of Tested Columns

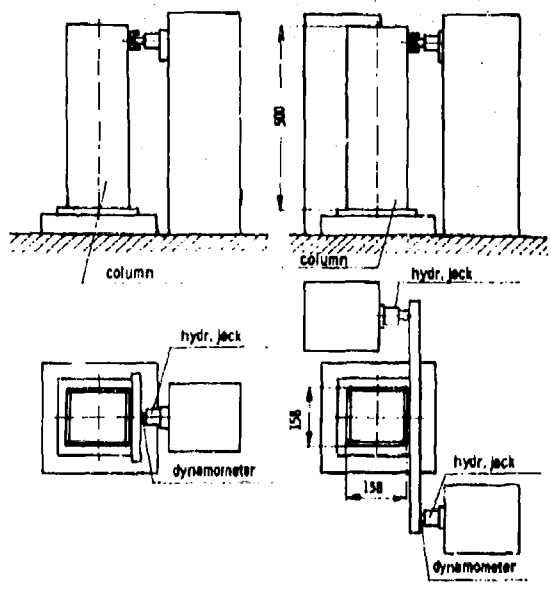

Fig. 3.33 Test Rig for Static Tests

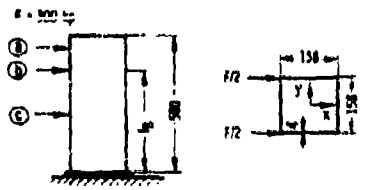

(all dimensions in mm)

Fig. 3.34 Calculated and Measured Deflections of a Column with Square Cross-Section

column without top-plate

force application		deflection x (µm)		
plane	l (mm)	calculated	measured	error (%)
a	455	62,5	59,5	- 5
b	370	38	40,5	+ 7
c	210	12	13	+ 8

column with top-plate

force application		deflection x (µm)		
plane	l (mm)	calculated	measured	error (%)
a	455	62,5	64	+ 2
b	370	38	41,5	+ 9
c	210	12	13	+ 8

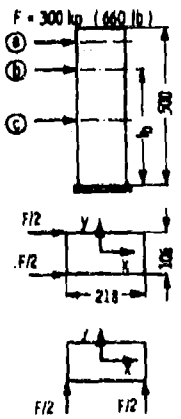

(all dimensions in mm ; µm
1 in ≙ 25,4 mm ; 1mm ≙ 10^3 µm)

load	force application		deflections x (µm) /y (µm)				
	plane	l (mm)	calculated	measured	error (%)	measured	error (%)
x-direction	a	455	34,5	37	+7	34,5	0
	b	370	22	21,5	-2	21	-5
	c	210	7	7,5	+7	7	0
y-direction	a	455	98,5	99,5	+1	93	-5
	b	370	61,5	65	+6	63	+2
	c	210	21	20	-5	21,5	+2
				without top plate		with top plate	

Fig. 3.35 Calculated and Measured Deflections of a Column with Rectangular Cross-Section

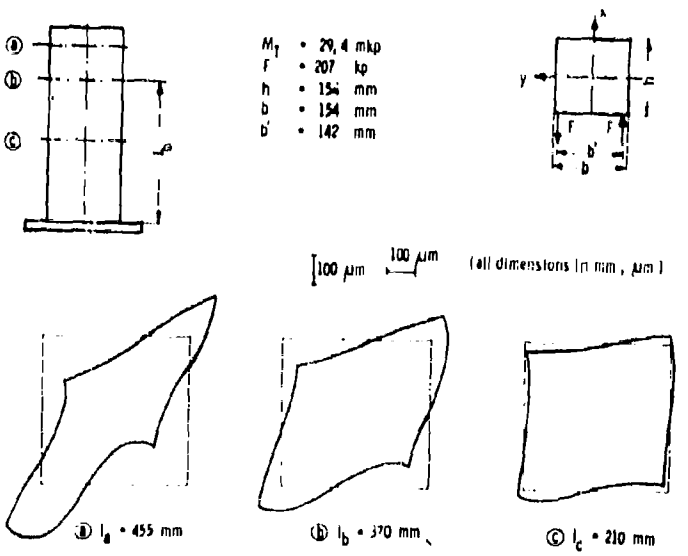

Fig. 3.36 Torsional Deformation with Cross-Sectional Distortion

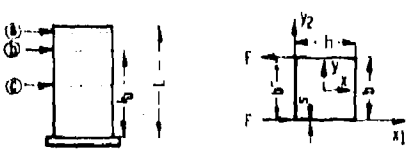

$M_T = F \cdot b' = 29{,}4$ kpm (= 213 ft lb)
F = 207 kp (= 455 lb)
h = 154 mm
b = 154 mm
b' = 142 mm
s = 4 mm
l = 500 mm

height of loading		deflection x_1 (µm)			deflection y_2 (µm)		
plane	height l (mm)	computed	measured	error (%)	computed	measured	error (%)
a	455	135	139	+ 3	119	100	- 16
b	370	78	82,5	+ 6	64,5	58	- 10
c	210	20	26,5	+ 32	11,5	9,5	- 17

Fig. 3.37 Calculated and Measured Torsional Deformation of a Column with Square Cross-Section

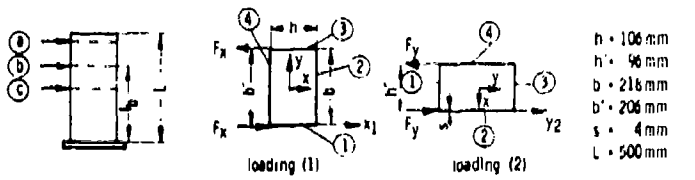

M_T = 29,4 kpm (= 213 ft lb) F_x = 143 kp (= 315 lb) F_y = 396 kp (= 870 lb) (all dimensions in mm)

height of loading plane	l (mm)	loading (1), deflection x_1 (µm) computed	measured	error (%)	loading (2), deflection y_2 (µm) computed	measured	error (%)
a	455	200	173	- 13,5	99,5	94	- 6
b	370	114	110	- 3,5	58,5	59,5	+ 2
c	210	26,5	32	+ 21	16,5	22	+ 32

Fig. 3.38 Calculated and Measured Torsional Deformation of a Column with Rectangular Cross-Section

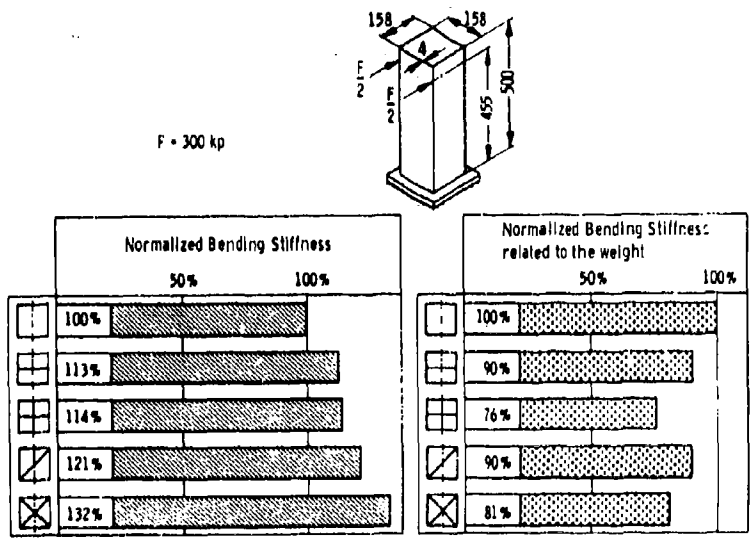

Fig. 3.39 Normalized Bending Stiffness of Columns

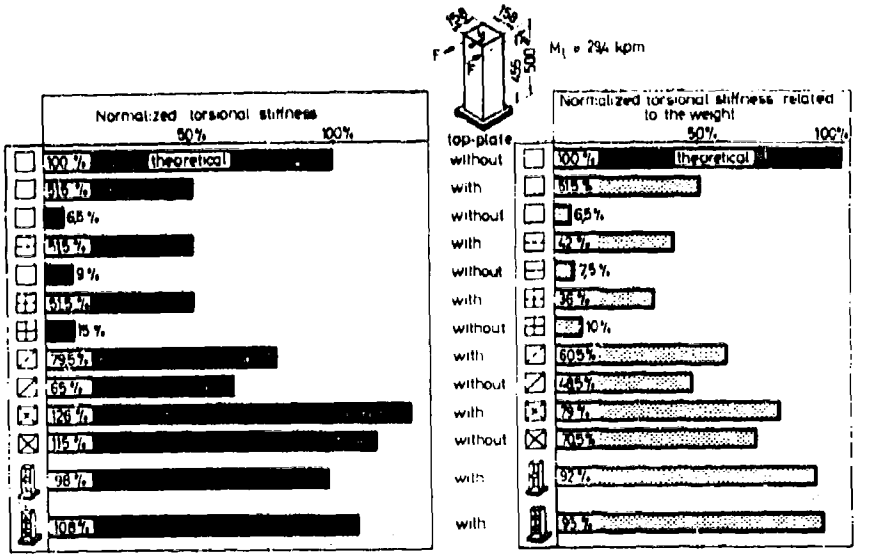

Fig. 3.40 Normalized Torsional Stiffness of Columns

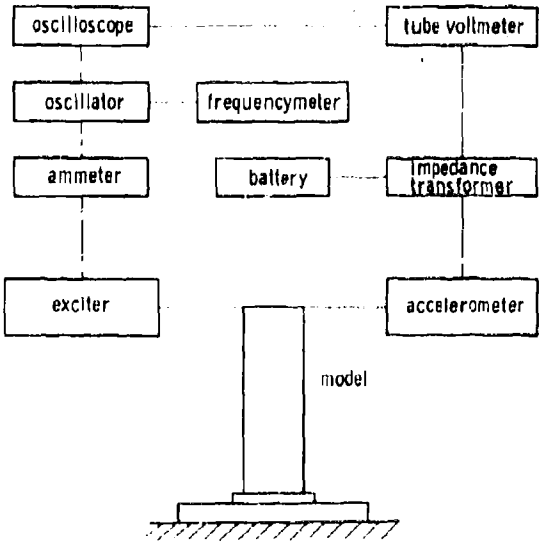

Fig. 3.41 Block Diagram of Dynamic Test Rig

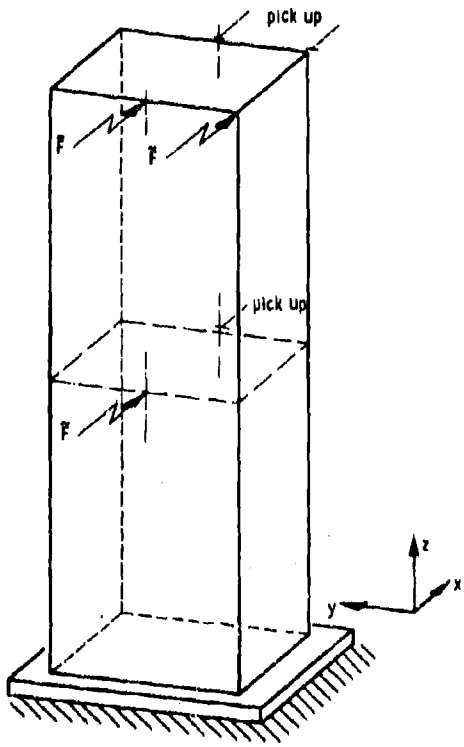

Fig. 3.42 Points of Force Application in Dynamic Tests

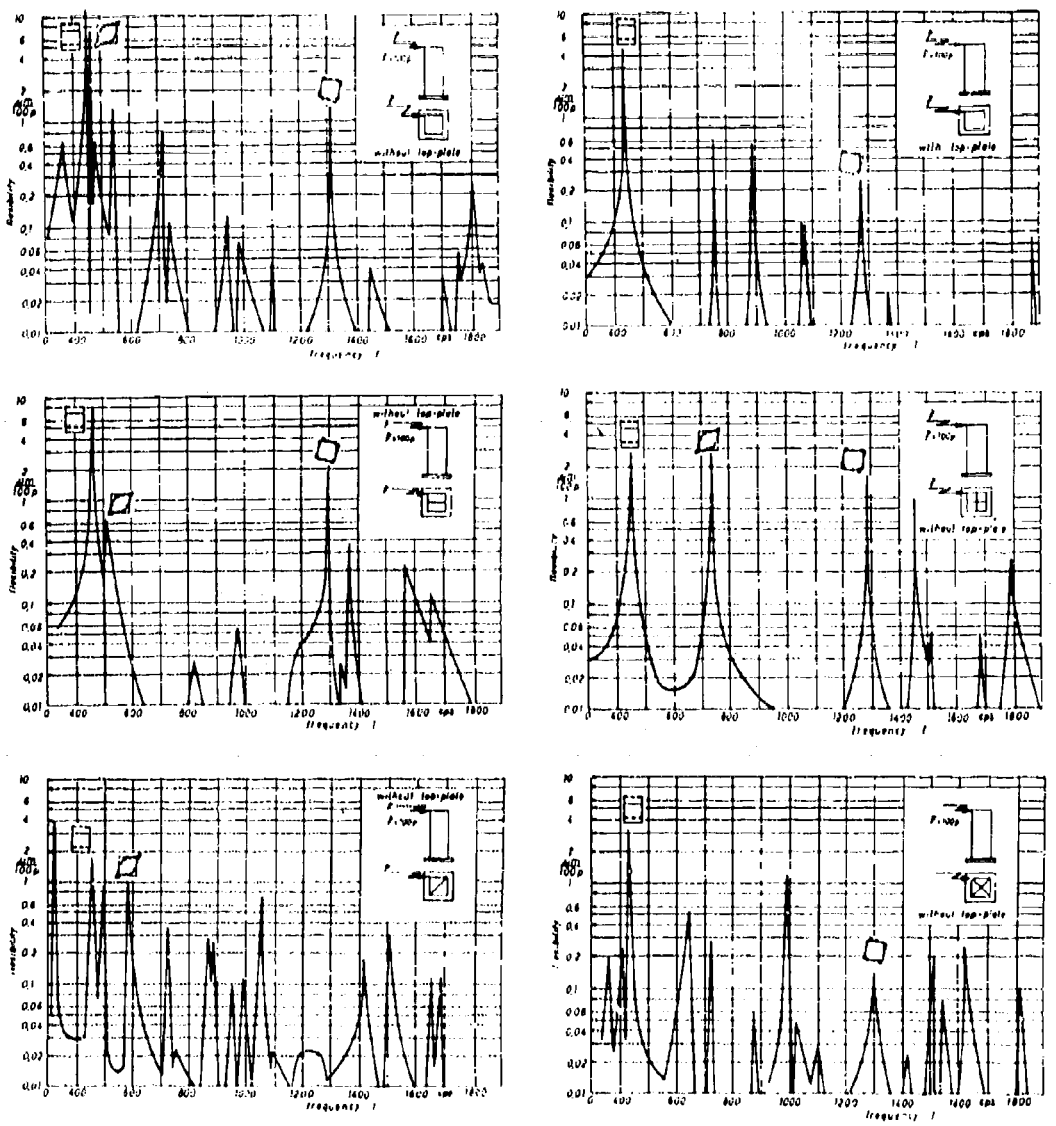

Fig. 3.43 Resonance Curves of Internally Ribbed Columns

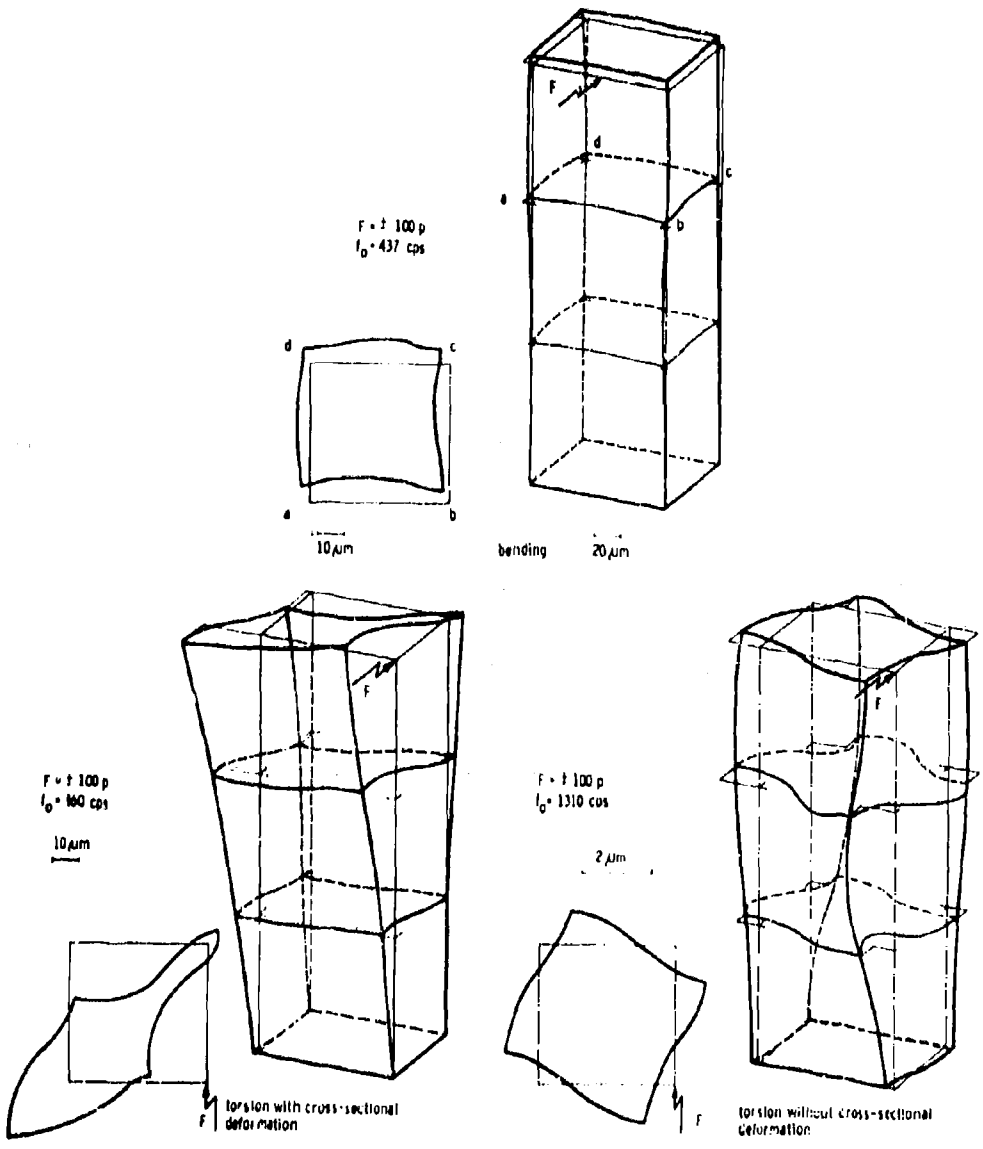

Fig. 3.44 Mode Shapes of Twisted Columns

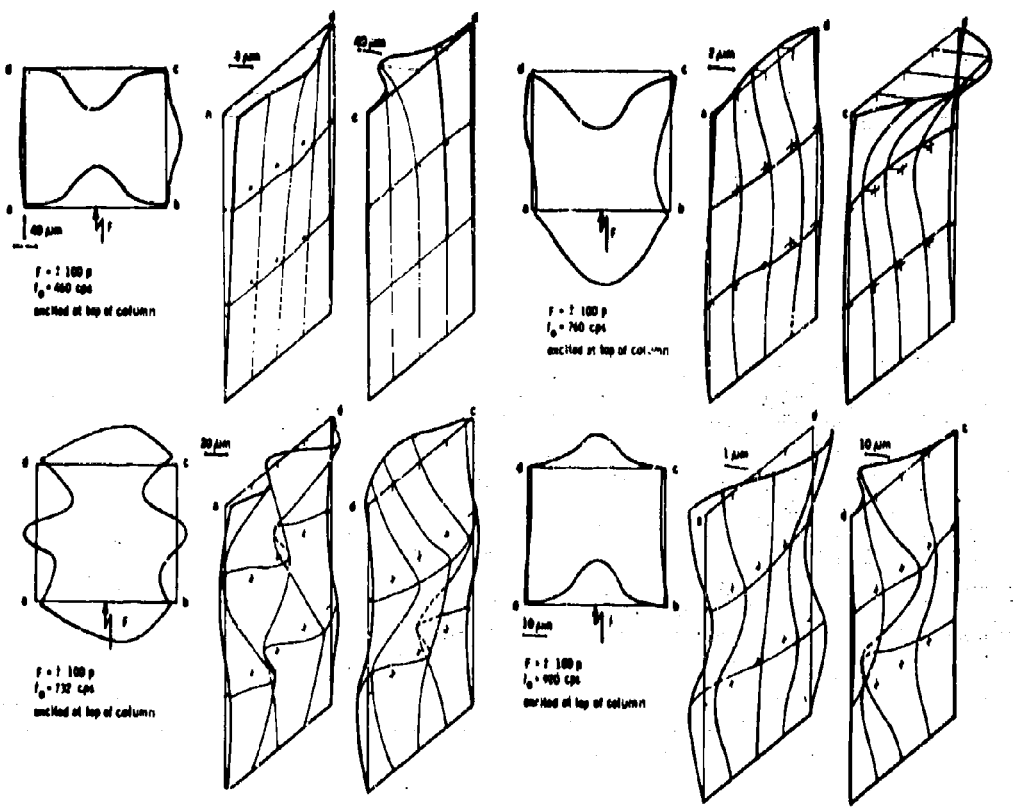

Fig. 3.45 Mode Shapes of Plate Vibrations

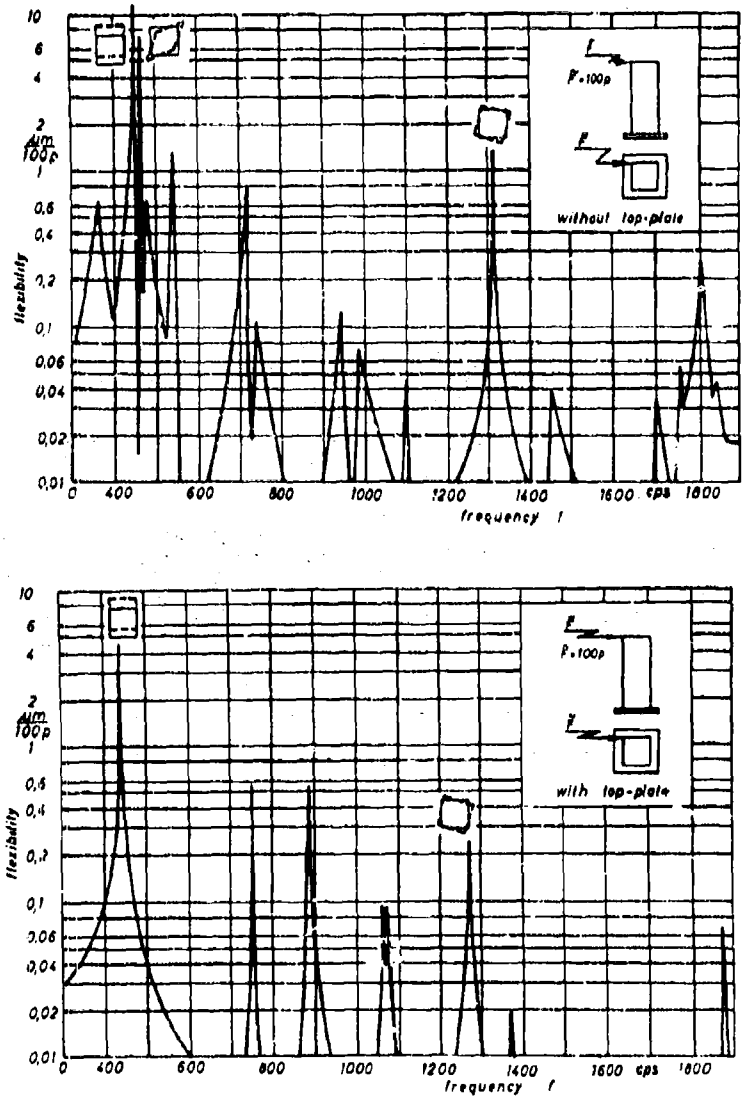

Fig. 3.46 Resonance Curves of Unribbed Columns

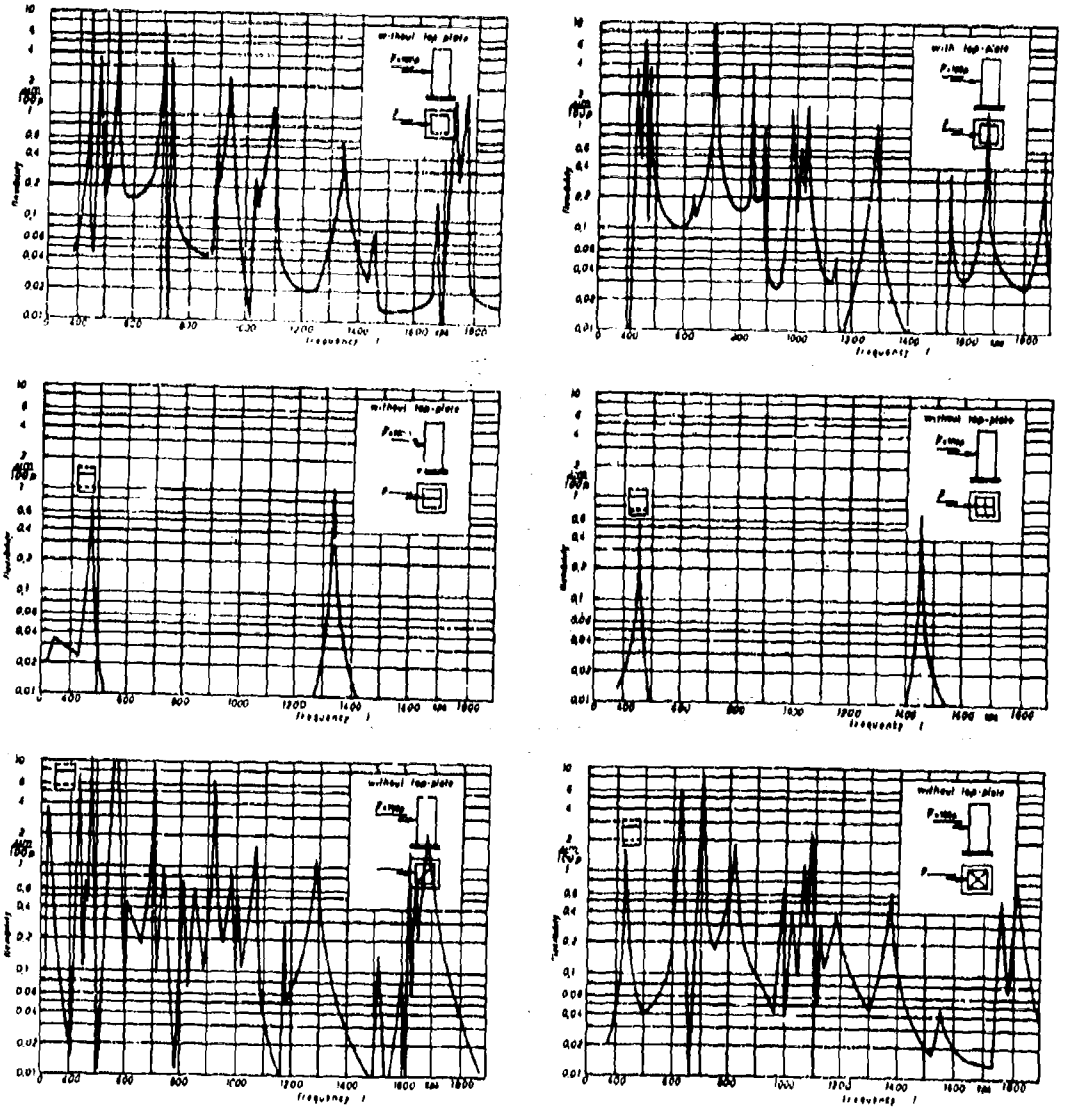

Fig. 3.47 Resonance Curves of Internally Ribbed Columns

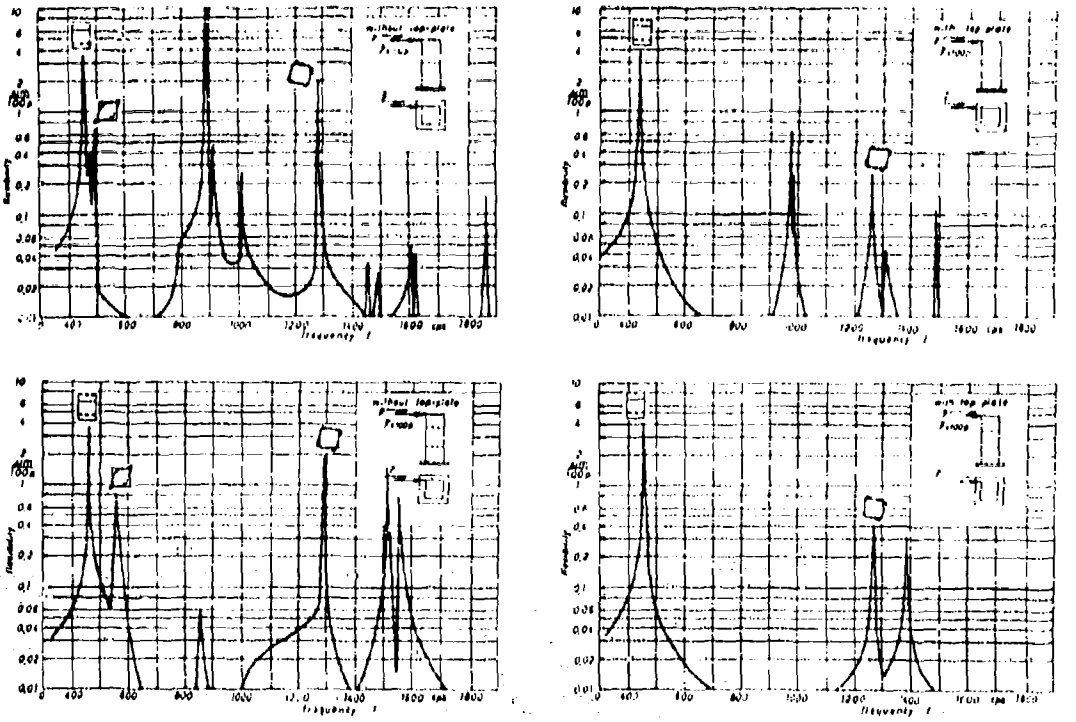

Fig. 3.48 Resonance Curves of Columns with Horizontal Ribs

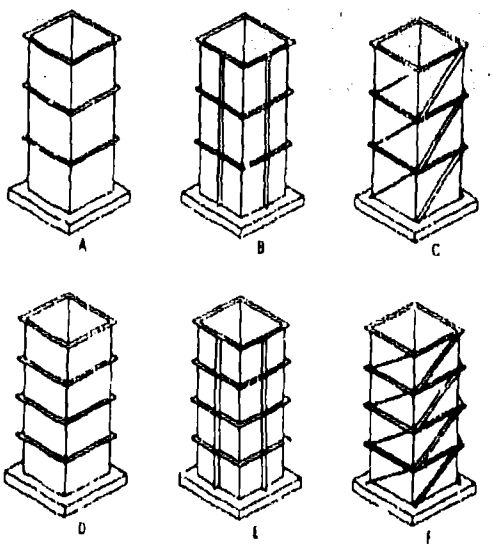

Fig. 3.49 Columns with Wall-Ribbing

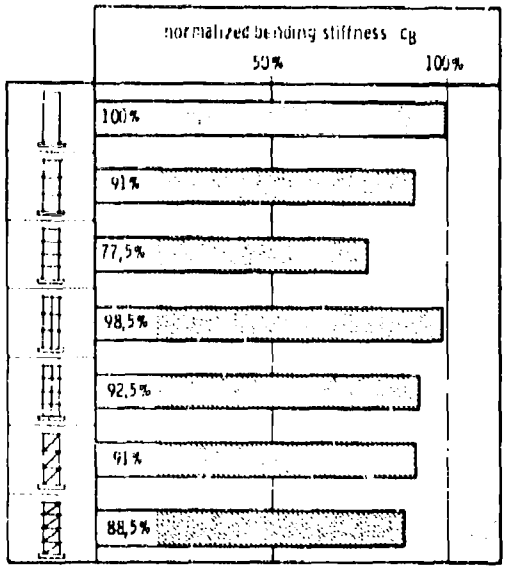

Fig. 3.50 Normalized Bending Stiffness of Columns with Wall Ribbing

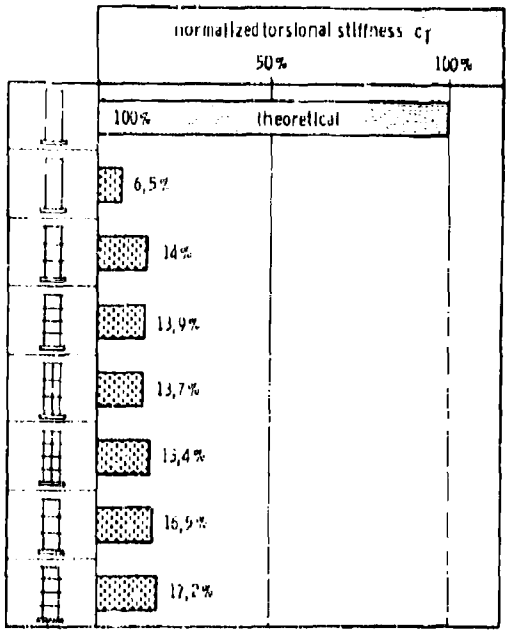

Fig. 3.51 Normalized Torsional Stiffness of Columns with Wall Ribbing

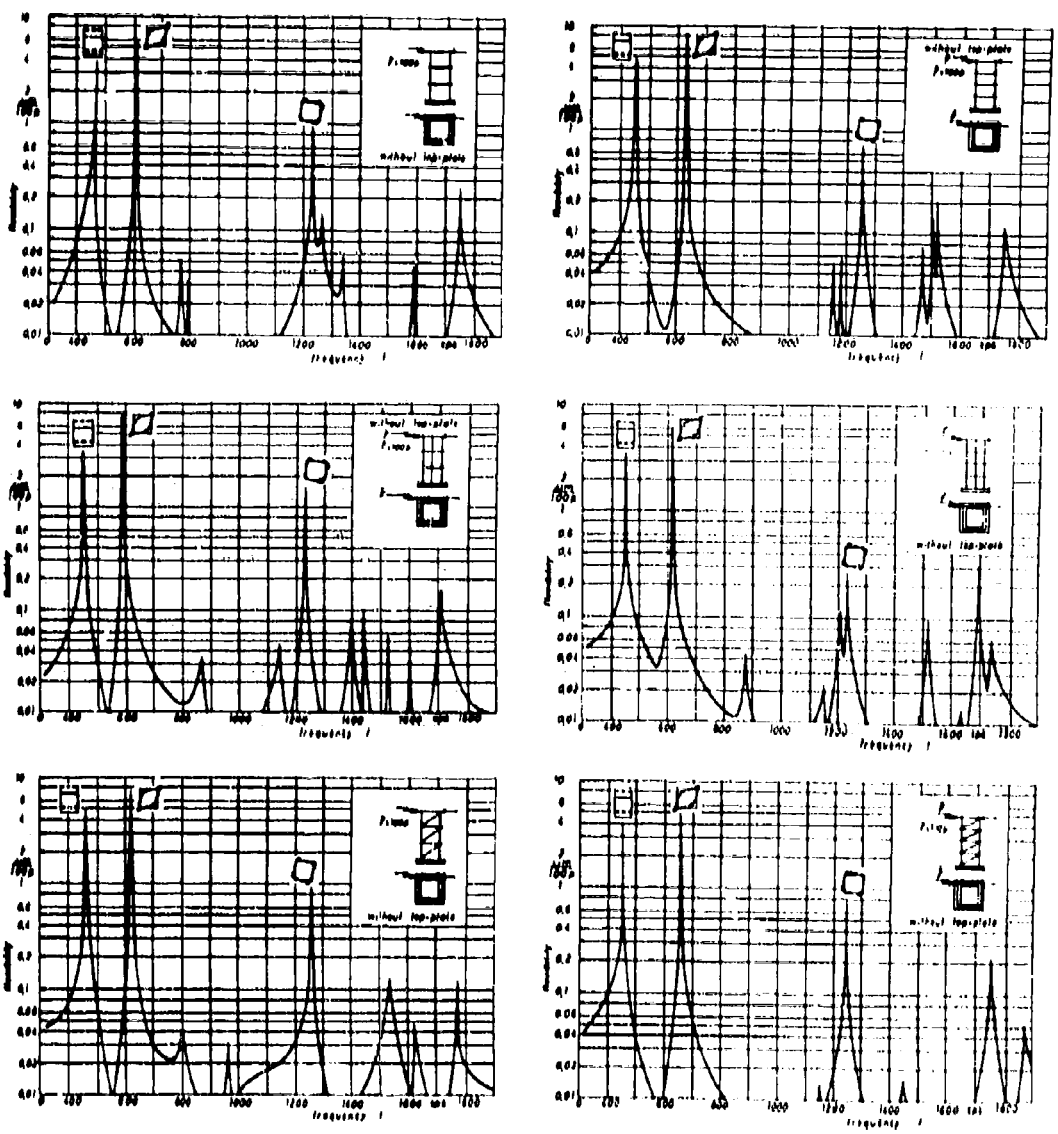

Fig. 3.52 Resonance Curves of Columns with Wall Ribbing

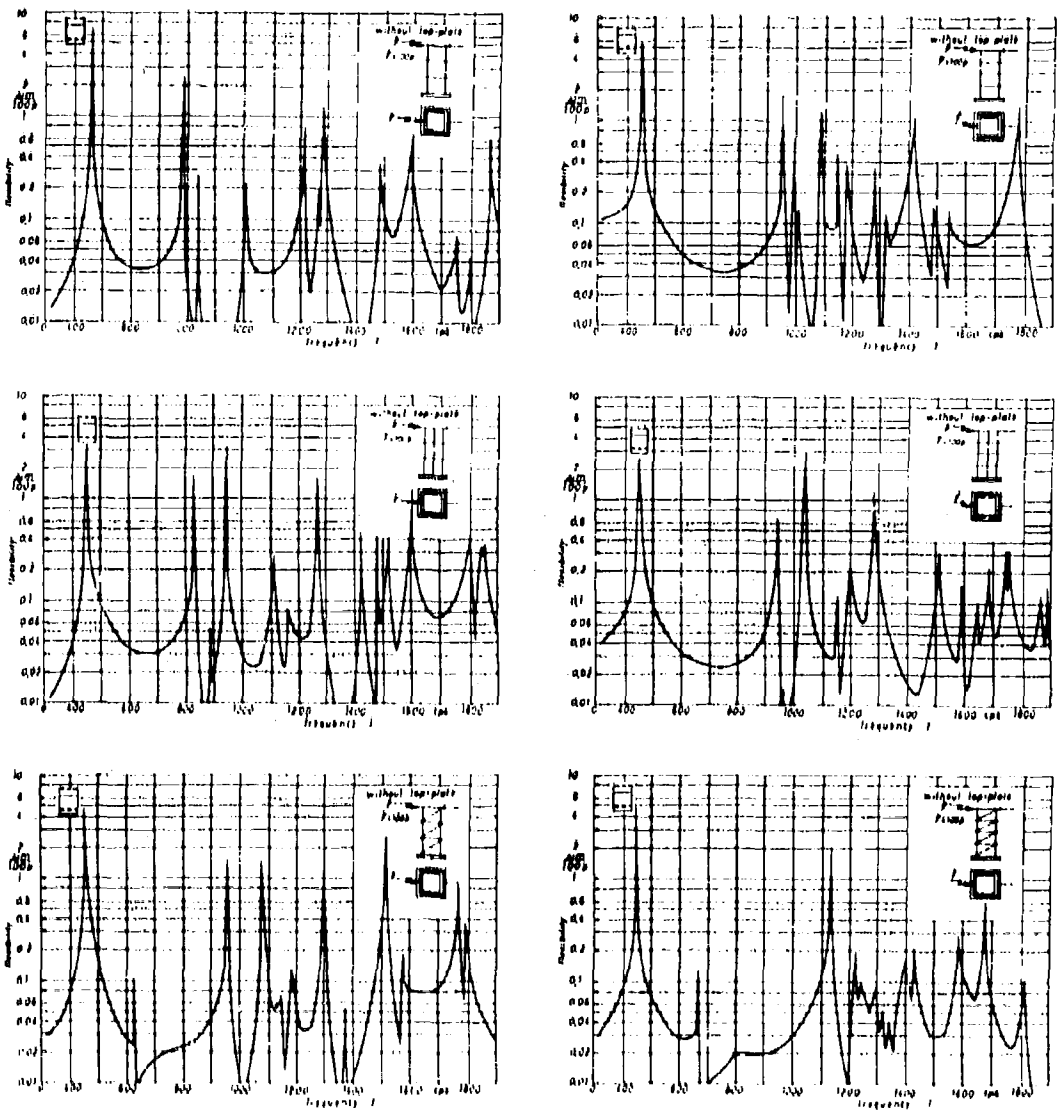

Fig. 3.63 Resonance Curves of Columns with Wall Ribbing

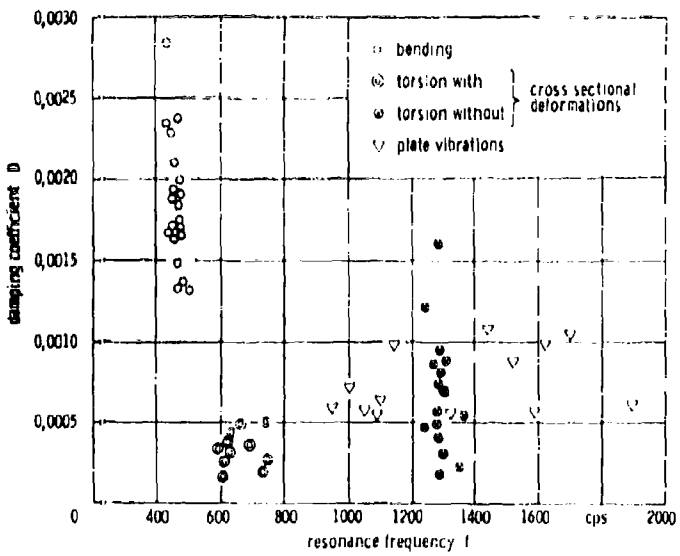

Fig. 3.54 Relationship between Damping Coefficient D, Resonance Frequency and Mode Shape

cross-section	wall thickness s (mm)	area A (%)	area moment of inertia I_x (%)	I_x/A (%)
	4	100	100	100
	4	124	110,5	82,8
	5	124	121,5	99
	5	125	128	101,5
	4	148	110,5	75,2
	6	148	143	97,5
	6	150	156	103
	4	134	115	86,4
	5,39	134	130	98,2
	5,39	135	139	102
	4	163	128	79,2
	6,78	165	159	96,5
	6,78	166	174	104

Fig. 3.55 Area Moment of Inertia of Unribbed and Ribbed Columns

Unclassified

Security Classification

DOCUMENT CONTROL DATA - R&D

(Security classification of title, body of abstract and indexing annotation must be entered when the overall report is classified)

1 ORIGINATING ACTIVITY (Corporate author) Laboratorium für Werkzeugmaschinen und Betriebslehre der Techn. Hochschule Aachen	2a. REPORT SECURITY CLASSIFICATION Unclassified 2b GROUP

3 REPORT TITLE

CHATTER BEHAVIOR OF HEAVY MACHINE TOOLS

4 DESCRIPTIVE NOTES (Type of report and inclusive dates)

FINAL SCIENTIFIC REPORT, 1 Jan 1966 - 31 March 1968

5 AUTHOR(S) (Last name, first name, initial)

Opitz, Herwart, Professor Dr.-Ing. Dr. h.c., D. Sc.

6 REPORT DATE	7a TOTAL NO. OF PAGES	7b NO. OF REFS
30 April 1968	152	22

8a CONTRACT OR GRANT NO.	9a ORIGINATOR'S REPORT NUMBER(S)
b PROJECT NO	
c.	9b. OTHER REPORT NO(S) (Any other numbers that may be assigned this report)
d	

10 AVAILABILITY/LIMITATION NOTICES

11 SUPPLEMENTARY NOTES	12. SPONSORING MILITARY ACTIVITY Air Force Materials Laboratory, Research and Technology Division, AFSC

13 ABSTRACT

Based upon the theory of regenerative chatter the system machine-tool - cutting process is reduced to a nonintermeshed closed control loop, of which the stability behavior is representative for the chatterfree cutting performance. For economically carrying out the stability analysis digital computer programs have been developed. Results of practical chatter investigations are finally detailed.

The discussion of different possibilities to provide data for chatter specifications showed, that further practical investigations must be carried out, before one of the discussed procedures can be finally stated to be fully suitable and before machine tool chatter specifications can be published respectively.

Methods and digital computer programs have been developed and tested for the precalculation of the static and dynamic properties of machine tool systems already in the status of design. A short general view over this research work is presented.

For calculating the deformation of columns with square and rectangular cross-section equations have been derived. They include the influence of shear force and a cross-sectional distortion under torsional loads can be considered as well. In model tests these equations have been proved. Furthermore the influence of different types of ribbing on the static and dynamic behavior of columns has been determined.

DD FORM 1 JAN 64 1473

Unclassified

Security Classification

Unclassified

Security Classification

14 KEY WORDS	LINK A		LINK B		LINK C	
	ROLE	WT	ROLE	WT	ROLE	WT
Machine Tool Vibrations						
Chatter						
System Analysis						
Metal Cutting						
Structure Analysis						

INSTRUCTIONS

1. ORIGINATING ACTIVITY: Enter the name and address of the contractor, subcontractor, grantee, Department of Defense activity or other organization *(corporate author)* issuing the report.

2a. REPORT SECURITY CLASSIFICATION: Enter the overall security classification of the report. Indicate whether "Restricted Data" is included. Marking is to be in accordance with appropriate security regulations.

2b. GROUP: Automatic downgrading is specified in DoD Directive 5200.10 and Armed Forces Industrial Manual. Enter the group number. Also, when applicable, show that optional markings have been used for Group 3 and Group 4 as authorized.

3. REPORT TITLE: Enter the complete report title in all capital letters. Titles in all cases should be unclassified. If a meaningful title cannot be selected without classification, show title classification in all capitals in parenthesis immediately following the title.

4. DESCRIPTIVE NOTES: If appropriate, enter the type of report, e.g., interim, progress, summary, annual, or final. Give the inclusive dates when a specific reporting period is covered.

5. AUTHOR(S): Enter the name(s) of author(s) as shown on or in the report. Enter last name, first name, middle initial. If military, show rank and branch of service. The name of the principal author is an absolute minimum requirement.

6. REPORT DATE: Enter the date of the report as day, month, year; or month, year. If more than one date appears on the report, use date of publication.

7a. TOTAL NUMBER OF PAGES: The total page count should follow normal pagination procedures, i.e., enter the number of pages containing information.

7b. NUMBER OF REFERENCES: Enter the total number of references cited in the report.

8a. CONTRACT OR GRANT NUMBER: If appropriate, enter the applicable number of the contract or grant under which the report was written.

8b, 8c, & 8d. PROJECT NUMBER: Enter the appropriate military department identification, such as project number, subproject number, system numbers, task number, etc.

9a. ORIGINATOR'S REPORT NUMBER(S): Enter the official report number by which the document will be identified and controlled by the originating activity. This number must be unique to this report.

9b. OTHER REPORT NUMBER(S): If the report has been assigned any other report numbers *(either by the originator or by the sponsor)*, also enter this number(s).

10. AVAILABILITY/LIMITATION NOTICES: Enter any limitations on further dissemination of the report, other than those imposed by security classification, using standard statemen such as:

(1) "Qualified requesters may obtain copies of this report from DDC."

(2) "Foreign announcement and dissemination of this report by DDC is not authorized."

(3) "U. S. Government agencies may obtain copies of this report directly from DDC. Other qualified DDC users shall request through

_____."

(4) "U. S. military agencies may obtain copies of this report directly from DDC. Other qualified users shall request through

_____."

(5) "All distribution of this report is controlled. Qualified DDC users shall request through

_____."

If the report has been furnished to the Office of Technical Services, Department of Commerce, for sale to the public, indicate this fact and enter the price, if known.

11. SUPPLEMENTARY NOTES: Use for additional explanatory notes.

12. SPONSORING MILITARY ACTIVITY: Enter the name of the departmental project office or laboratory sponsoring *(paying for)* the research and development. Include address.

13 ABSTRACT: Enter an abstract giving a brief and factual summary of the document indicative of the report, even though it may also appear elsewhere in the body of the technical report. If additional space is required, a continuation sheet shall be attached.

It is highly desirable that the abstract of classified reports be unclassified. Each paragraph of the abstract shall end with an indication of the military security classification of the information in the paragraph, represented as (TS), (S), (C), or (U).

There is no limitation on the length of the abstract. However, the suggested length is from 150 to 225 words.

14. KEY WORDS: Key words are technically meaningful terms or short phrases that characterize a report and may be used as index entries for cataloging the report. Key words must be selected so that no security classification is required. Identifiers, such as equipment model designation, trade name, military project code name, geographic location, may be used as key words but will be followed by an indication of technical context. The assignment of links, rules, and weights is optional.

Unclassified

Security Classification